Design of a Thin Concrete Shell Roof

for a Basketball Arena of 20,000 spectator capacity

Niladri Kanta

Master of Science Thesis

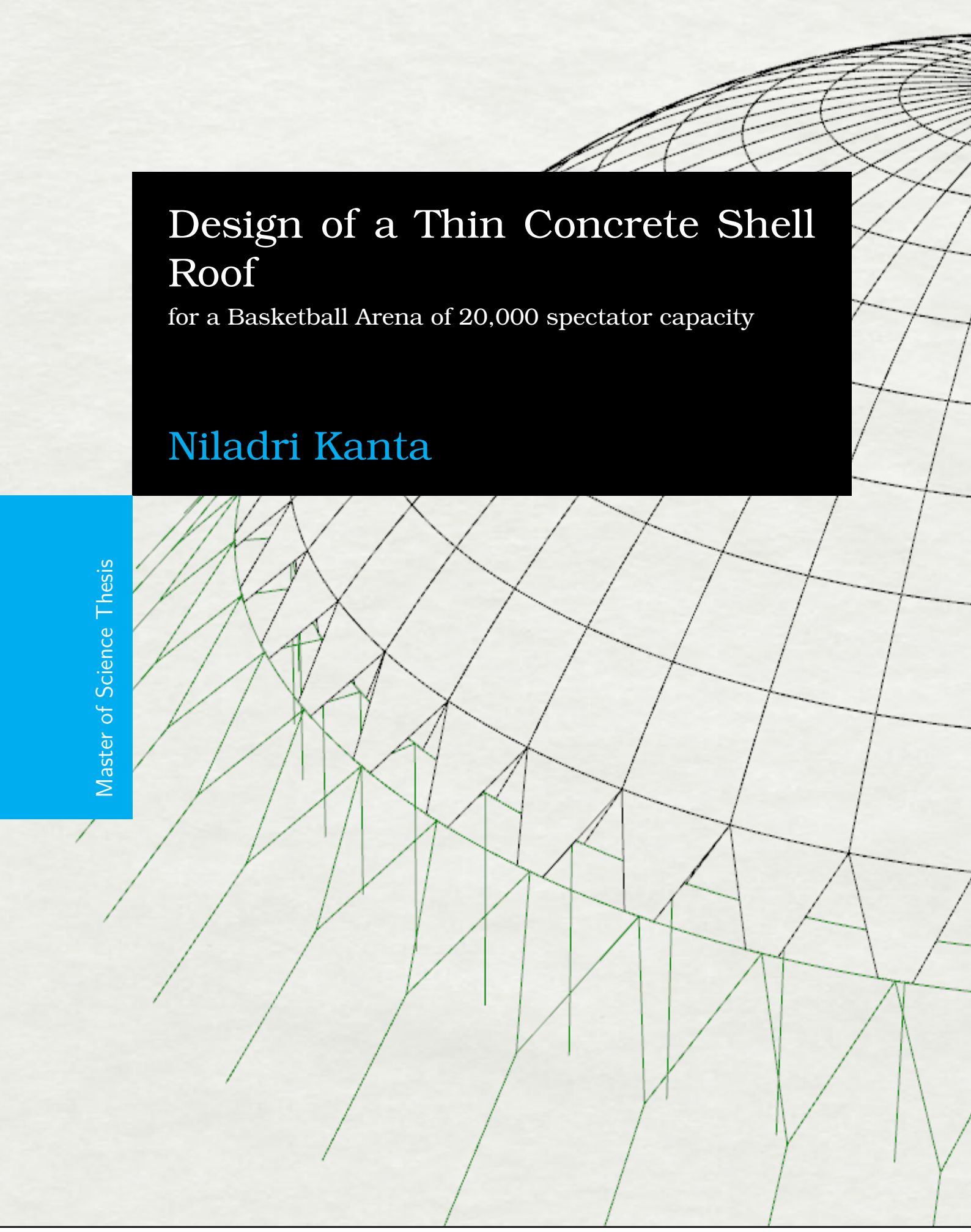

TU Delft Delft University of Technology

Civil Engineering and Geosciences

Design of a Thin Concrete Shell Roof

for a Basketball Arena of 20,000 spectator capacity

Master of Science Thesis

For the degree of Master of Science in Structural Engineering at Delft University of Technology

Niladri Kanta

June 23, 2015

Faculty of Civil Engineering and Geosciences · Delft University of Technology

Delft University of Technology
Department of
CITG

The undersigned hereby certify that they have read and recommend to the Faculty of Civil Engineering and Geosciences for acceptance a thesis entitled

Design of a Thin Concrete Shell Roof

by

Niladri Kanta

in partial fulfillment of the requirements for the degree of

Master of Science Structural Engineering

Dated: June 23, 2015

Supervisor(s):

Prof. ir. R. Nijsse

Dr. ir. P.C.J. Hoogenboom

Ir. A. Borgart

Abstract

This master thesis involves the design of a roof for a basketball arena, which has a capacity of 20,000 spectators and it needs to be designed as a concrete shell structure. The size of the stadium is large enough to demand a long spanned shell structure. This thesis attempts to find an elegant solution to this problem, which combines aesthetic and structural beauty with efficiency during construction. These points are judged to be important aspects of a complete structural design.

A literature study is done in an attempt to create a plan for the design of the shell roof. The general theory of shells is studied to understand their forms, structural behaviour and modes of failure. This helps the designer to understand the mechanics of shells which heavily influence the design procedure. Prominent shell designers of yesteryears and some of their projects are the next object of interest. Existing basketball arenas are also examined to find out the loading requirements for the roof in this thesis. The literature study is concluded by gathering details of high strength concrete and finite element software, both of which are relatively new in the shell industry.

A design procedure is defined based on the findings of the studies mentioned above. The shell is chosen to be designed as a spherical dome. The initial geometrical details are stipulated after conducting sightline analysis, capacity calculations and hanging model analysis. Varying values of the span and thickness are chosen, leading to multiple design formulation, one of which is chosen based on a linear stability analysis. The selected design is then structurally investigated with inclusion of nonlinear effects and imperfections. The above mentioned process is executed using a combination of different softwares, for modelling, meshing and analyzing. Once the structural behaviour of has been verified, the stresses are checked and the design is finalized by defining the structural framework, and proposing the paneling and connection details.

Table of Contents

List of Figures

List of Tables

Preface

I offer my sincerest gratitude to Mr. Rob Nijsse, Mr. Pierre Hoogenboom and Mr. Andrew Borgart for guiding me to the path of becoming a structural designer. With them I was able to discuss my professional ambitions which enabled them to suggest a thesis topic, which aligned perfectly with my interests.

Being a designer at heart my thoughts, at the initial stages, were uncontrolled and aimless. This is where the members of my committee were able to mentor me towards a much organized way of designing structures. The discussions, questions and comments during the many interactions with them played a crucial role in the completion of this thesis.

I would also like to thank Peter Eigenraam for his help to model the structure. This phase of the thesis was particularly time consuming and his knowledge of working with modeling softwares benefited me a lot.

I also thank my family and friends for their constant support during this phase of my life. Lastly, I specially thank my housemates for tolerating me during this difficult period.

Delft, University of Technology — Niladri Kanta
June 23, 2015

Chapter 1

Introduction

1-1 Concept of Structural Designers

Structural designers are a new breed of engineers, who act as bridges between conventional structural engineers and architects. Their role requires them to formulate the best possible design based on certain requirements, which depends on several factors. Thus, it is fair to say that they define the backbone of project. This causes a lot of responsibilities to fall on the designer. A good structural designer tries to incorporate several factors to make a complete design. This includes taking into account aesthetic, structural and constructional factors. Incorporating every factor heavily influences the design, as will be evident from this particular project. This approach obviously causes several obstacles, which can cause complications in the design process. This makes it imperative for a structural designer to have intuition and foresight, along with good structural knowledge to deal with these problems. It remains the primary responsibility of the structural designer to ensure that the structure performs all the functions, it was meant to perform before the start of the design process.

The design process of any structure ultimately determines its 'structural life'. This motivates a designer to check the behaviour of the structure, when it is in a state of service. In the past, some shell structures have collapsed due to increasing influences of nonlinear parameters. The collapse of the hypar shell roof of a high school in the USA [1] is one such example. Structural failure is the biggest nightmare of any designer. Shells experience something called 'snap-back' behaviour, which is characterized by sudden loss in load carrying capacity, leading to immediate failure. Furthermore shells collapse without warning, unlike other structures which show considerable visual deformations before collapse. This warning is unavailable to shell designers adding more significance to checking nonlinear effects in the design process. Now, finite element softwares can be used to incorporate such effects in computational design. Together with numerous available modelling softwares, they provide the most essential tools for a structural designer.

1-2 Beauty of Shell Structures

Shell structures are very interesting due to their impressive strength-to-weight ratios. They are able to span over large areas, while having an exceptionally less thickness. This is primarily due to their form based structural behaviour. The geometry, that is their initial curvature, along with the boundary conditions and type of loading, dictates the way they transfer load or the way they fail (in case the load exceeds their load carrying capacity). Shells exhibit membrane like behaviour which will be explained further in this thesis. The beauty of shells lies in the fact that a designer is able to design the shell as thin as possible, even in the presence of loads that disrupt its characteristic membrane behaviour. The shell is able to confine this disturbance within regions which can be designed or optimized separately.

The properties mentioned above are highlighted by the various shell structures in existence today. Shells provide a means to obtain an aesthetical and structurally efficient design. They can take several shapes and forms, which lie at the mercy of the designer. Coupled with the fact that they take up less material for construction, shells became increasingly popular in the last seven decades. Since then there have been several hindrances in their growth, but these difficulties are a thing of the past. Development of advanced analysis methods, and new innovative developments in the construction field, have led to a resurgence in shell design. As a result, new designs for shells are gaining prominence, some of which were impossible in the past.

1-3 Objectives

This thesis is essentially a design project, which attempts to create the roof of a basketball arena. This arena is expected to have a capacity of 20,000 spectators, and the shell is proposed to be made of concrete. This can lead to a very complicated design process as a whole and therefore a set of objectives are listed out to ensure an efficient and sound structural design. These objectives are stated below:

- **Aesthetical Efficiency**

  Basketball is a very popular indoor game and has a large fan following. Having a stadium which looks beautiful, also has its advantages. It has the potential of becoming an iconic structure and an object of pride for the city or town. Hence, it is very important to design not only a functional but also a aesthetically efficient structure. Having a structure which looks elegant, has unparalleled advantage in capturing the attention of people.

- **Structural Efficiency**

  There are several structural solutions for any kind of criteria. Nevertheless, the designer has to formulate a design which is structurally sound, and transfers the load to the ground in the most efficient way possible.

- **Constructional Efficiency**

  Detailed investigations in the temporary decline of shell structures revealed that one of the problem was high constructional costs. This was due to the complex nature of

frame work required for shell structures. Reacting to this, the shell needs to be designed such that it can be easily constructed. Furthermore, concrete is favored to create the shell as it is generally inexpensive and easily available as compared to other materials like steel.

It is important to point out, that the fulfillment of the criteria defined above is subjective. This is because some aspects like beauty of a structure, mean differently to different people. It may look aesthetically pleasing to one, but not the other. Also matters like constructional efficiency can depend on factors like money. Nevertheless, the final outcome of this design tries to reach a balance between all three objectives.

1-4 Design approach

A specific design approach is defined to fulfill all of the objectives mentioned earlier. Design is an iterative process which can become extremely taxing, if not preplanned beforehand. The overall order of the design strategy adopted in this project is mentioned below.

1. All theory related to shell design is acquired and studied. This includes study of different shell surfaces, their structural behaviour and also the possible ways they can fail.
2. The entire history of concrete shell industry is studied, along with important associated people and structures. In the 1950s several shell designers rose to prominence. An attempt is made to learn about their ways and methods. Between these designers, they have an impressive list of shell structures that exist and function today. Some of these bear similar characteristics and aspects, compared to the expected shell design for this project.
3. Currently functioning basketball arenas are studied to have a better understanding of loads expected on the roof. If there are any special loads that need to be taken into account, then they are found out in this step.
4. Based on the three steps mentioned above, pre-design considerations are drawn up. They essentially serve as design boundaries or constraints, only within which, the designer can freely operate. This step marks the beginning of the actual design process.
5. Once all factors are taking into consideration, the outline of the main design process is created. This procedure is strictly followed during the entire course of design.
6. Finally the behaviour of the designed shell is studied and recorded, under various load combinations, to ensure proper functioning of the structure.

The first three steps constitute the literature study performed, before commencing the actual design of the roof of the basketball arena. They help to create a sound design process which is then applied to obtain the final proposal. This design process is explained in detail during the course of this thesis.

Chapter 2

Existing Knowledge relevant to concrete shell design

2-1 Classification of Shell Surfaces

2-1-1 Gaussian Curvature

Shell surfaces are usually classified based on their gaussian curvatures. For a three dimensional surface, the product of the maximum and minimum principal curvatures gives us the gaussian curvature. They are orthogonal to each other and can be found out by intersecting infinite planes with the surface at any point. Based on the product of the principal curvatures we can further classify the gaussian surfaces as discussed below.

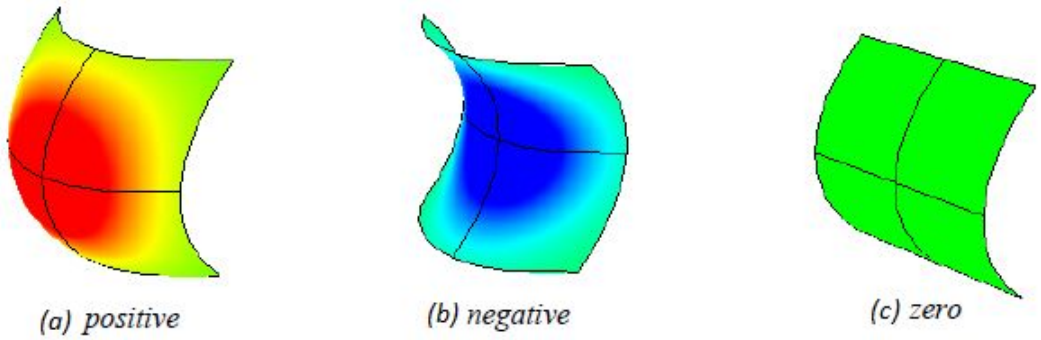

Figure 2-1: Types of Gaussian Curvatures [1]

1. **Synclastic**

A Synclastic surface has a positive gaussian curvature and is shown in figure 2-1 (a). Both the principal curvatures have the same sign. They generally exhibit in-plane meridional and circumferential stresses to carry loads. Spheres and elliptical paraboloids are common examples of this kind of surface.

2. **Anticlastic**

   In this type of surface both the principal curvatures have different signs resulting in a negative gaussian curvature (figure 2-1 (b)). Having opposite signed principal curvature enables these surface to act with a combination of compressive and tensile arch behaviour under perpendicular loads [12]. Hypars are good examples of anticlastic surfaces.

3. **Monoclastic**

   If one of the principal curvatures is zero then it gives rise to monoclastic surfaces. They have zero gaussian curvature as seen in figure 2-1 (c). Cylindrical shells are the most common examples of this type of surface.

2-1-2 Developed and Undeveloped Surfaces

This basis of classification depends on whether the surface can be 'opened' or deformed to obtain a plane form. Figure 2-2 show examples of both.

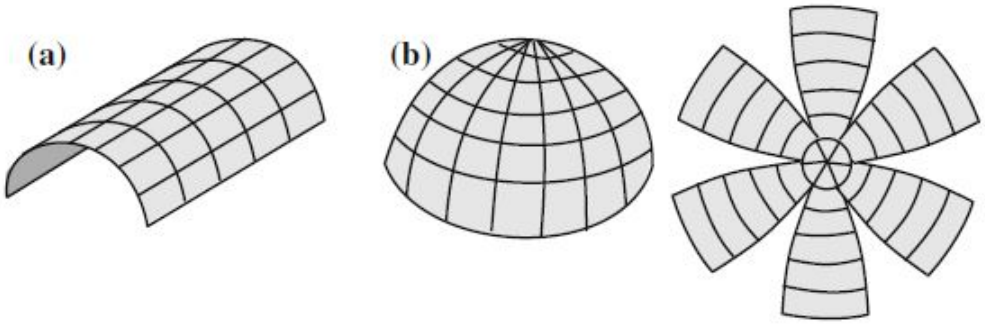

Figure 2-2: Examples of developable and undevelopable surfaces [2]

Developable surfaces can be deformed and developed to obtain a plane surface, without any cutting or stretching. Cylindrical roofs as shown in figure 2-2a are an example of this type of surface. We can imagine that the roof can be easily deformed to obtain a plane. All monoclastic shells are developable surfaces.

Undevelopable surfaces (figure 2-2b), unlike their developable counterparts, cannot be deformed into their plane forms without alterations, which were mentioned before. All synclastic and anticlastic surfaces fall in this category. They have significant advantage over comparable developable surfaces in having more strength and stability. This stems from the fact that more external energy is required to cause any kind of deformation [2].

2-1-3 Generation of surfaces

Surfaces described above can be created using geometric or non-geometric techniques. The former uses mathematical functions while the latter uses natural processes like form-finding.

1. **Geometrical Surface generation**

   They include surfaces of revolution, surfaces of translation, ruled surfaces and free-form surfaces as shown in figure 2-3. Surface of revolutions are created by rotating a *meridional curve* about the an *axis of revolution*. Translational surface requires sliding of a constantly oriented *generator* curve over a *directrix* curve. Constructing ruled surface requires another method, where we slide two ends of a straight line on their own curve while keeping them parallel to an arbitrary direction or plane. Lastly, free-form surfaces can be generated using NURBS (Non-Uniform Rational B-Spline). They are different from the other geometrical methods as they cannot be described by fixed equations but can be used to make any possible shape.

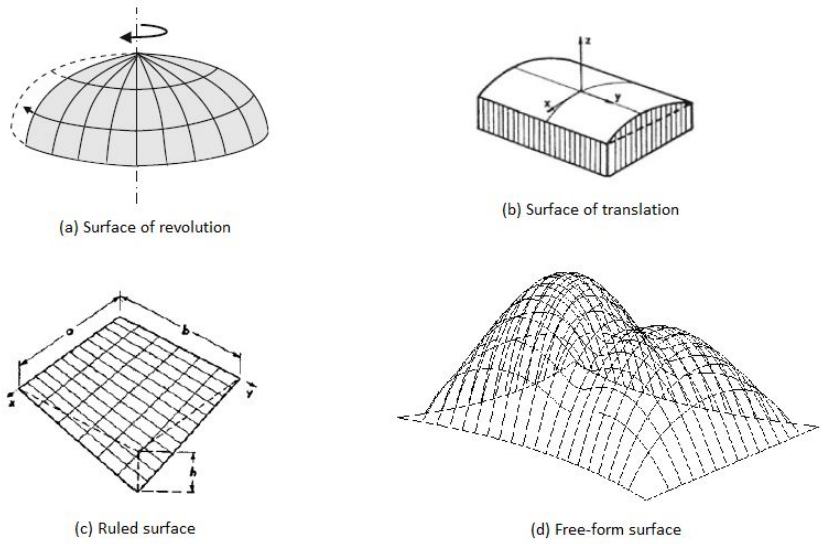

Figure 2-3: Examples of geometrically generated surfaces

2. **Non-Geometrical Surface generation**

   There are several physical and computational methods of form finding. They involve finding a shape which is at equilibrium with the forces that act upon it. Here we study the hanging model analysis which is the most native form physical form-finding. This method is extremely useful to obtain shapes for thin shells. Generally cloths or chain nets can be used for this analysis. These materials cannot absorb bending moments, so when they hang it is safe to assume they experience only tension due gravity. Keeping this in mind we can create hanging models as shown in figure 2-4. This shape represents the equilibrium shape of the cloth at that particular moment. If we were to freeze the model and invert it, logic dictates that the entire cloth is in compression. For a structural designer this is a very important aspect as the cloth acts like a membrane

which, as discussed earlier, is very structurally efficient. Although, it should be known that presence of other dominant loads can cause problems.

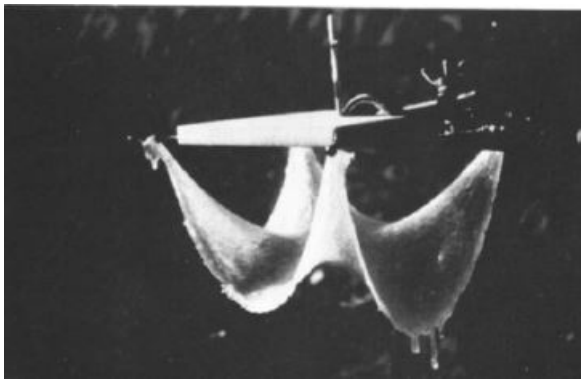

Figure 2-4: Example of a hanging model using cloth [3]

2-2 Structural behaviour of Shells

A good knowledge of the structural behaviour of shells is imperative for good shell design. It can vary hugely depending of kind of loads the shell is expected to carry. Shells are form-based structures where the shape influences the shell's load carrying capacity. This structural geometry largely dictates the development of stresses in the shell elements. This has to kept in mind to avoid unwanted deformations and structural failure.

2-2-1 Membrane behaviour

Membrane theory attributes to the membrane-like behaviour of shells, which enables it to carry out-of-plane loads. They transfer these loads by generating in-plane membrane forces, a fact that separates them from plates. Shells, unlike membranes, stretch and contract without producing significant bending or changes in local curvature[10]. Ideally a designer would prefer to design the shell only for membrane forces, as this enables the shell to be thin and hence be more economic.

This is not possible always due to presence of unfavorable loading and boundary conditions. These conditions are shown in figure 2-5. In such cases the membrane stress are not enough to reach a state of equilibrium giving rise to disturbed regions with additional stresses. Thus a bending theory is required for a complete analysis of the shell [2].

2-2-2 Bending behaviour

The bending behaviour of shell is very interesting. It only occurs at parts of the shell where the membrane stresses are insufficient to carry the applied loads. The bending moments developed in these regions only compensate for the inadequacy of membrane behaviour and do not carry any load [12]. In figure 2-5 we can see, the presence of concentrated forces or geometry changes creates a disturbed region with bending moments. But these moments are

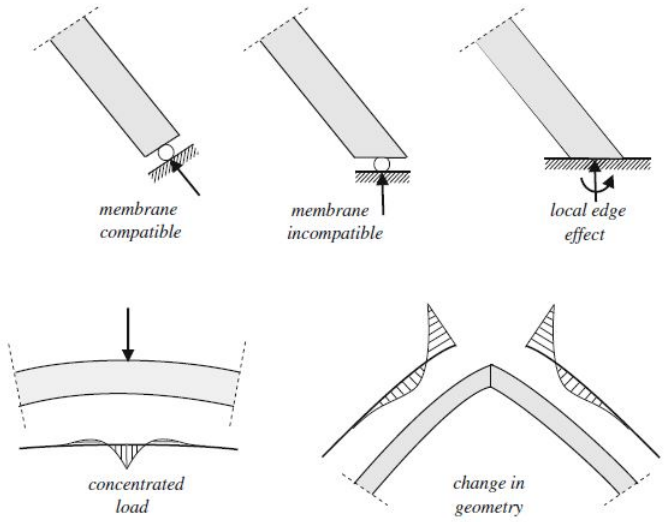

Figure 2-5: Conditions for membrane and bending theory [2]

confined to small region around the point of disturbance defined by its 'influence length' (l_i). This means the rest of the shell will still possesses a true membrane field. The influence length for a spherical done is shown in figure 2-6.

This behaviour of shells is a boon to designers as it highlights the structural efficiency of shells. In a practical sense, this enables the designers to design a relatively thin shell, even in the presence of membrane incompatible conditions. Special optimizations or other structural solutions can be found to tackle these conditions, while expecting large parts of the shell to still behave like a true membrane.

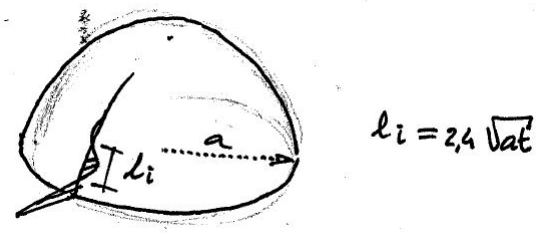

Figure 2-6: Influence length of edge in for a spherical dome [1]

2-3 Structural Failure of Shells

It is important to know a structure might fail, because this knowledge helps the designer to design the structure accordingly. In this project, the aim is to design a thin shell which motivates us to study the various modes of shell failure. Shells can fail due to increasing deformations, failure of material or a combination of both (Figure 2-7). The former is called 'buckling instability' while the latter is referred to as 'strength failure' [4].

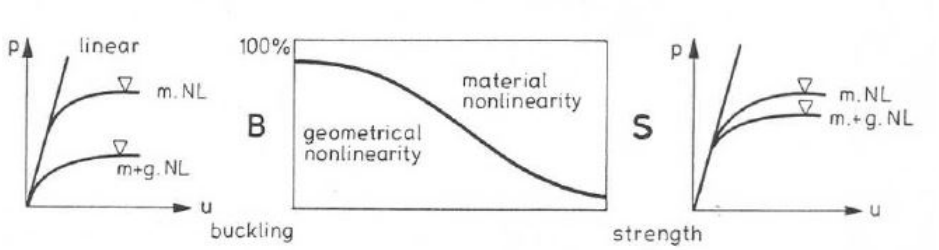

Figure 2-7: Structural failure modes for shells [4]

2-3-1 Strength Failure

Strength failure occur as a result of deterioration of material properties and are characterized by lower deformations. Tensile forces can cause the concrete to crack, or it might undergo compressive crushing which ,in turn, will reduce the strength of concrete. In most cases of thin shells the stresses are not too high, hence this type of failure does not govern design, although this can lead to buckling failure[12]. Usage of high strength concrete further decreases the possibility of this type of failure.

2-3-2 Buckling Instability

Shells, for the most part, are expected to carry in-plane compressive forces. Initial imperfections in geometry can give rise to eccentricity of these forces, which threaten the stability of the structure. Usually one or more structural components can fail, at a lower stress than the design ultimate compressive value of the failing concrete member. Following this the structure undergoes a drastic loss in load carrying capacity finally leading to collapse. Nonlinearities in materials further adds to this phenomenon. There are some more important points associated with shell buckling which are discussed below.

1. **Snap-back behaviour**

   This type of behaviour is typically seen in shell structures. When the shell is loaded it starts following a path of equilibrium. This part is shown by the linear line in figure 2-8. This path is followed till the bifurcation point is reached, after which the shell experiences sudden loss in its load carrying capacity. This is shown in figure 2-8 as the curved line which represents snap-back. This behaviour is dramatic and catastrophic, as it happens suddenly and quickly without any warning.

   This curve represents the post buckling behaviour of the structure. The transition between the two paths of equilibrium can be smooth or sudden depending on the geometry of the shell. This phenomenon is further intensified with the presence of imperfections, hence the dotted line in figure 2-8 is a closer assumption of the path of equilibrium a shell will follow in real life.

2. **Imperfection Sensitivity**

   Imperfection sensitivity of shells was first established when scientists found discrepancies, between the calculated critical load and the actual load that a shell could carry.

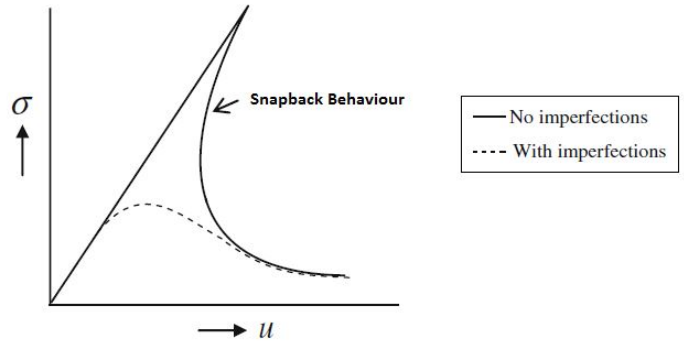

Figure 2-8: Stress-Deflection curve showing snapback behaviour of a shell [2]

Experiments were performed on axially loaded cylinders resulting in failure, much before reaching the critical load. Eventually it was realized that these cylinders were extremely sensitive to even a minute imperfection, which would otherwise be hidden from the naked eye. The effect of imperfections was first quantified by Professor Koiter during the second world war.

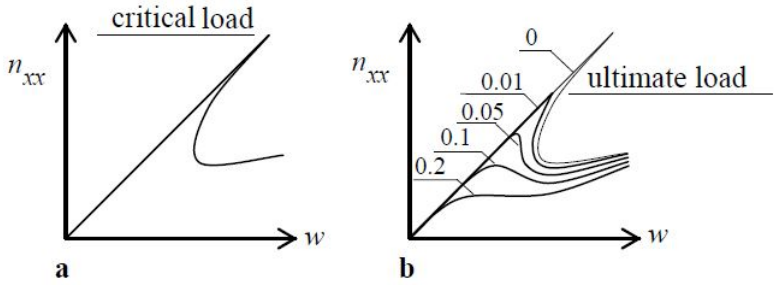

Figure 2-9: Buckling of cylinders over different imperfection amplitudes [5]

Figure 2-9 shows us how increasing imperfection amplitudes can drastically reduce the load carrying capacity of the cylindrical shell. Although, not all shell are so sensitive to imperfections.

3. **Compound Buckling**

Thin shells are specially sensitive to imperfections due to the occurrence of 'compound' or 'multi-mode' buckling. This happens due to interactions between the different buckling modes as all of them are associated with the same linear critical buckling load. Thin shells exhibit membrane dominant behaviour, hence have closely related buckling modes. This is due to the absence of shorter influence lengths of bending regions [12]. As a result, thin shells are more susceptible to compound buckling than thick shells. Consequently, this is a major reason for snap back behaviour in thin shells.

Type of Shell	Type of Loading	Imperfection Sensitivity
Open Cylinders	Radial	No
Open Cylinders	Axial	Yes
Open Cylinders	Torsion	No
Hyperboloid	Axial	Yes
Closed Cylinders	Uniform	Yes
Spheres	Uniform	Yes
Domes	Uniform	Yes
Hypars	Uniform	No

Table 2-1: Imperfection sensitivity of some elementary shells [1]

item **Knock down factor**

It was discussed earlier how experiments showed a large difference between the theoretical and actual critical load. This posed significant problems to shell designers as the various factors (a few discussed above) could not be separately incorporated in design. A solution to this problem was found by applying a factor, which accounted for all the factors causing snap back behaviour. This factor is called 'Knock down' factor.

The knock down factor for a particular design is the sum of the individual factors, for each negative effect on the load carrying capacity of the shell. These effects are shown for a spherical dome in figure 2-10. For this project the value of knock down factor (C) is chosen as $\frac{1}{6}$, as is the norm in the absence of a stipulated value.

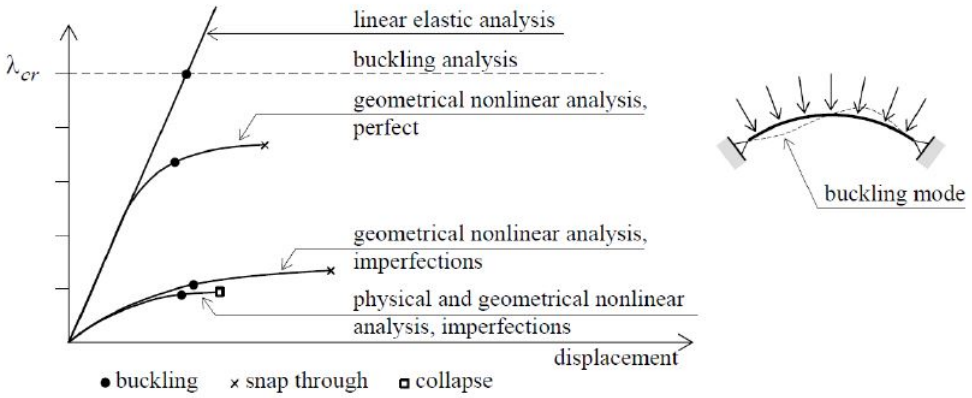

Figure 2-10: Negative effects causing fall-back in load carrying capacity [6]

2-4 Prominent Shell Designers

2-4-1 Pier Luigi Nervi

Born in 1891, Mr. Nervi graduated from the faculty of Civil Engineering, University of Bologna in 1913. In 1923 he started his own company, himself filling the role of a designer and contractor. Mr. Nervi believed that reinforced concrete is the most beautiful constructive system that mankind ever found[8]. He also created a shell specific version of concrete called 'Ferrocement' in the latter years of his life.

Mr. Nervi has an impressive list of iconic buildings in Italy. At that time in Italy important civil projects were given to contractors based on the proposals they put forward. They were invited to submit their ideas for the project which was awarded to the best overall design. This is where Mr. Nervi was particularly famous for submitting proposals which were beautiful, efficient and cheap to construct. His structures were magnificent fusions of science and art. The competition he won in 1930, for the designing the stadium in Florence, is a good example of his legacy.

Mr. Nervi is also known for his extensive model testing techniques. He always believed that the value of intuition is indispensable for an engineering as it leads to innovation. His design for the 1935 Italian Air Force competition is a testament to this fact [13]. Due to lack of theoretical knowledge and calculation instruments, he created an experimental celluloid model to understand stresses in the structure more carefully. He improved the model for the second design to incorporate ribs and stiffeners. He used prefabricated elements in this design, something which had not been done before.

2-4-2 Nicolas Esquillan

Mr. Esquillan, born in 1902 in France, was another pioneer in the field of shell structures. He was an active member of IASS (International Association of Shell and Spatial Structures) and contributed significantly to the development of lightweight spatial structures [7]. Most notable projects include several record breaking long span bridges, followed by the majestic CNIT completed in 1958, which remains the longest span shell structure till date. The details of this project will be studied and discussed in following sections.

2-4-3 Heinz Isler

Mr Isler was a swiss civil engineer well known for thin concrete shell design. He did not deal with long spanning shell structures. Most of his projects had a span of 40-60 m, like the Burgi Garden Center and the SICLI Company building. Nonetheless, his work in the field of shape and form finding was unprecedented during that time. One of his notable contributions was in the first congress of IASS in 1959, where he introduced the ideas of "the freely shaped hill, the membrane under pressure and hanging cloth reversed" in his presentation "New Shapes for Shells"[14]. It is also important to bring forward Isler's views on shell structures at that time. He was specially curious about shells and shapes which occurred in natural form in

the environment. These included simple objects like egg shells, onion peels and nuts to more complex shells obtanied from clams, oysters, etc. He believed that these natural forms, are the most efficient forms of shells and perceived them as "stiffened shells, double-curved shells, rotation shells and several other variations".

2-5 Existing similar shell structures

2-5-1 CNIT, Paris

The 'Centres National des Industries et des Techniques', also known as CNIT, is the longest spanning concrete shell structure standing till date. It has a triangular plan with each face spanning 218m. Another notable feature of the structure is that it is made up of double shell in concrete. The most remarkable fact of this project was the how it was able to gather the leading structural engineers of that time [7].

The CNIT was decided to be built to create an exhibition building to display of French machines on an international level. The clients required the design to provide maximum area, for display of heavy machinery on the ground floor and lighter machines on the upper floors. Nervi, Esquillan and other leading engineers namely Mr. B. Laffaille and Mr. J. Prouve submitted designs for this project. Towards the end Nervi's and Esquillan's proposals were the front runners. Subsequently, ideas with metallic solutions and cables were discarded resulting in approval of Esquillan's proposal.

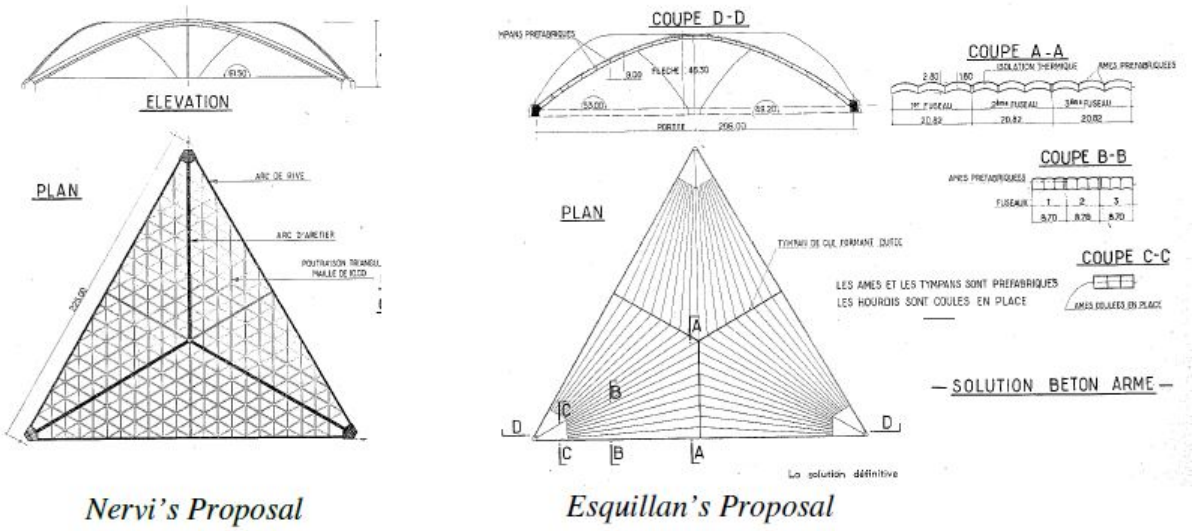

Figure 2-11: Main proposals for CNIT design [7]

Now we look into the proposal that was submitted by Esquillan, to understand how he deals with structural problems in that design. He decided to use a honeycomb structure and incorporated it form a double skinned shell structure [15]. This was ingenious way to counteract buckling without adding additional material weight to the structure. Additionally, the panels

used in the roof construction, have local curvature introduced in design to prevent local buckling as well. The plan from figure 2-11 containing Esquillan's proposal shows the varying cross sections across the roof. This is done to compensate for reduced material near the supports making it structurally sound.

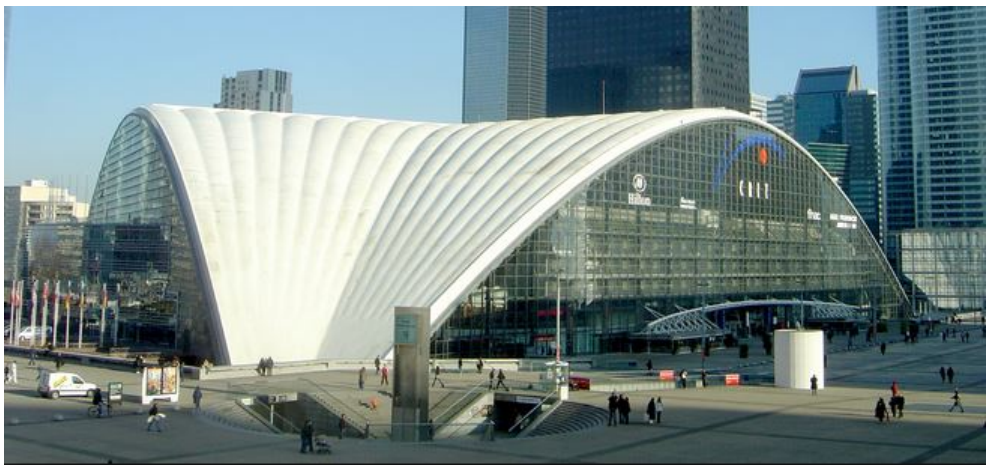

Figure 2-12: CNIT as it stands today

Today it is one of the few iconic structures which combine structural efficiency with beauty and validity.

2-5-2 Palazzo dello Sport (Sports Palace), Rome

This structure was designed and constructed by Pier Luigi Nervi and Marcello Piacentini for the 1960 Rome Olympics. Every detail in this structure has been carefully designed to create a perfect union of architecture and engineering. The main dome spans approximately 100 m and houses 16,000 spectators [16]. It is made up of radial prefabricated units which are joined to form 'V' sections as shown in the figure 2-13. The upper slab has a thickness of 9 cm only.

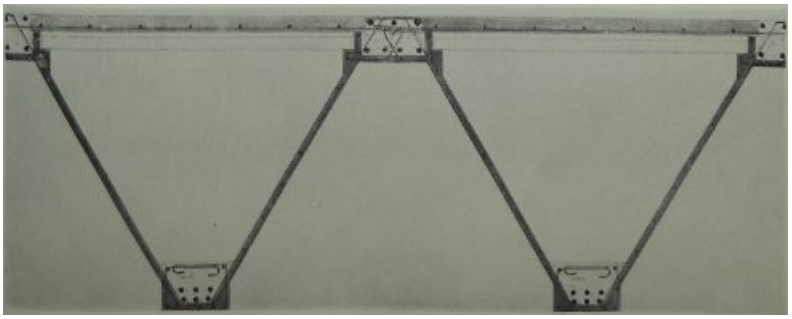

Figure 2-13: Section of prefabricated roof units [8]

The efficiency of the structure is evident in every detail. Figure 2-14 shows the structural fans and the underlying pilasters which transfer load from the dome to the foundation. The

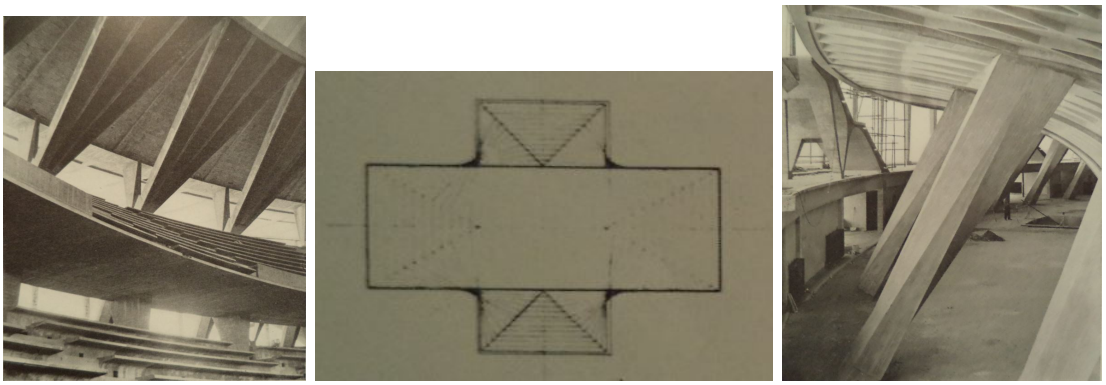

Figure 2-14: Structural fans, section and on-site view of pilasters supporting the dome[8]

structural fans have been specially designed with ribs to counter buckling. The important aspect about these fans are that they allow natural light to flood the arena. In the same figure we can notice the warped surfaces of the pilasters, which have been provided to facilitate conversion of radial to longitudinal load transfer. These two examples provide enough evidence of how different elements of the structure perform multiple functions. This fact is key to Nervi's philosophy of combining knowledge with imagination [8].

Figure 2-15 shows the dome of the structure from a distance. Closeup pictures are difficult to find since the dome remains hidden by the glass facade surrounding the structure.

Figure 2-15: Dome of Palazzo dello Sport

2-6 Current Major Basketball stadiums

Currently there are a few state of the art basketball stadiums in the United States which have roughly the same capacity as ours. This exercise is carried to find any special requirements specific to basketball arenas. The two major stadiums studied for this thesis have been mentioned below:

1. Amway Center, Orlando, USA with a capacity of 20,000[17].
2. Bradley Center, Wisconsin, USA with a capacity of 19,000[18].

We find out that for a basketball arena of our size we need to provide a central video screen. This is almost mandatory and present in all major stadiums in the USA. This adds a special load to the design of our roof. Also studying them from an architectural point of view gives us an idea of the arrangement of spectators, rings and video screen displays. This is expected to influence the shape and size of the roof which is important for geometry based shell structures.

2-7 Evolution of the Concrete shell industry

As a designer it is easy to overlook the arising complexities of construction. Usually it has less of a significance but these complications caused major problems for shell structures. In fact this was the main reason for the sharp decline in their construction after a promising start in the 1950s [19]. Lack of advanced methods led to use of conventional form-work being used for shell construction, which is costly and more prone to errors. But this started changing in the last two decades. This rise is mainly owing to the development of new innovative construction techniques coupled with new softwares which enable digital modelling and analysis.

At present there are numerous creative methods available for shell construction like balloon or inflatable formworks and vacuumatics which enable creation of smooth curved surface[20]. The designer also has the option of dividing the shell into smaller prefabricated elements which are manufactured and transported to site for assembly. This method was adopted by Nervi in many of his constructions[13]. Ribs and stiffeners can be added during connection of individual slabs which makes this method particularly useful.

2-8 Finite Element Analysis

Increase in computational power in the recent years has fueled the use of finite element analysis (FEA) for structural design. Complex calculations which could not be done before can now be easily performed, using one of many finite element method (FEM) softwares available to us now. Shell design has particularly benefited from this rise, as designers are now able to model and analyze complex shell geometries with numerical solutions to most complicated stress problems. While this is highly advantageous, we should keep in mind that errors with modelling and other input parameters can yield inaccurate results. This highlights

the importance of designer's knowledge to ensure proper modelling. In general FEA requires a designer to follow three primary steps which are discussed below[21].

1. **Preprocessing**

   This step includes construction of a digital model of the structure. Presently, all major FEM softwares allow importing of an initial geometry in the form of CAD files. These softwares can read this initial geometry to create a mesh of the structure, using elements and nodes. The main idea behind this step is to discretize the structure into subregions and points, for easier calculation.

   There are three types of elements available for shell modelling. Flat elements, elements based on the Sanders-Koiter equations and elements based on reduction of solid elements. Examples for each are shown in figure 2-16 (a),(b) and (c) respectively.

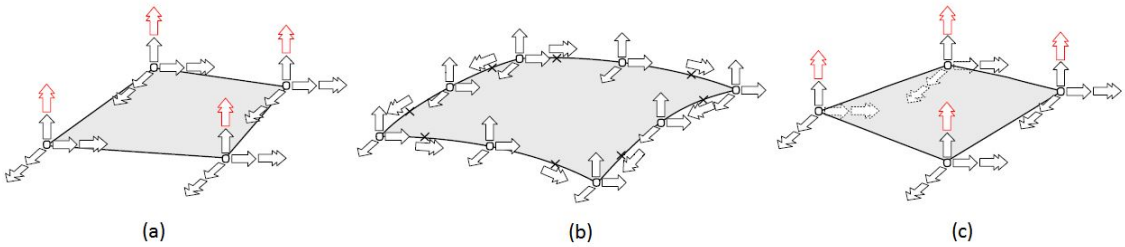

Figure 2-16: Degrees of freedom of different types of shell elements [1]

2. **Analysis**

   The meshed model created in preprocessing is used as input to the finite element code which creates and solves a system of equations based on the type of analysis chosen [21].

$$K_{ij}.u_j = f_i \tag{2-1}$$

   In this equation 'u' and 'f' refer to the nodal displacements and externally applied forces respectively. 'K' is the stiffness matrix which depends on the formulation of our structural problem. The system of equations can be linear or nonlinear.

3. **Postprocessing**

   Reading the results of the analysis can be a tedious process. Earlier this was a bit tricky due the absence of graphical representations. But in the present time we have several viewing options which can help a designer to easily find crucial stress areas or trends. A postprocessor uses superimposed colored contours to display levels of stresses, forces, displacements and other parameters. Often softwares have the option to average the computational results in the nodes to obtain smoother plots. This removes any real jumps in stresses in the presence of shell elements of different thickness.

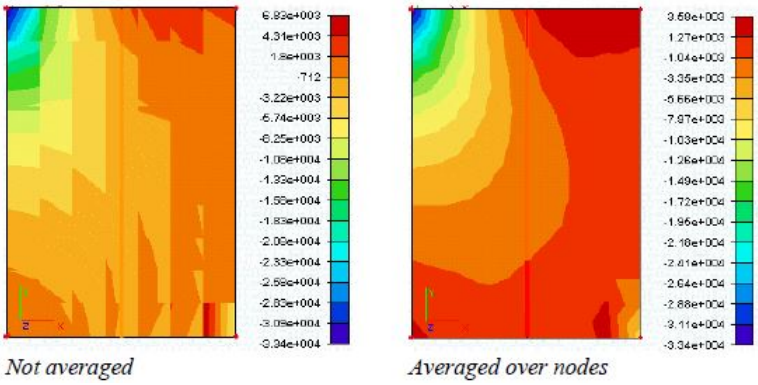

Figure 2-17: Example of nodal averaging of contour plots [1]

2-9 Nonlinear Analysis

We can perform a nonlinear analysis on our structure by applying the load in steps. Each step is iteratively checked for convergence, of the internal and external forces. Schematic details of this process are shown in figure 2-18. A good knowledge of the working of nonlinear finite element analysis is required by the designer. Most softwares offer more than one way to incorporate nonlinear properties in the structural model using different kinds of material models and settings. Application of these settings varies based on a wide range of factors, depending on what behaviour we are studying. To have a better understanding of nonlinear computational mechanics Professor Sluys handbook[22] is studied.

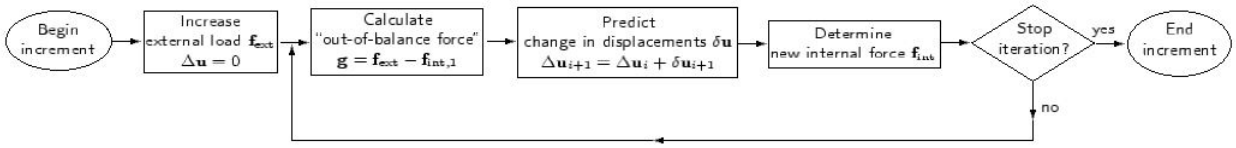

Figure 2-18: Scheme of an Incremental-Iterative Procedure

We have studied the structural failure of shells in the previous sections, which suggest that accounting for nonlinear behaviour intensifies failure of shell. Therefore a nonlinear study provides a more realistic behaviour of our structure [12]. Exceedingly large displacements and rotations, including imperfections, are incorporated in geometrical nonlinear analysis (GNLA). Whereas the physical properties of concrete like plasticity, creep, shrinkage, etc. are included in a physical nonlinear process (PNLA).

Chapter 3

Pre-Design Considerations

One has to deal with a lot of aspects before starting the actual design process. They can include anything, from client requirements to ensuring structural integrity and adequate functionality. Usually a designer has lot of options to deal with these requirements. Therefore it is important to list the major requirements to create a more specific design. These conditions can be imagined as design constraints. Only within these constraints does the designer have free will. Study of previous designs, related to shells and basketball arenas, helps in defining some requirements for the roof.

3-1 Capapcity of the Arena

The first design requirement is the size of the roof, which depends on the amount of people the arena is expected to hold. The arena for this project needs to house 20,000 spectators. Exact calculations are done further on in this project, but at the moment it can be intuitively said this shell will have a large span, i.e. in excess of 100 meters. A large shell is particularly harder to design since it is more susceptible to buckling failure. Thin shells are very sensitive to imperfections and buckle really easily, even before the buckling load is reached. These imperfections make large span shells even more vulnerable to buckling, something which the designer needs to pay special attention to.

3-2 Centrehung Display

The primary requirement in every basketball arena is that of a âĂŸcentrehungâĂŹ display. This is a common and essential feature in all the major arenas across the world. The arena being designed in this project is large enough to require a mounted display on the roof, which is more efficient than providing closed-circuit television receivers among the seats [19].

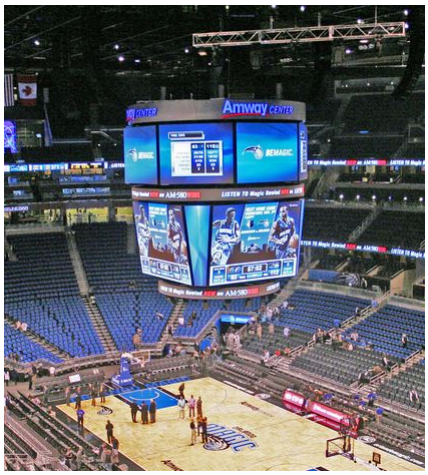

Figure 3-1: Centrehung display at the New Amway Centre

The weight of the display needs to be determined to calculate the magnitude of concentrated force, the roof needs to be designed for. This kind of a centre-hung display is usually made to order for special arenas, hence exact specifications can only be gauged through existing examples.

For this reason the display at the Amway Centre arena, USA is chosen. This arena has a capacity of around 19,000 spectators and is a close approximation considering the size of our arena. The centre-hung display in the Amway Centre, provided by American audio and visual company Daktronics, is arguably one of the most advanced of its kind [17]. It has two rows of four sided LED displays which collectively weigh 40 tons. This weight can imagined as a concentrated force on the shell roof.

3-3 Choice of construction material

These days several high performance concrete types are available. This development has enabled designers to building thinner shells due to their advanced properties. As a result Ultra High Performance Concrete (UHPC) is chosen as the final construction material. There are several reasons for doing so which are noted below [23]-

- UHPC is the latest advancement in concrete technology with improved homogeneity, packing density, micro structure and ductility, hence are specially suited to special structures.
- It has steel fibers as reinforcement, which contribute to material toughness and ability to withstand concentrated forces. The presence of the centre-hung display makes the choice of this material ideal.
- UHPC has improved durability properties with increased resistance to transport of harmful materials within the pores.

- One of the objectives of this thesis is to design the shell in a way which facilitates efficient construction. The designer has an option to use prefabricated panels for this purpose. UHPC is specially suited to this kind of construction as it needs state-of-the-art production facilities from where it has to be transported to the construction site.

3-4 Choice of construction method

Concrete shell construction was extremely popular in the 50s and 60s but there was a marked decline in their construction thereafter. This occurred due to the expensive nature of concrete shell construction. The form-work required would cost a lot since conventional scaffolding techniques were used. But now the invention of advanced methods has led to a more efficient construction techniques for shells.

Nevertheless, it is decided to construct the shell using prefabricated roof elements. This step could solve a lot of construction problems. The shell can be divided into smaller plate or shell elements which can be prefabricated and transported to the construction site. At the site the elements need to be hauled into position connected to each other. Although this adds to extra transportation costs but it is preferred since it reduces the probability of errors during construction. Some benefits of dividing the shell into smaller elements are mentioned below:

- This allows us to use prefabricated elements for the shell construction. This is a relatively easier construction method where the elements can be hauled into place and connected by pouring concrete.
- This approach also enables us to provide ribs and stiffeners easily as they can be formed while making connection between the various roof elements. This will depend on the geometry of elements used.
- We chose UHPC as the desired construction material which can only be produced in specialist manufacturing facilities [23]. This rules out in-situ pouring of UHPC due to financial considerations. Prefabrication of elements at the UHPC facility and then transportation to the construction site is the most viable option. This aligns perfectly with the decision to divide the shell.
- Lastly the prefabricated elements are produced off-site under careful observation which reduces the probability of geometrical errors that would usually occur on-site. This leads to lesser imperfections in the final shell.

Chapter 4

Design Process Outline

The outline of the design process is formulated in this section, and has been shown in the previous page. Some of the boxes are color coded to highlight the influence of the aforementioned objectives, on the design procedure. The key to the color code is explained below.

- Orange: In this part of the procedure the roof's aesthetics are established. Once the shape is established, the overall model of the stadium is created. This helps in perception of the roof as a part of the complete structural system.
- Green: In this part of the procedure the structural efficiency of the roof is improved. The shell is designed to be as thin as possible. This is achieved by choosing the preferable failure mode as buckling, the reason for which is explained in further sections. Also the panel cross sections are established using the concept of effective material distribution.
- Red: Panels and connections as described for the chosen design. They are designed in such a way that the panels need to be just hauled and fixed in their appropriate positions. The merits of this construction method have already been discussed in pre-design considerations.

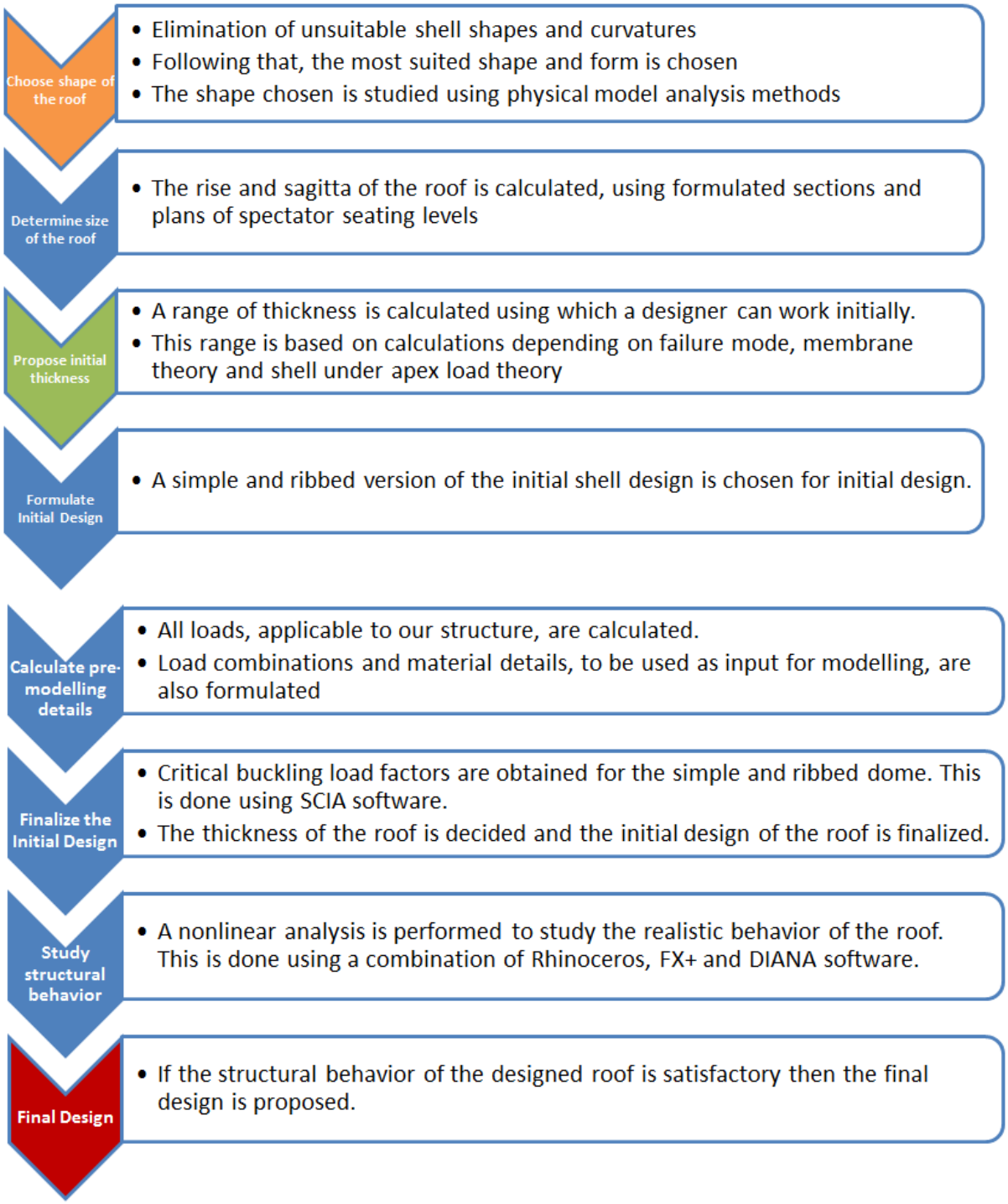

Figure 4-1: Overview of the followed design process

Chapter 5

Shape of the Roof

There are a lot of shapes that can be chosen for the arena. It is ultimately going to influence the entire design process as shells are shape based structures. The type of geometry influences the way they transfer load. The roof for this project, having a large span, needs to carry its own self-weight and natural loads, along with a concentrated force attributing to the video display. It has been studied that this type of loading is membrane incompatible, and can give rise to bending regions. It becomes necessary to choose a shell geometry which would not aggravate these regions. This choice is governed mostly by a combination of intuition and knowledge of load transfer mechanisms in shell structures.

5-1 Elimination of possible shapes

It is decided to eliminate some elementary shell types to aid with choice of the final shape. There are three different types of gaussian curvatures which give rise to synclastic, anticlastic and monoclastic shells. All these shells can be easily designed to be stable under their own weight. Therefore the behaviour of these shells under a point load is investigated, to pass a judgment on their suitability for this design.

Anticlastic shells, e.g. hypars, are point not suited to carry concentrated apex loads. The yellow arrows in figure 5-1 (a) show the flow of load along the middle line (red) in case of self weight only. If we add a concentrated load on this shell it will add to instability along the middle line and intensify buckling. Furthermore the presence of free edges are not advisable, as they develop additional moments (figure 5-2) which will increase instability.

Monoclastic roofs face a similar problem of additional bending moments at the free edges. In figure 5-1 (b) the cylindrical roof under a point load can be seen. It can be imagined that the concentrated load is resisted due to geometrical interlocking in one direction, as shown by the yellow arrows. Yet this system would be unsupported in the other directions, making it highly susceptible to failure.

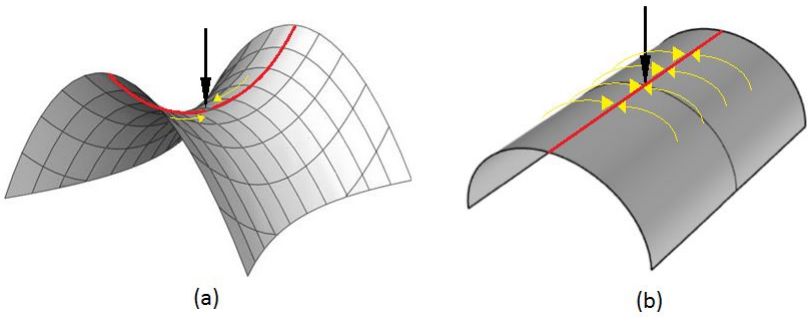

Figure 5-1: Behaviour of anticlastic and monoclastic shell under point load

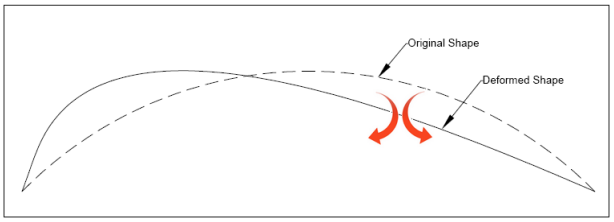

Figure 5-2: Possible bending moments and deformation at edge

5-2 Initial Decision on shape

After elimination of the rest, a look at synclastic shells is taken. Figure 5-3 shows their efficiency over anticlastic and monoclastic shells. This arrangement provides good stability to the entire structure due to geometrical interlocking of shell elements under the point load. This is shown using yellow arrows. Visualize how the shell would resist deformation due to this interlocking. Unlike in a cylindrical shell this resistance is offered from all directions.

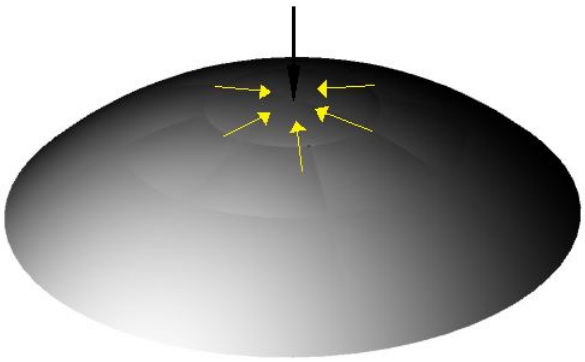

Figure 5-3: Behaviour of spherical dome under point load

In the end it is evident that for this project and shell roof with positive gaussian curvature will be the best option. To this effect we choose a spherical shell as the shape of our roof. As discussed earlier, a spherical shell will require most external energy (i.e. a larger concentrated

load) to undergo the same deformation as an equivalent cylindrical shell or hypar.

5-3 Hanging Model Analysis

The best possible shape for the roof has now been chosen. Logically the next step would be to determine the dimensions of the roof. But it is done, the final geometry of the roof needs to be physically study. Physical model analysis is a useful way to find any weak design spots as one can study the cracking patterns on the models. This analysis is a common practice amongst shell constructors. The structural integrity of shells was purely based on intuition in the earlier days of shell construction. Even though now this has been replaced by the rapidly growing finite element technology, it is still advisable to perform a physical model analysis to obtain valuable insight into how a shell structure might fail. This analysis is imperative to obtain an initial design.

Figure 5-4: Supporting framework for the hanging model

The framework for the hanging model was set up as shown in figure 5-4 (a). The circular ring of cardboard, which supports the model, is adjusted to be horizontal. Pins are punched in this ring in a radially equidistant manner to support the model in a uniform way. Two different types of cloth exhibiting separate characteristics are used. One exhibits orthotropic properties which can resemble the behaviour of wood for example. The other is an isotropic cloth which shows same properties in all direction. It can be assumed that this material can mimic fiber reinforced concrete. A mixture having equal parts of gypsum and water, is used to stiffen the hanging cloth as can be seen in figure 5-4 (b).

It is extremely difficult to form a dome shape using cloth without a small degree of incisions, stretching or folding of the cloth. This modification ruins the properties of the cloth nullifying its ability to carry load, which can be confirmed looking at the failed structure in figure 5-5 (a). To work around this problem it is decided to cut out portions of the cloth to imitate an arrangement of a dome resting on 'structural fans'. This portions are areas in tension which fold upwards and have been marked in figure 5-5 (b).

Once the gypsum dries, the model is turn upside down, left to rest in that position for a day and studied thereafter. Figure 5-6 the behaviour of the orthotropic cloth as it clearly

fails. Tensile cracks develop where the dome is connected to the fans. This was expected as the cloth is strong only in two directions. An orthotropic material would be more suited to, for example, a cylindrical shell. On the other hand, we can see in figure 5-7 that the model made out of isotropic cloth still stands. This means that material isotropy is essential for the structural integrity of our structure. The geometry of a spherical shell is such that uniformity of material strength in all directions is imperative as it makes deformation of the shell more difficult. This strengthens the choice of UHPC as the construction material for this project.

Figure 5-5: Modifications of cloth used in analysis

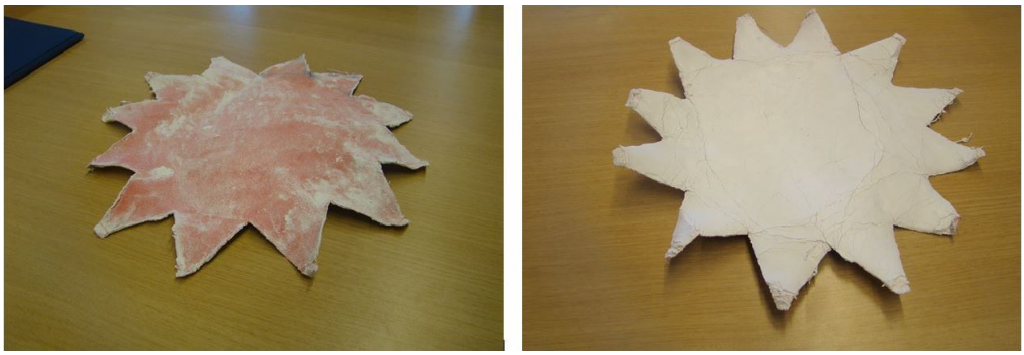

Figure 5-6: Model made out of orthotropic cloth

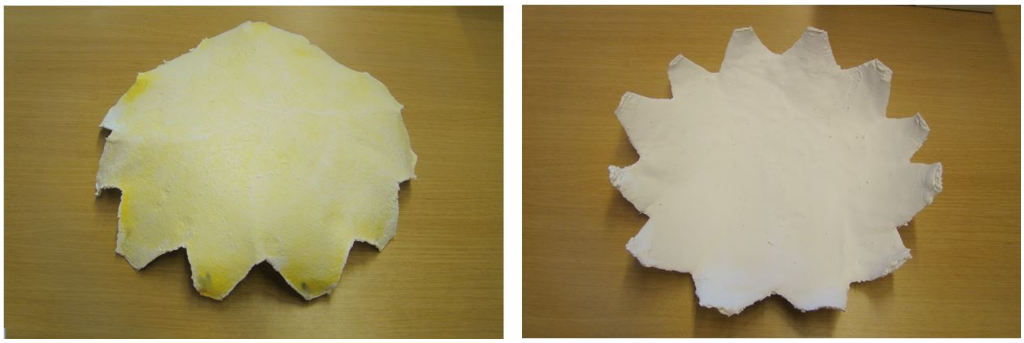

Figure 5-7: Model made out of isotropic cloth

5-4 Propose arena design based on shell shape

The shell roof in itself can be considered as a beautiful structure, but it can be visually represented in a much better way. The idea behind this step is to portray the aesthetics of the shell, by providing the reader with a complete picture of the stadium. This is achieved by creating a computational model of the roof, along with the rest of the arena.

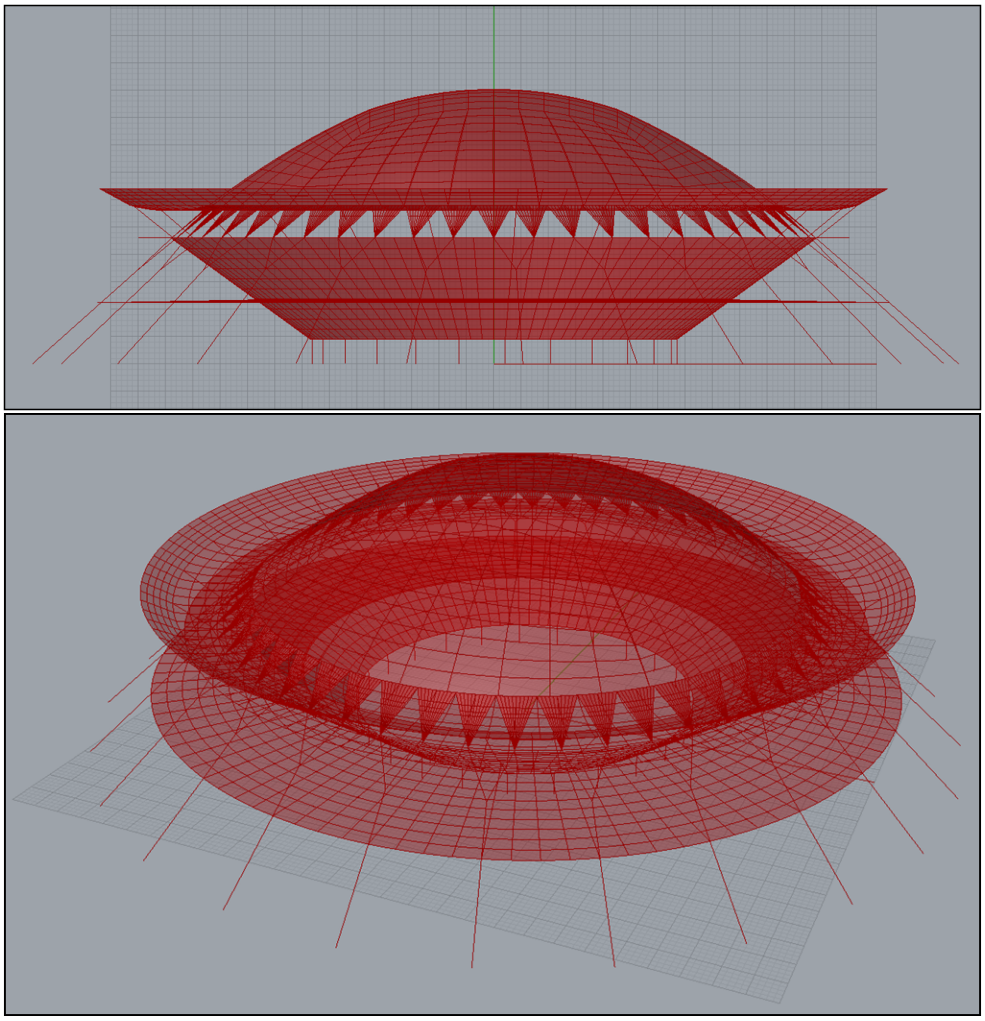

Figure 5-8: Proposed design for the entire basketball arena

Rhinoceros is the software used for modelling the arena. It offers a special plug-in called 'Grasshopper', which helps the designer create models which are flexible to changes. Figure 5-8 depicts the complete model of the proposed stadium, which tries to incorporate a modern aesthetic sense in conventional structural design. 'Y-shaped' columns are provided to improve the rotational stability of the roof. These columns are provided with the same inclination as the edge of the shell, to facilitate a smoother load transfer to the ground. An additional overhanging shell is provided as the continuation of the roof. The purpose of this roof is to cover the additional areas of the arena. This space is provided for amenities, shops and other recreational services.

Chapter 6

Dimensioning of the Roof

After making a decision on the shape the next step is to dimension the roof. In this section the span and sagitta of the roof will be defined. These two parameters are very important for shell design as ultimately they govern it's structural behaviour.

6-1 Span of the roof

The span is based on the amount of people the arena is expected to hold. The cross section of the seating arrangement is designed first, and based on that a the plan of the arena is formulated. This gives a better representation of the structure, which is used to determine a favorable value for span. This process in done in steps and is explained in the following paragraph.

1. **Basketball court dimensions**

   The plan of the basketball court need to be defined first. This needs to be done as a prerequisite, for the analysis which we will perform next, which requires a point of focus for the spectators. The outermost line of the finalized court plan will be chosen as the point of focus.

   Several regulations are available for court dimensioning. The National Football Association (NBA) of USA and the International Basketball Federation (FIBA) are the two main organizations which stipulate rules which govern the layout of the court. These values can be checked on their official websites. For this project it is decided to use the design guidelines provided by Neufert in the widely used book 'Architects' Data' [9]. The exact dimensions are shown in figure 6-1.

2. **Formulation of cross-section for seating levels**

   The court dimensions have now been established. Using the outer edge of the court as focal point the seating sections are designed. This is done by performing a sightline analysis. This concept assigns âĂŸC-valuesâĂŹ to spectator rows depending on the

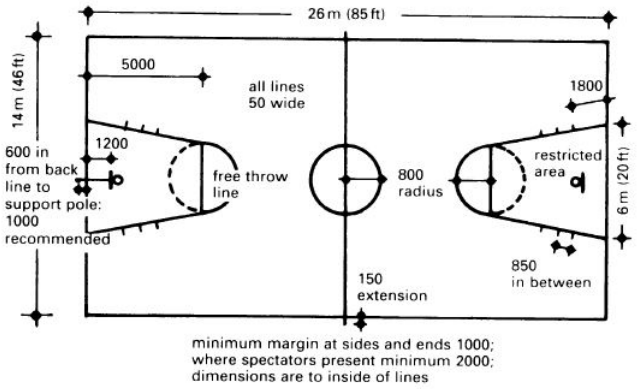

Figure 6-1: Court Dimensions adopted for our design [9]

distance and height from the point of focus [24]. Detailed explanation and calculations for this analysis can be viewed in appendix A. The seating arrangement is designed for different C-values for separate tiers of seats namely bottom, middle and top tier. The final arrangement can be seem in figure 5-7 while a 3D cross section is shown in figure 6-6 for better visual representation.

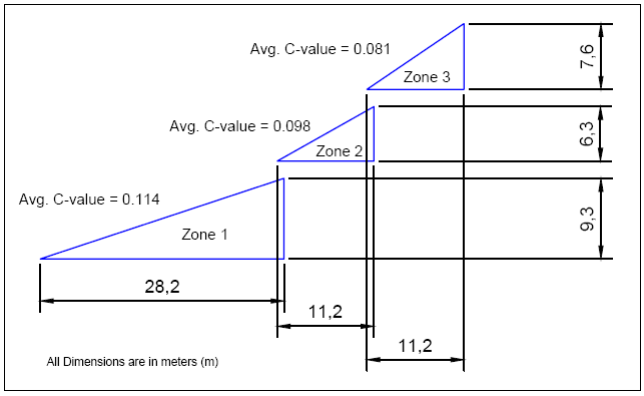

Figure 6-2: Cross-section of seating levels

3. **Formulation of plan of seating levels**

Now that the cross sections are drafted, they can used to create a seating plan for the spectators. This is the final step which helps in obtaining the span of the shell. A seating plan is designed and is shown in the figure below.

This plan used to check the capacity of the arena. This is necessary as the plan has to be redesigned if all the 20000 spectators cannot be accommodated. Therefore, a capacity analysis is performed which involves simple geometrical calculations. More details for this can be found in appendix B, where it can be verified successfully verify that the arena has sufficient space to hold the required number of people.

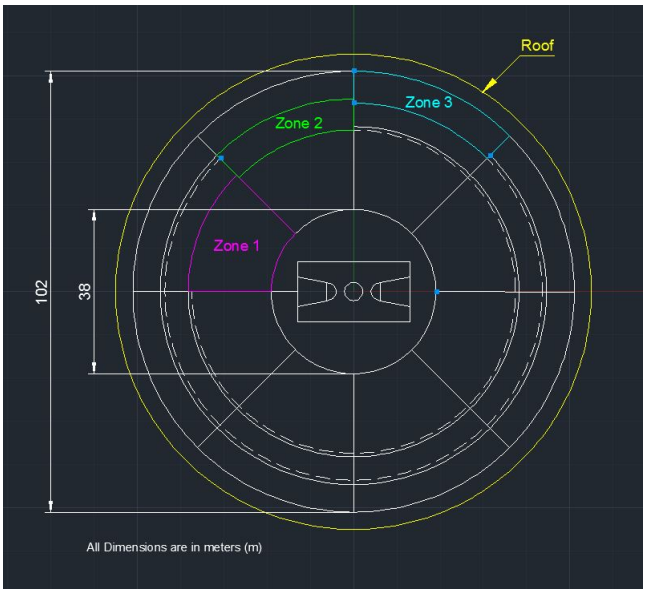

Figure 6-3: Arena seating plan

From the calculations performed above it can be adjudged that the last row of spectators are 49m away and 27.2m above the point of focus which is the edge of the basketball court. Accounting for some space from the farthest row we adopt a radius of 55m. The covering roof can be seen as the yellow line in figure 6-3. Thus the span of the roof is chosen to be 110m.

6-2 Sagitta/Rise of the roof

Before establishment of the rise of the roof, the flow of forces in a roof, subjected to concentrated load, need to be investigated. Since shells are geometry based structures, it is only obvious that different geometries for the spherical roof can result in separate structural behaviour.

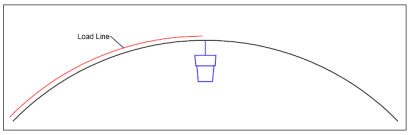

Figure 6-4: Stress flow for shallow spherical dome

Consider the behaviour of a shallow roof as depicted in figure 6-4 and of a higher roof in figure 6-5. The shallow roof has a gentler load line thus we can intuitively say that buckling is more likely to occur at the apex of the shell resulting in the disturbed region being present around the centrehung display. On the contrary the higher shell should behave differently because it has a steeper load line. It this arrangement the buckling focus shifts towards the edges of the shell. In theory, this arrangement should be preferred as logically it would be more resistant to buckling. But having a higher dome would require more material for construction

due to the extra height and providing extra thickness in the edges of the shell. Owing to this thought, it is decided to test three designs having different sagittas. Details of this are given in table 6-1. These designs will undergo buckling analysis, after which final decision on the sagitta-ti-span ratio will be made.

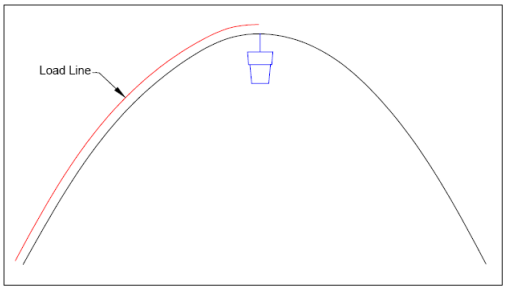

Figure 6-5: Stress flow for higher spherical dome

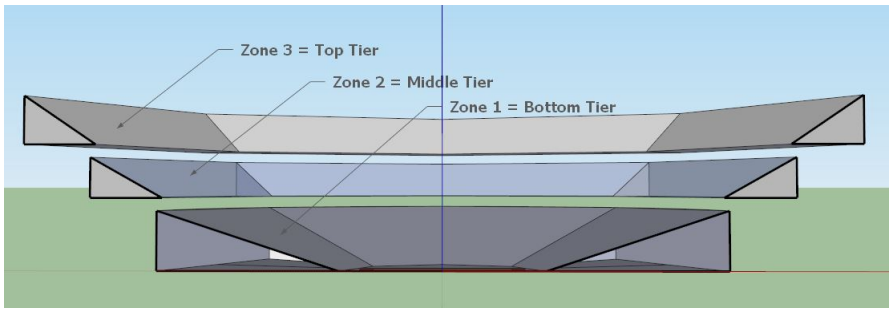

Figure 6-6: 3D cross section of the seating levels

Design	Span(m)	Sagitta(m)	Sagitta-to-span ratio
1	110	23	**1/4.78**
2	110	30	**1/3.67**
3	110	35	**1/3.14**

Table 6-1: Design details

Chapter 7

Thickness of the Roof

In this part of the design process the most crucial aspect of our roof is defined. Thickness has a direct influence on how a shell structure fails. Moreover shell design is largely based on which failure mode the designer chooses. For this reason the thickness is chosen based on several considerations which are discussed in subsequent subsections.

7-1 Based on failure mode

Structural failure of thin shells can be a combination of crushing and buckling. Studies have been conducted on spherical shells to obtain a relation between the thickness and mode of failure. Results of this study are shown in table 7-1. The values shown have been computed in a scenario where it is assumed that the shell experiences buckling and crushing at the same time. The only loads considered are self-weight of the structure. The shell in this design is subjected additional loads, yet this approach is considered due to the shells ability to confine disturbances in regions, as was discussed in earlier sections.

R/t	<58	58−336.4	>336.4
Failure mode	Crushing	Crushing and/or Buckling	Buckling

Table 7-1: Failure modes for different R/t ratios [10]

It is decided to choose a R/t ratio which prefers buckling as the failure mode. The aim is to create a thin shell which is more likely to fail due to buckling. On the other hand a thick shell would experience crushing failure, which is evident from table 7-1 (R/t<58 $\Rightarrow$ t>1332.76mm). Increasing the thickness is unfavorable since it requires more material and adds to the self weight of the structure. Overall this leads to inefficient design as it contradicts the whole idea of designing a thin shell. This gives a workable range of values for the shell thickness. One limit for the thickness is calculated below.

$$\frac{R}{t} \geq 336.4 \tag{7-1}$$

$$\Rightarrow t \leq \frac{77300}{336.4} \approx 230mm$$

Further sections involve calculation of the other ranges, in which the thickness of the shell can vary. The shell is individually analyzed under self weight and the centrehung display at the apex.

7-2 Based on membrane theory

A membrane analysis is conducted, although it should be noted that a pure membrane field cannot be realized in the presence of a point load at the shell apex. Due to this reason the point load is omitted here and a nominal thickness is calculated considering the normal force (n) in a pressurized spherical shell due to self weight only.

$$n = \frac{1}{2}pa \tag{7-2}$$

and the critical membrane force n_{cr} is given by the equation

$$n_{cr} = \frac{-1}{\sqrt{3(1-\nu^2)}}\frac{Et^2}{R} \tag{7-3}$$

The membrane stress needs to be below the critical levels. As a result the two above mentioned equations are equated ($n \leq n_{cr}$) to find the thickness(t). The knockdown factor (C=$\frac{1}{6}$) is introduced in this equation-

$$t^2 \geq -\frac{paR\sqrt{3(1-\nu^2)}}{2EC}$$

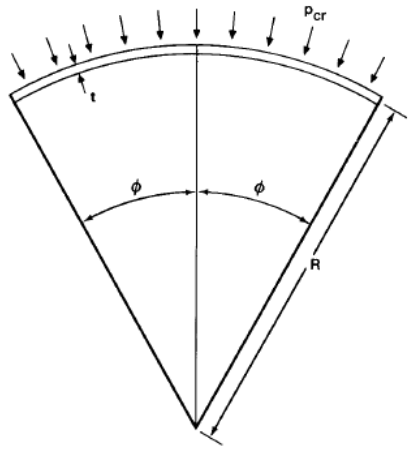

Figure 7-1: Shell under self weight

$$\Rightarrow t^2 \geq 6 \times \frac{25 \times 1000 \times 110 \times 77.3 \times \sqrt{3 \times (1-0.2^2)}}{2 \times 58000 \times 10^6}$$

$$\Rightarrow t \geq 0.013363m \approx 14mm$$

(The negative sign in the formula above disappears due the negative vertical direction of the dead load.)

The thickness obtained here is so small as the shell is assumed to carry self weight. It is highly underestimated for the actual roof design as the value is calculated for a perfect shell only subjected to self weight. These are ideal conditions which are seldom achieved at the site of construction. Yet it points out the extreme structural efficiency of shells as no other concrete structure can span a space of 110 m having a theoretical cross section of one centimeter. Nevertheless, it is obvious that the shell thickness will definitely be more than the value calculated above.

7-3 Based on theory of shell under point load at the apex

The Sanders-Koiter equations are used, for a spherical cap loaded by a point load perpendicular to the surface. The deflection (u_z) under a point load ($P = 500kN/m^2$) is given by the following equation-

$$u_z = \frac{\sqrt{3}}{4}\frac{Pa}{Et^2}\sqrt{1-\nu^2} \tag{7-4}$$

The deflection at the top of the shell is limited to minimum possible value (as shells are extremely sensitive to minute imperfections). An arbitrary value of 100 mm is chosen.

$$t^2 = \frac{\sqrt{3}}{4}\frac{Pa}{Eu_z}\sqrt{1-\nu^2}$$

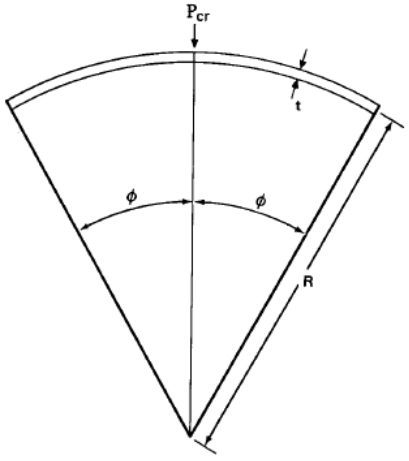

Figure 7-2: Shell under point load at apex

$$\Rightarrow t^2 = \frac{\sqrt{3} \times 500000 \times 110}{4 \times 58000 \times 10^6 \times 0.1} \times \sqrt{1-0.2^2}$$

$$\Rightarrow t \geq 0.073241m \approx 75mm$$

This is used as the lower limit for the range of our of thickness. This value is greater than the thickness obtained for membrane theory. The bending moments caused due to the apex load necessitates extra thickness for flexural rigidity.

The calculation performed above makes it easier to propose a thickness for the shell roof. The range of values can be stipulated between 75mm and 230mm. For further analysis three values are selected: 100, 150 and 200 mm.

Chapter 8

Initial Design Formulation

This section involves formulation of multiple designs to be used for further analysis. Linear stability analysis is performed on these designs, which eventually leads to finalizing the final design. The designs proposed here are based on varying sagitta and thickness consideration which have been identified in previous sections.

1. **Design 1**

   s/d=1/4.78; **R/t**=515.33

   - Simple Shell

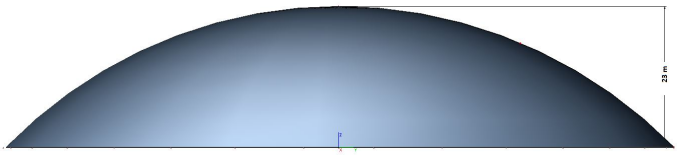

   - Ribbed Shell

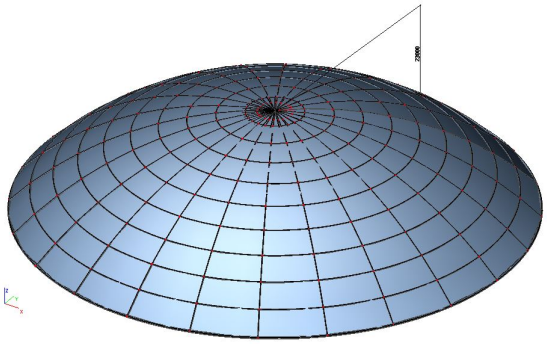

2. **Design 2**

   s/d=1/3.67; **R/t**=429.33

   - Simple Shell

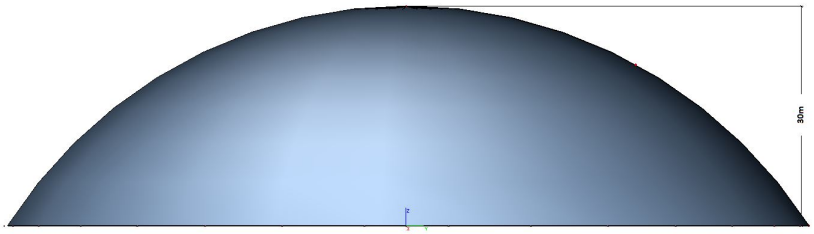

   - Ribbed Shell

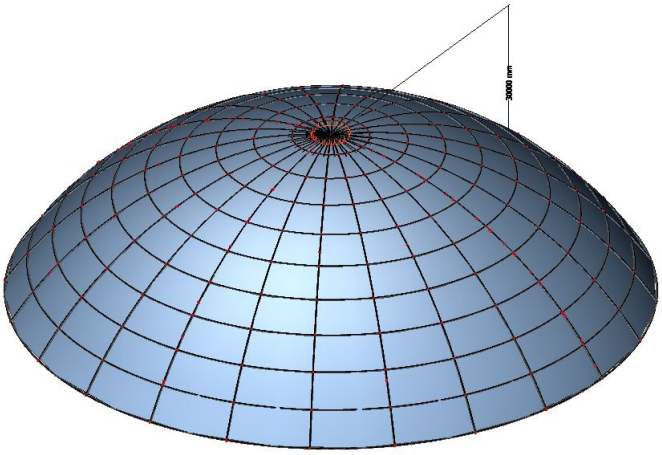

3. **Design 3**

   s/d=1/3.14; **R/t**=404.67

   - Simple Shell

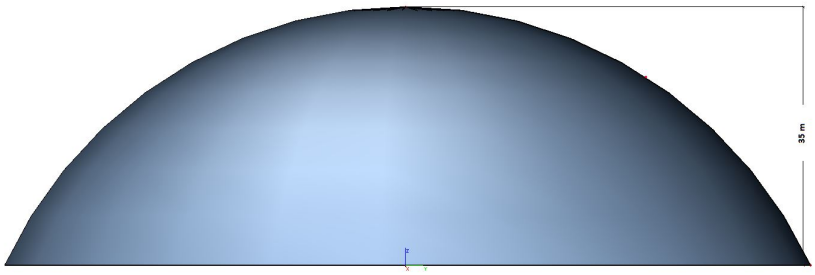

- Ribbed Shell

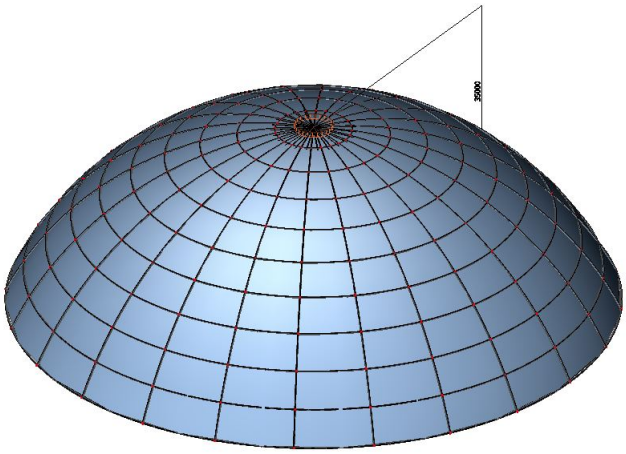

All the design are thin shells which can be verified using the classification provided in [1]. All R/t values are greater than 30, hence all designs conform to thin shell standards.

Chapter 9

Pre-modelling Details

9-1 Calculations of Loads

The next process in design is to identify the loads acting on the structure. Load factors are calculated using Eurocodes which lead to design values of several kinds of loads. This section describes how and what loads are assumed to act on our structure.

9-1-1 Permanent Loads

Permanent loads are referred to as the dead or static loads acting on the structure and are calculated using Eurocode EN1991-1-1 [25].

1. **Self Weight**

   One of the dead loads is the self weight of concrete used in shell construction and other finishing installations. UHPC is known to have a specific weight between 25-28 kN/m^3. In this design a specific weight of 25 kN/m^3 is adopted. This weight multiplied by the thickness of the shell gives the dead load acting on the surface of the shell in negative z-direction.

   $$q_{selfweight} = 2.5 \times 10^{-5} \text{ N/mm}^3$$

2. **Load due to video display**

   The other major dead load is due to the presence of the centre-hung display at the apex of the shell. This screen is introduced in the analysis as a circular load at the apex. The weight of the display has to be known to calculate the magnitude of the force on the roof. As discussed earlier, the video display at the New Amway Centre, USA is a 40 ton configuration. In this design the weight of the centrehung video display is chosen to be 50 tons.

The centrehung will be hung from a special beam which also acts as a stiffener for the shell at the top. The radius of this circular beam is 4.16 meters. The final load calculations are shown below.

$$q_{centerhung} = \frac{500 \times 1000}{2 \times \pi \times 4160} = 19.1 \text{ N/mm}$$

9-1-2 Variable Loads

Variable or Live Loads are categorized into wind and snow loads for our structure. All calculations regarding these types of loads have been performed with reference to Eurocodes EN1991-1-3 [26] and EN1991-1-4 [27].

1. **Wind Loads**

   Wind loads are calculated in the form of pressure coefficients acting over the surface of the shell. The wind pressures have to be calculated taking into account the shape and size of the structure. This process begins with the determination of basic wind velocity (v_b). The constants c_{dir} and c_{season} are directional and seasonal constants which have a recommended value of 1. The fundamental value of basic wind velocity is denoted as $v_{b,0}$. This value is assumed to be 27 m/s for wind region II according to article 4.2 in the National Annex.

   $$v_b = c_{dir}.c_{season}.v_{b,0}$$
   $$\Rightarrow v_b = 27 \text{ m/s}$$

   Now the peak velocity pressure is calculated using the expression obtained from article 4.5 of the eurocode.

   $$q_p(z) = [1 + 7.l_v(z)].\frac{1}{2}.\rho.{v^2}_m(z) = c_e(z).q_b$$

   where q_b is obtained using the air density(ρ), which has a recommended value of 1.25 kg/m^3, and the basic wind velocity as shown in the expression below.

   $$q_b = \frac{1}{2}.\rho.{v_b}^2$$

   $c_e(z)$ which is found out using the figure provided in the Eurocode. This value is found out for terrain category I as shown in the following figure.

   $$\therefore q_p(z) = 3.8 \times \frac{1}{2} \times 1.25 \times 27^2 = 1.73 \text{ kN/m}^3$$

   Thereafter the global external pressure coefficient is determined using the specifications provided in the eurocode. This procedure is shown below.

   The three different pressure zones can be seen in figure 9-2 namely A, B and C. These coefficients are calculated using linear interpolation of values obtained from Figure D2 in the eurocode. The sagitta by span ratio is ranged between 0.20 and 0.32. Value of h/d adopted is 0.168.

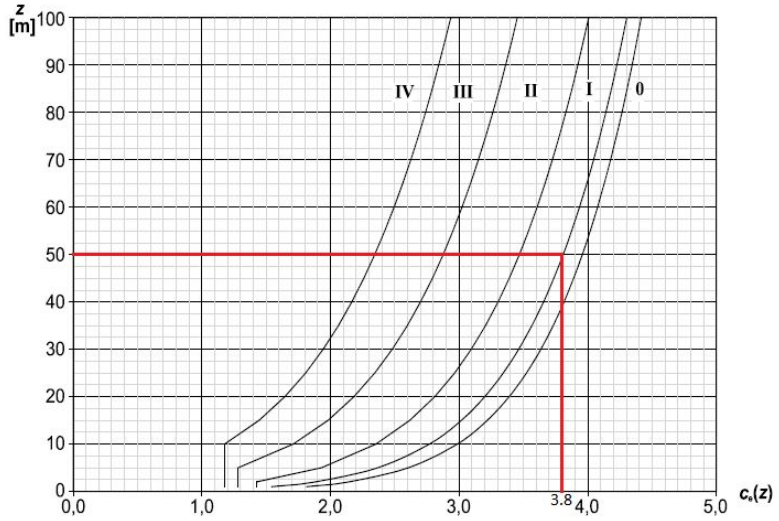

Figure 9-1: Determination of exposure factor

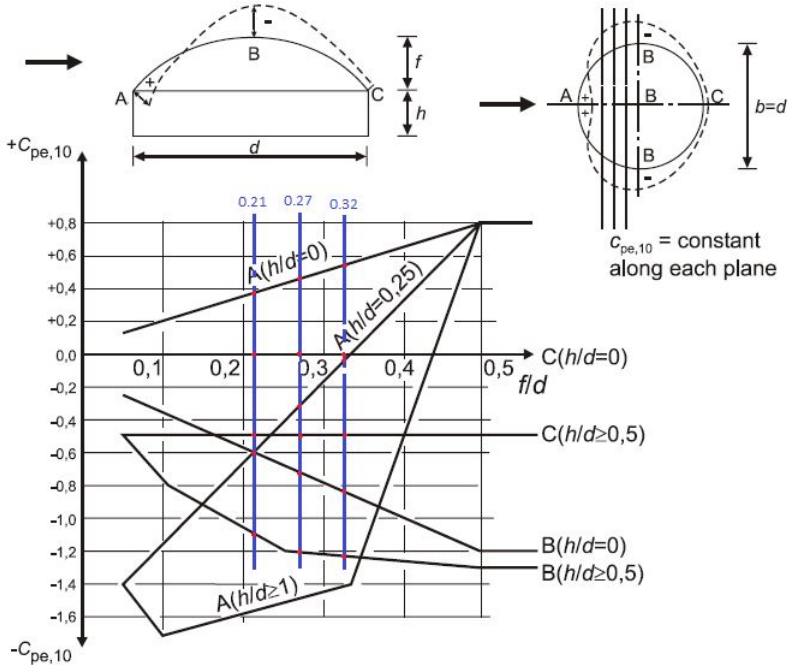

Figure 9-2: External wind pressure coefficients for spheres

$$h \approx 18.5m; d = 110m \Rightarrow h/d = 0.168$$

This value is used in the second part of figure 9-2 to get the various pressure coefficients ($c_{pe,10}$). Once they are obtained it is applied in the following expression to get the external wind pressures(w_e).

$$w_e = q_p(z_e).c_{pe}$$

In the expression $q_p(z_e)$ is replaced by $q_p(z)$ which was calculated earlier. Once the external wind pressures are obtained we have to distribute the three different pressure regions on the surface of the roof.

Design	**1**			**2**			**3**		
Zone	**A**	**B**	**C**	**A**	**B**	**C**	**A**	**B**	**C**
C_pe	-0.28	-0.77	-0.17	-0.053	-0.885	-0.17	0.15	-0.97	-0.17
W_e (kN/m3)	-0.484	-1.33	-0.29	-0.092	-1.53	-0.294	0.26	-1.68	-0.294

Table 9-1: Wind coefficients and forces for all three design sets

For the distribution of force previously conducted studies [10] are referred to. A similar procedure is followed and the wind forces are distributed as shown in the following figures.

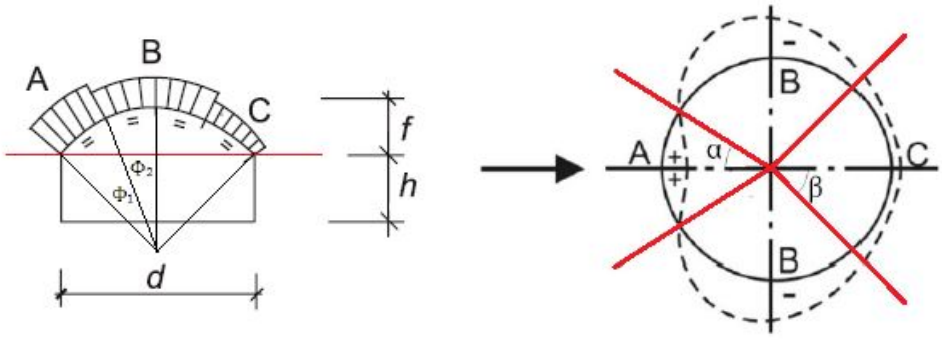

Figure 9-3: Distribution of wind loads

From figure 9-3 we can assume that Φ_1 and Φ_2 are equal. From earlier calculations we know that $\Phi_1 + \Phi_2 \approx 45.2°$.

Figure 9-3 is derived from the plan provided in the top right of figure 9-2. The values of α and β are approximated as 32°and 45°respectively. Thus the magnitude and orientation of the wind loads are known.

2. **Snow Loads**

Snow can have a considerable effect on shell structures as they add to the self weight. In our design the Eurocode En 1991-1-3 is used to obtain snow loads. The following expression is used for this calculation.

$$s = \mu_i.C_e.C_t.s_k$$

where:

s_k= characteristic value of snow load = $0.7kN/m^2$ (for all of Netherlands)

C_e= exposure coefficient = 0.8 (assumed for Windswept topography)

C_t= thermal coefficient = 1.0

μ_i= snow load shape coefficients

The eurocode provides snow load coefficients for cylindrical roofs only as shown in figure 9-4

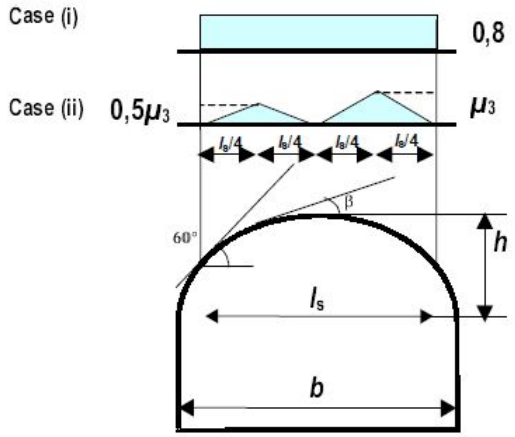

Figure 9-4: Snow load shape coefficients for cylindrical roofs [10]

Case (i) is indicative of undrifted load arrangements which corresponds to evenly distributed snow load. Case (ii) implicates drifted load arrangements which is a result of rearrangement of the snow(e.g. due to wind). Since figure 9-4 is for cylindrical roofs only we formulate an alternating pattern for minimum and maximum values for the distributed snow. This is shown in the figure 9-5.

The value of shape coefficient is calculated as it would be for cylindrical roofs. Using the expression given in article 5.3.5 of the eurocode μ_3 is approximated.

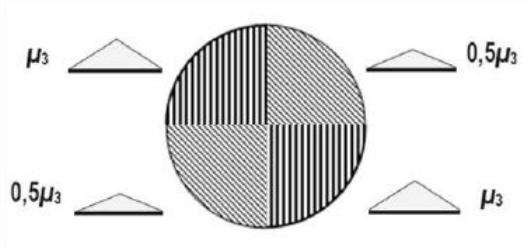

Figure 9-5: Snow load shape coefficients for dome [10]

$$for \beta > 60°, \mu_3 = 0$$
$$for \beta \leq 60°, \mu_3 = 0.2 + 10h/b$$

- **Case (i)** Load values for undistributed snow are calculated below. .

$$s = 0.8 \times 0.8 \times 1.0 \times 0.7 = 0.45 kN/m^2$$

- **Case (ii)** Load values for redistributed snow are shown below for all three designs.

The loads are applied on the shell using the scheme as shown below. The original non uniform load distribution is approximated as smaller uniform loads for easier modeling.

h(m)	b(m)	h/b	μ_3	$0.5\mu_3$	s(μ_3) kN/m^2	s($0.5\mu_3$) kN/m^2
23	110	0.209	2.3	1.15	1.28	0.64
30	110	0.273	2.9	1.46	1.64	0.82
35	110	0.318	3.4	1.69	1.89	0.95

Table 9-2: Snow loads calculated for all three designs

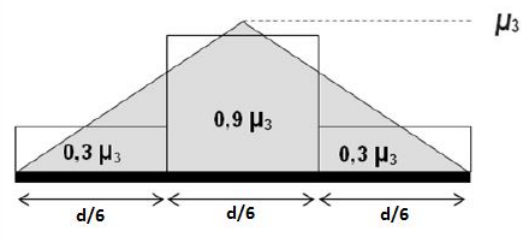

Figure 9-6: Loading scheme for redistributed snow [10]

9-2 Load Combinations and Factors

The eurocodes [28] are referred again to obtain suitable load combinations and design safety factors for this design. Article A1.3 and A1.4 in the eurocode [28] provides design values for the various actions on a structure in ultimate and serviceability limit states. The combinations and factors used in this project are mentioned hereafter.

- **Load Combinations**
  1. Self weight + Point Load + Wind Load
  2. Self weight + Point Load + Undistributed Snow Load
  3. Self weight + Point Load + Redistributed Snow Load
- **Load Factors**

Limit State		**Permanent Loads**	**Variable Loads**
SLS	Unfavorable	1.35	1.5
	Favorable	0.9	0
ULS	Unfavorable	1.0	1.0
	Favorable	1.0	1.0

Table 9-3: Load Safety Factors

In this design project, the behaviour of our structure is analyzed in serviceability limit state conditions. Ultimate load combinations are not considered as they relate to the ultimate load of the structure, which leads to collapse. Whereas in this project the roof will only be designed for basic functionality. Hence, the behaviour of the roof during failure is not part of this study.

9-3 Material Details

A decision on the type of concrete, that will used in this project, has already been. The merits of this decision have been mentioned in pre-design requisites. UHPC type Ductal ®BS1000 is chosen for this design due to its popularity in construction of several special structures worldwide [10]. The presence of discontinuous fibers makes it the perfect isotropic material for shell construction. Some of its properties used in this design are shown in the table 9-4.

Property	**Value**	**Unit**
Density	25	kN/m^2
Compression (Mean)	180	MPa
Compression (Design)	150	MPa
Tension (Mean)	10	MPa
Tension (Design)	8	Mpa
Young's Modulus	58	GPa
Tensile Fracture Energy	0.2603	N/mm
Poisson Ratio	0.2	
Thermal expansion coefficient	11.8	μm/m/°C

Table 9-4: UHPC Properties

The fiber characteristics are provided below

- Fiber Length = 14 mm
- Fiber Diameter = 0.2 mm
- Fiber Content (approx.) = 2 % Vol.

Chapter 10

Finalizing Initial Design

Once the size and shape of the roof have been established, the physical model analysis complete and all additional data for modeling are obtained, the mathematical model of the structure is created. Three designs for the roof, were proposed earlier, based on varying sagittas. In this part of the design process it is attempted to finalize one of these designs, which will then be further studied. Meanwhile it is decided to obtain the critical buckling load factors (λ_{crit}). This can easily be obtained using finite element softwares which allow linear buckling analysis.

For this analysis the software 'SCIA Engineer' is chosen. It is a good example of commercial civil engineering software package. It has a very user friendly interface and is very flexible to modifications in design. This makes this an ideal choice for many structural designers. A special feature of this program is its ability to perform buckling analysis which is essential for shell structures. In addition to this the shell elements used in this program are better compared to other FEM programs. The designs are analyzed for 'Linear stability' in SCIA. Some aspects of this analysis are discussed below.

1. **Modeling details**

   The roof is first modeled as a simple shell with no ribs or stiffeners. This is done to observe the behaviour of the smooth shell structure under varying sagittas. We had earlier studied how a higher shell can perform differently than a shallow shell for our specific load case. This behaviour of shells is studied here.

   Next the same designs is modelled into ribbed shells by adding ribs and stiffeners as 1D elements. Thereafter buckling coefficient are obtained and compared to their smoother counterparts to see if they behave in the same structural way.

2. **Material details**

   The material to be used in modeling is decided next. The possibility of using UHPC has special advantages in shell construction, as mentioned earlier. Properties from table 9-4 are accordingly entered in SCIA.

3. **Loading Details**

   Three different loading combinations are used for this analysis. Since buckling is being considered we obtain load factors for Ultimate Limit State. The overview of these are given in table 9-3.

4. **Boundary Conditions**

   Fixed or clamped boundary conditions are chosen to be applied as line support on the edge of the shell. Previous studies [12] show that fixed supports are more favourable for buckling considerations in case of uniformly distributed loading. This is because the stiffness of the shell is increased near the edge beam.

10-1 Analysis of simple shell roof

A linear stability analysis is performed on the proposed simple shell designs. Each design has a three varying values of thickness and three separate load combinations, each of which gives 4 buckling modes on analysis. In all cases the first buckling mode was found out to be the critical one. Furthermore, the first load combination established as the decisive one, based on obatined results of critical buckling coefficients. Hence, only the first buckling modes for load combination 1 are figuratively shown for each design.

1. **Design 1:**

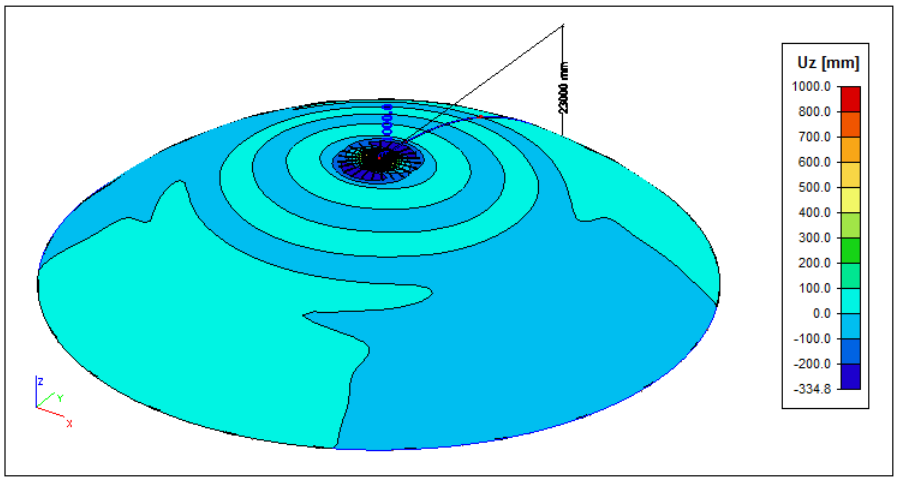

Figure 10-1: Design 1: First buckling mode for t=100 load combination 1

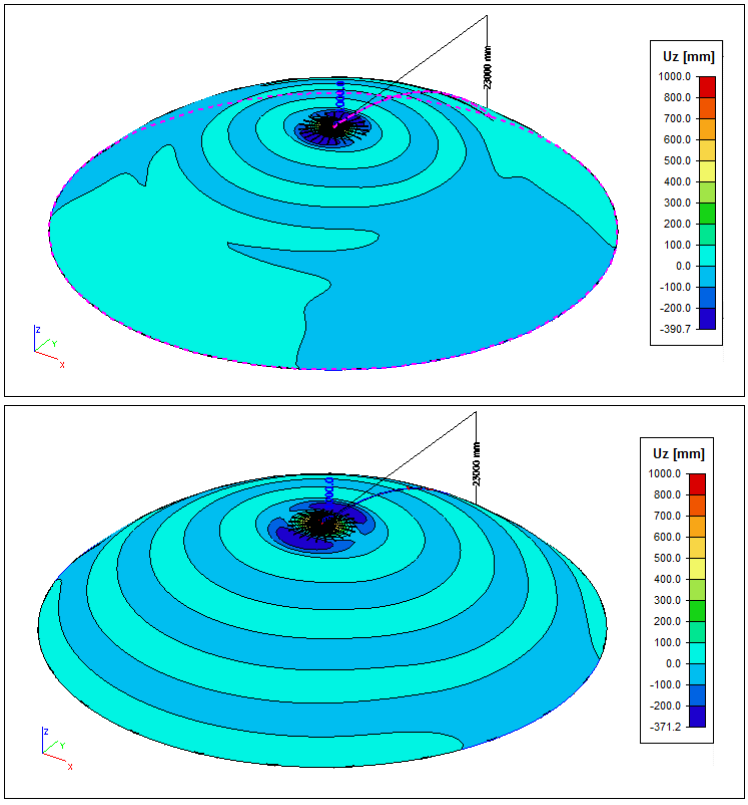

Figure 10-2: Design 1: First buckling mode for t=150 and 200mm, for load combination 1

2. **Design 2**

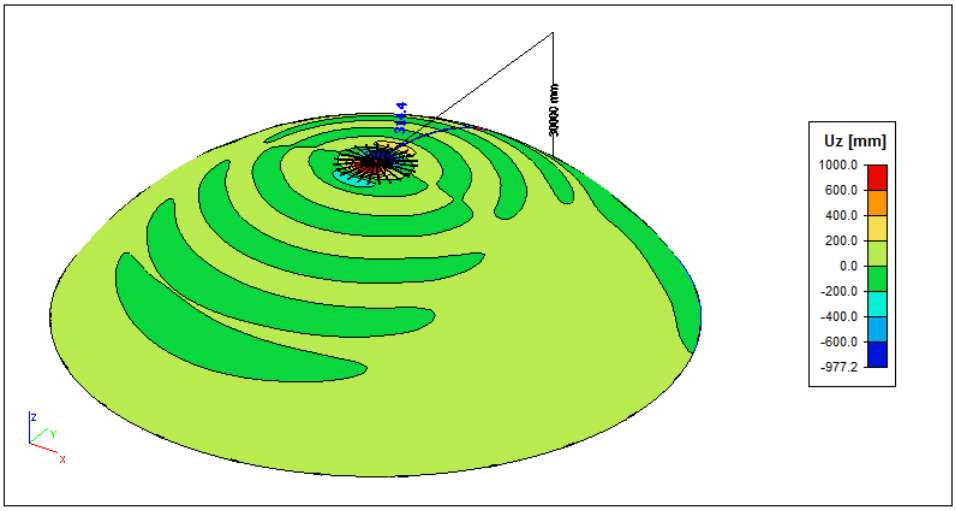

Figure 10-3: Design 2: First buckling mode for t=100 load combination 1

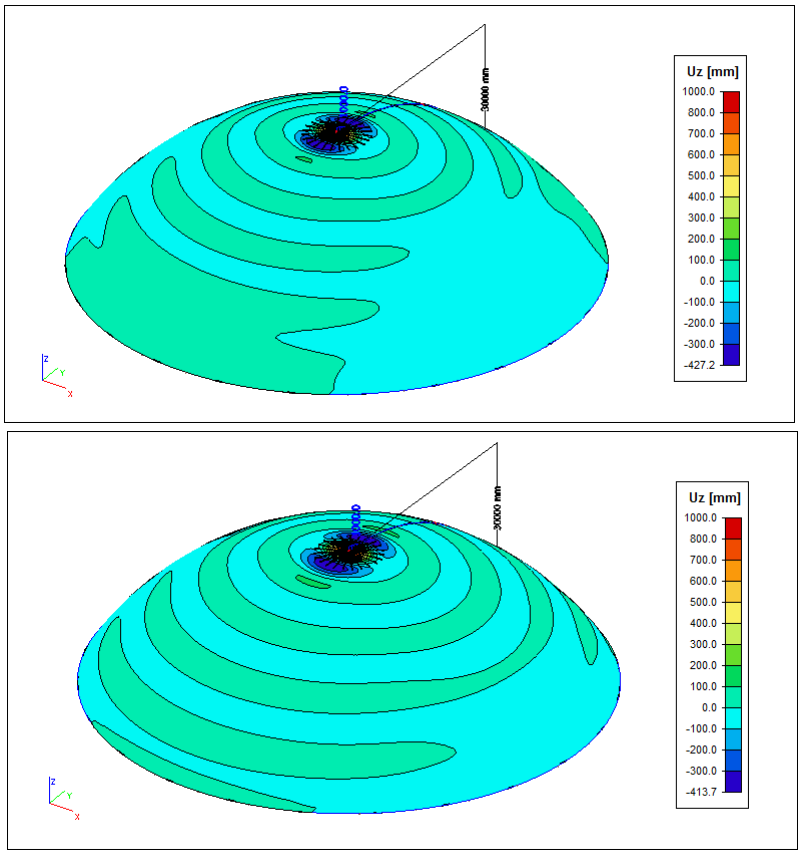

Figure 10-4: Design 2: First buckling mode for t=150 and 200mm, for load combination 1

3. Design 3

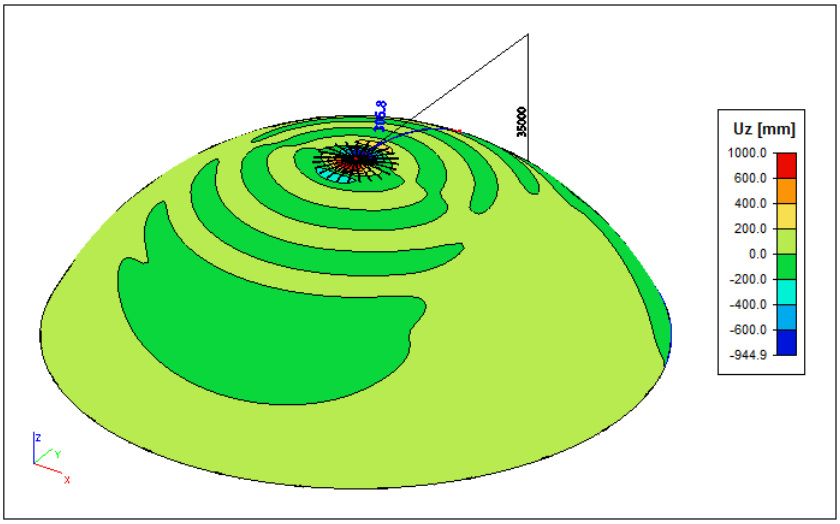

Figure 10-5: Design 3: First buckling mode for t=100 load combination 1

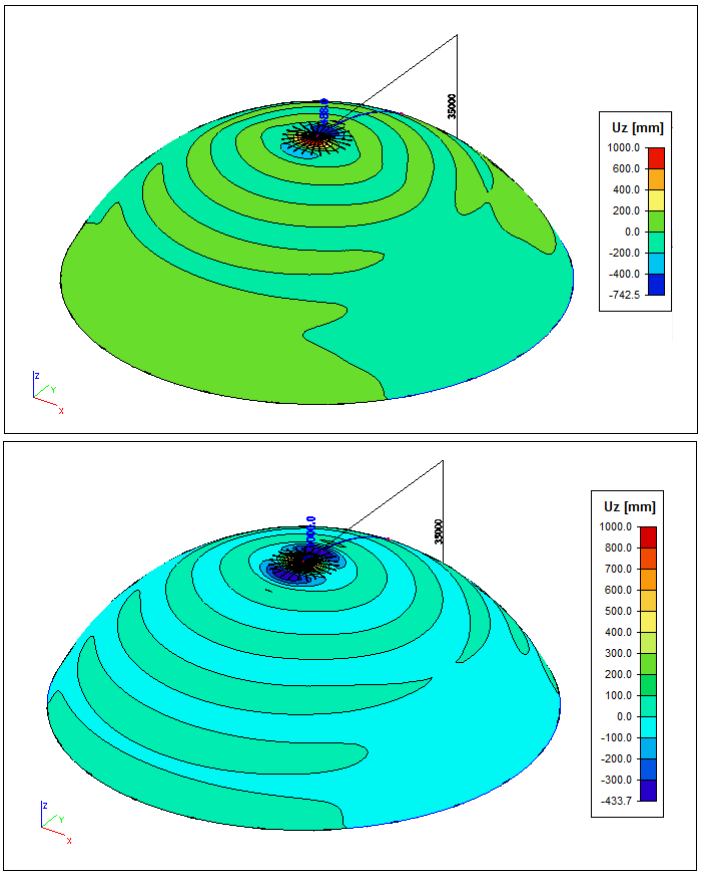

Figure 10-6: Design 3: First buckling mode for t=150 and 200mm, for load combination 1

Once the critical load coefficients (λ_{crit}) are obtained, the susceptibility of the structure to buckling can be checked. Recall choosing a Knockdown factor of 1/6 earlier which is use now used to verify the structure. The load factor (λ) are calculated in the following way:

$$\lambda = \frac{\lambda_{crit}}{6} (\text{if} > 1, \text{ then OK})$$

For Design 1 the lowest critical coefficient is 9.82 and it is greater than 6. Hence the structure is safe against buckling for all three thicknesses. The same observation is made for the remaining two designs. Design 2 has the lowest λ_{crit} of 13.59 while for Design 3 the least value is 15.39. Hence it is concluded that all three designs are safe against buckling.

Previously a discussion had been made about the influence of sagitta on the structural behaviour of shells. This can now be studied with the analysis performed above. It is noticed that the buckling capacity of the shell keeps increasing in an increase in rise of the shell. This leads to the conclusion that a steeper load-line shown in figure 6-5 is more structurally efficient. This behaviour is attributed to the decrease in eccentricity of the major load on the structure which is video display at the apex. This facilitates better membrane behaviour and decreases the overall bending moment on the structure.

Table 10-1 concludes the analysis of the simple shell design. In the next section the design is studied for varying shell thickness, which is used to define the geometry of the panels.

	Buckling Mode	Critical Load Coefficients		
		t=100mm	t=150mm	t=200mm
Design 1	Mode 1	9.82	21.06	35.41
	Mode 2	10.03	21.95	36.9
	Mode 3	11.42	24.74	41.09
	Mode 4	12.83	28.44	46.41
Design 2	Mode 1	13.59	29.12	49.18
	Mode 2	13.71	29.62	50.48
	Mode 3	16.22	34.84	58.48
	Mode 4	16.78	38.19	64.61
Design 3	Mode 1	15.69	33.68	56.54
	Mode 2	16.00	33.79	57.11
	Mode 3	19.12	41.57	68.72
	Mode 4	19.85	43.11	72.83

Table 10-1: Critical load coefficients for simple shell for load combination 1

Thereafter the panels are used to build up the ribbed shell. Once this has been done the a design can be chosen, to proceed with nonlinear analysis.

10-2 Design of shell panels

The influence of differing thickness on the shell also needs to be studied. The aim is to finalize the geometry of the shell panels to complete the initial design. A comparative study is performed using the figure 10-7. Initially a range of values was chosen for the thickness, which can be seen in the graph. It is observed that all values of thickness provide a safe design, but they apply to a simple shell. In order to obtain the ribbed cross section, the shell surface is divided into panels which are redesigned using redistribution of material. They are designed in such a way as to increase the buckling capacity of the structure while implementing structural efficiency.

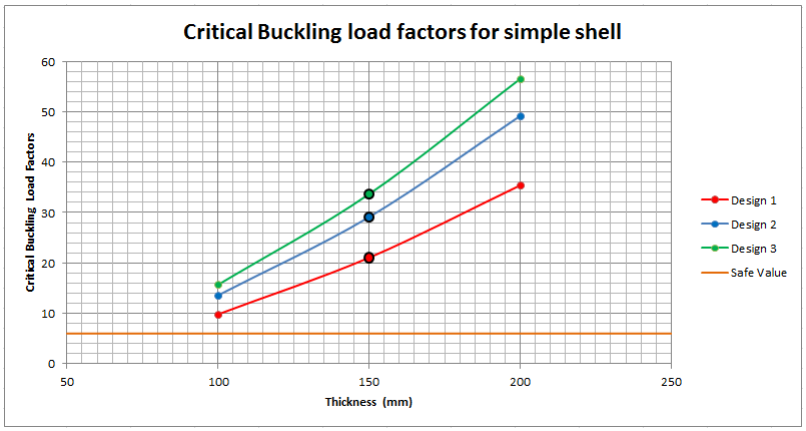

Figure 10-7: Comparison of buckling factors for varying shell thickness

The idea is to remove a section of UHPC from middle of the panel and applying it to the edges of same panel, where it is more useful structurally. This can be easily explained using figure 10-8. Initially, the middle pieces of the panel were adding more weight to the structure without any major influence on the buckling strength. But if they are removed and added to the panel edges then this greatly increases the buckling capacity. This is because the flexural stiffness of the panels increases with the order of cube of the thickness. Hence, these edges now perform as ribs and stiffeners which, when built up together, produce a ribbed dome.

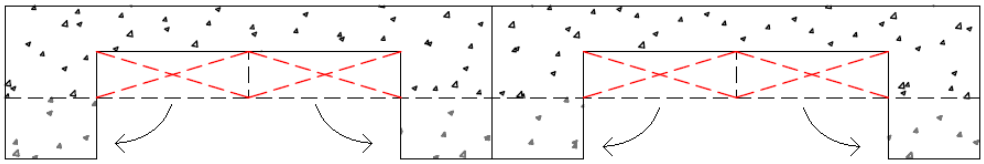

Figure 10-8: Redistribution of material in shell panels

Figure 10-7 now used to determine a nominal value for thickness to create the necessary cross section of the panel. A thickness of 100 mm is adjudged to be too close to dropping below the line for a safe design. Furthermore the higher value of 200 mm requires additional material would could decrease the structural efficiency, based to strength to weight considerations. Consequently, a thickness of 150 mm is chosen from the simple shell design, and is used to obtain panel cross sections for a ribbed shell. This procedure is shown in the figure 10-9. The length of the slab varies at different cross section which means that the amount of material removed varies, depending on the position of the panel. Although, for ease of modelling, the dimensions of the ribs remains constant for all panels.

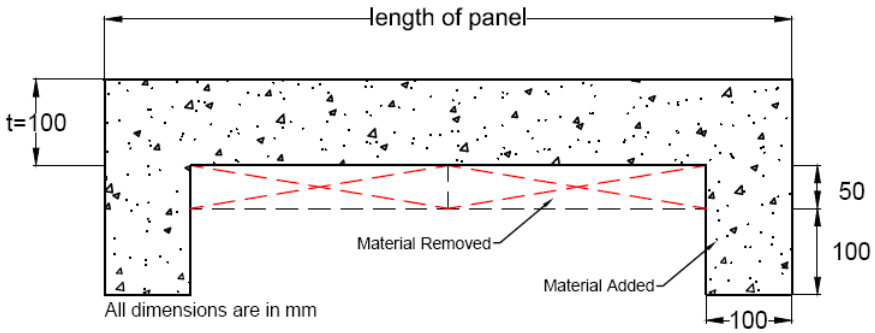

Figure 10-9: Final cross sectional geometry of the shell panel

Geometrical details of the rib can now be calculated for modelling purposes. From the figure above, it can be easily observed, that the dimensions for one rib will be 150×200 mm. The width of the ribs are doubled owing to two panels being side by side. These dimensions have been determined intuitively. The amount of material removed may not necessarily be the same as the amount added to form the ribs. Care has been taken to provide extra height to give more space for panel to panel connections.

10-3 Analysis of ribbed shell roof

The simple shell has now been converted into a ribbed dome using the panel design from the previous section. This used to model a ribbed dome in SCIA engineer and the respective critical elastic buckling coefficients are calculated for design 1,2 and 3. From simple shell analysis, it is inferred that the shell with the highest sagitta will form the most stable design. This might change for a ribbed shell due to modifications of the cross section. Another point to be mentioned here is that the thickness of the ribbed shell is reduced to 100 mm due to aforementioned changes.

The linear buckling analysis is performed for all designs and shown below. Only the first mode of buckling is shown for all shells. Thereafter, the critical coefficients are compared to the simple shell design of 150 mm thickness, to analyze how the addition of ribs affects the performance of the design. A decision on the final design will be made after this step has been completed.

1. **Design 1**

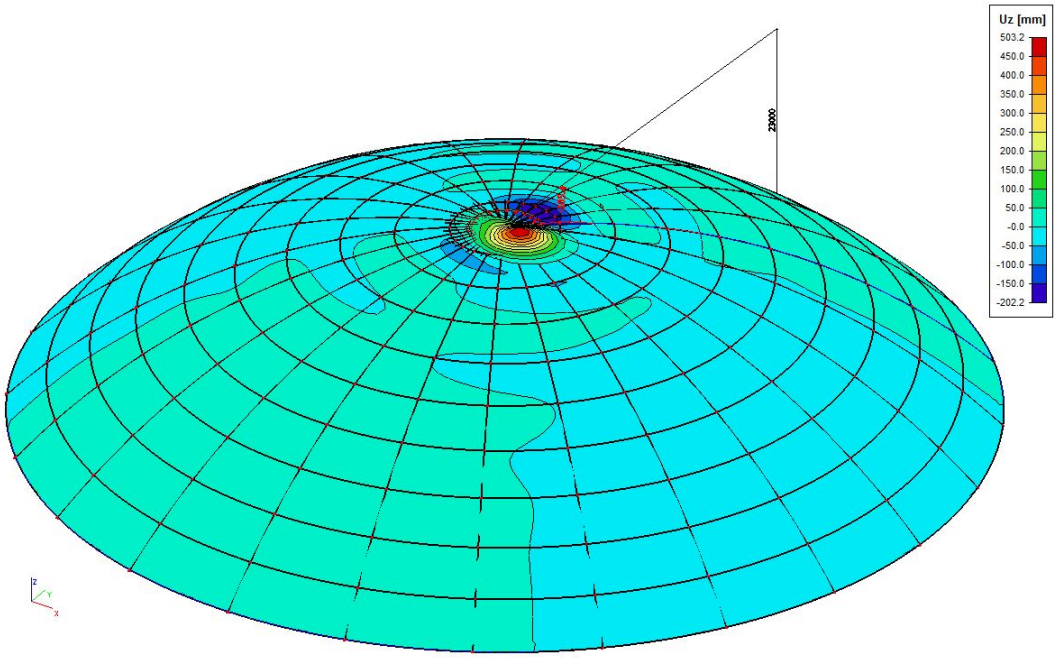

Figure 10-10: Buckling combination 1 Mode 1 for Design 1

2. **Design 2**

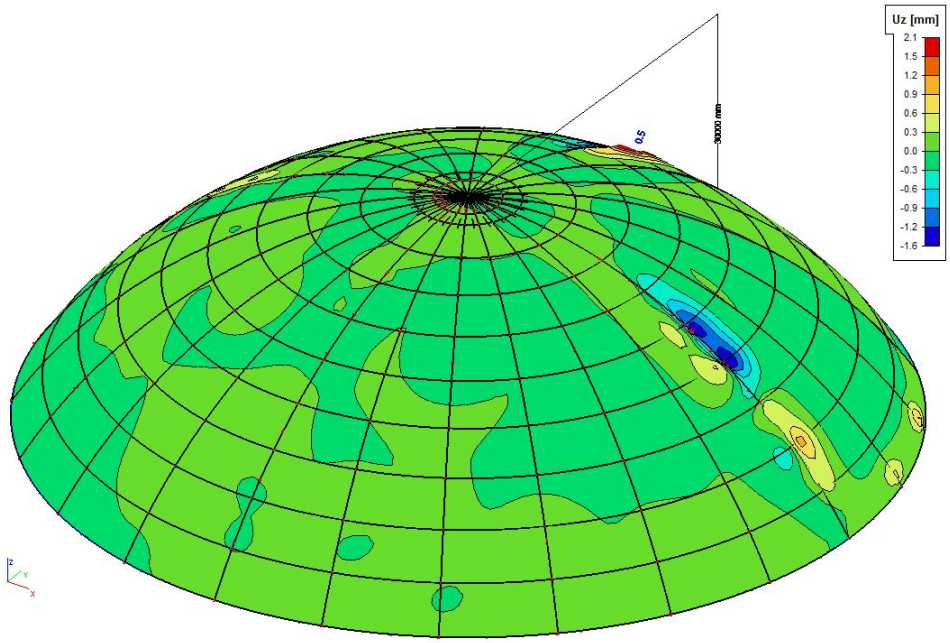

Figure 10-11: Buckling combination 1 Mode 1 for Design 2

3. **Design 3**

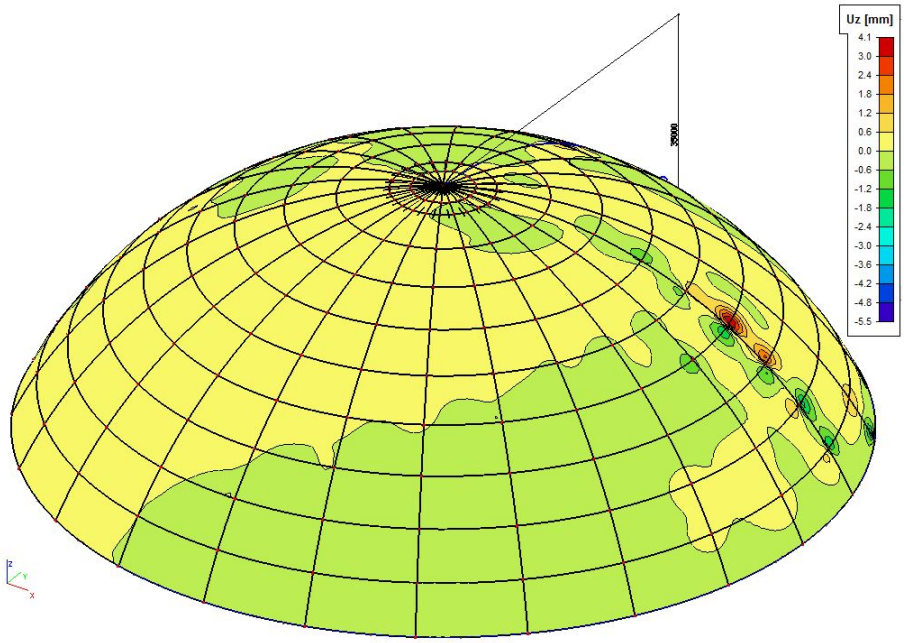

Figure 10-12: Buckling combination 1 Mode 1 for Design 3

4. **Results**

	Buckling Mode	Critical Load Coefficients
Design 1	**Mode 1**	18.93
	Mode 2	19.64
	Mode 3	20.41
	Mode 4	22.15
Design 2	**Mode 1**	5.55
	Mode 2	5.62
	Mode 3	6.61
	Mode 4	6.69
Design 3	**Mode 1**	7.10
	Mode 2	7.25
	Mode 3	8.11
	Mode 4	8.26

Table 10-2: Critical load coefficients for ribbed shell for load combination 1

The critical buckling coefficients are obtained and listed in table above. This analysis give interesting results when each design is checked for safety against buckling. Table 10-2 verifies the ribbed design for the shallow shell (with the lowest sagitta). From the graph 10-13 the improved buckling performance of Design 1 can be identified. This can be associated with the addition of ribs and stiffeners which provide extra stability, a behaviour which is expected. But the next two designs do not show the same pattern. Notice how the addition of ribs leads to a decrease in buckling capacity of Design 2 and 3. In fact both designs fall below the safe value.

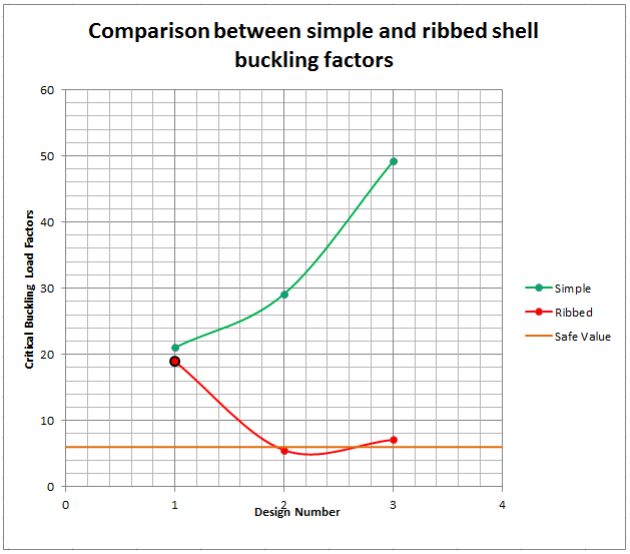

Figure 10-13: Buckling factors for the simple vs ribbed shell design

It is hypothesized that this sudden and significant loss of load carrying capacity can be explained due to the extra weight added to the initial structure. The addition of ribs and stiffeners increase the self-weight and consequently the uniform vertical load on the structure. This has a reverse effect and instead of strengthening the structure against buckling it make it more prone to it.

The conclusion of this analysis results in the finalization of the ribbed version of Design 1, as the best suited the roof. It performs well in linear stability analysis from the graph above. The choice in this design will now be verified by performing a nonlinear analysis on the shell.

Chapter 11

Structural behaviour of Initial Design

The previous analysis results in the final initial design, which is studied further by performing a nonlinear analysis. As mentioned earlier this captures a more realistic behaviour of our structure. Linear analysis assumes elastic properties of the material, which is not the case every time. UHPC is known to exhibit considerable ductile properties, which give rise to nonlinear nature. Additionally imperfections can cause geometrical changes, leading to a nonlinear response as well. It seems necessary to check the performance of the designed shell, incorporating nonlinear effects as they can dramatically reduce the load carrying capacity.

The following sections describes the entire procedure followed, to perform a complete nonlinear analysis. First the modelling strategy is described, which highlights the use of multiple existing software. Some important details of structural model are also shared. Prior to analysis, the nonlinear material models and settings need to be set. The choice of some important options are explained and justified. Thereafter, an order of analysis is chosen, which is used to perform a physical nonlinear analysis.

11-1 Modeling Strategy

In the previous section a single software was used ,for modeling and analysis, which was very convenient, but for nonlinear investigations we use multiple softwares. It is extremely time consuming to model a complex structure, using just the DIANA interface. This is because geometrical inputs can only be made by defining individual points. To simplify this process popular modeling software 'Rhinoceros' is used. The shell can be easily modelled as a combination of surfaces.

Once the shell model is created it is exported to Diana using the *.iges file format. While this approach works for simpler models, unexpected problems were encountered while transferring the shell geometry. It was noticed that the co-ordinates of the shell got distorted, resulting in the creation of an incorrect model. Initially it was thought that this was due to inaccurate modeling in Rhinoceros. But eventually, the cause of this problem was found out to be the

inability of DIANA to recognize trimmed surfaces. As a result, the shell is remodeled in Rhinoceros using the *patch* function which enables the designer to create untrimmed surfaces.

After facing the aforementioned problem in DIANA, the modeling software 'FX+ for DIANA' is chosen to create the meshed structural model. This software has a better user friendly graphical interface, unlike the initially chosen software. This allows the structure to be modelled easier and faster. Furthermore changes in geometry, material and physical properties can be easily performed. The final meshed structural model is shown in figure 11-1.

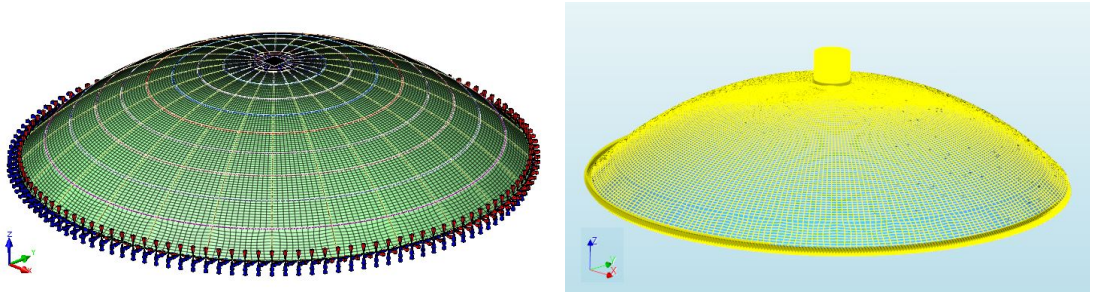

Figure 11-1: Meshed model in FX+ and transferred model in MeshEdit

The model is chosen to be edited using 'MeshEdit' for DIANA, which enables us to add a nonlinear material model to UHPC. It also allows us to create required load combinations, using the different types of loads imported from FX+. Figure 11-1 shows the meshed shell model under the first load combination. Further study is performed in this software using special analysis commands. An overview of the explained modeling can be seen in figure 11-2 while details are discussed in further sections.

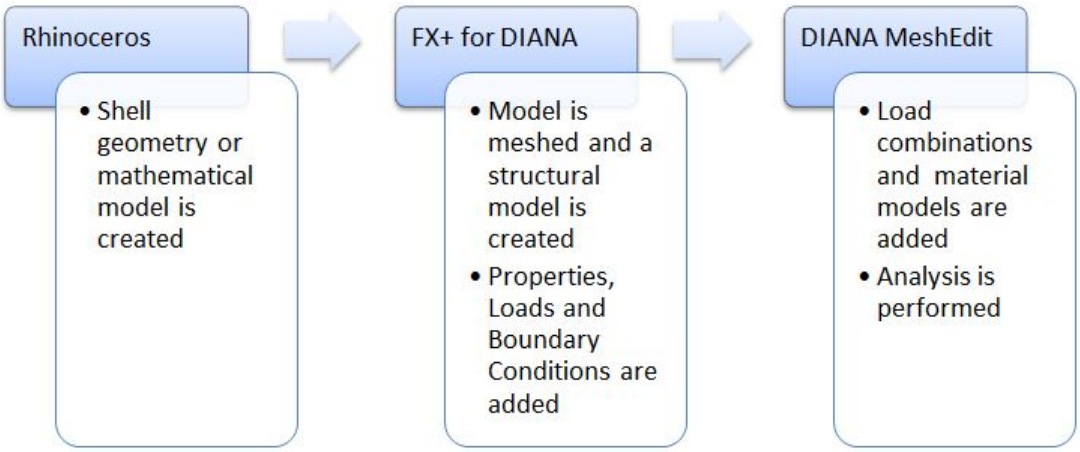

Figure 11-2: Overview of modeling approach

11-2 Model Details

The bulk of the modelling is done using FX+ for DIANA. Some of the details for this procedure are explained below.

1. **Material Properties**

   The properties of UHPC Ductal BS1000 are shown in Table 1. These parameters are entered into the software, to create an appropriate isotropic material property which is applied to the entire structure.

2. **Physical Properties**

   This includes definition of cross sections and element types for the components of the roof. Four different physical properties are created for modelling purposes.

   (a) **1D-Properties**

Property	Cross-section Details	Element type
Edge Beam	200 X 250 mm	BE3 CL18B
Stiffeners	200 X 250 mm	BE3 CL18B
Ribs	200 X 250 mm	BE3 CL18B

Table 11-1: Physical properties for beams

   All beams in the roof are modeled as a 1D-property. Details of the beams are mentioned in table 11-1. The element type chosen to model the beam is a 3D line element belonging to Class III. Further details can be found on the DIANA website or manual.

   (b) **2D-Properties**

   Shell panels are modeled under 2D-properties, using curved quadrilateral shell element type QU8 CQ40S. In this type, it is possible to have both in and out-off plane deflections. Spherical elements are chosen and a thickness of 150 mm is adopted from the initial design.

3. **Mesh Details**

   The edge beams, ribs and stiffeners are meshed, using the Auto-Mesh function for edges, while the shell panels are meshed, using the Face Map-Mesh function. In both cases mesh sizes are based on 10 divisions of each subsurface (which make up the entire shell). Mid-side nodes are generated during the meshing of all elements.

   While meshing the top of the dome, care is taken to avoid generation of quadrilaterals with acute corners. This is done by adopting a meshing pattern as shown in figure 11-3.

4. **Boundary Conditions**

   Boundary conditions are introduced as hinged supports, along the outermost edge of the shell roof. This can be seen in figure 11-1.

5. **Loading Conditions**

   Loads expected on the shell roof are the same as calculated previously, in pre-modeling details. The values for self-weight, load due to centrehung, wind loads, undistributed snow and redistributed snow loads remain unchanged from that section. The load combinations will be illustrated further.

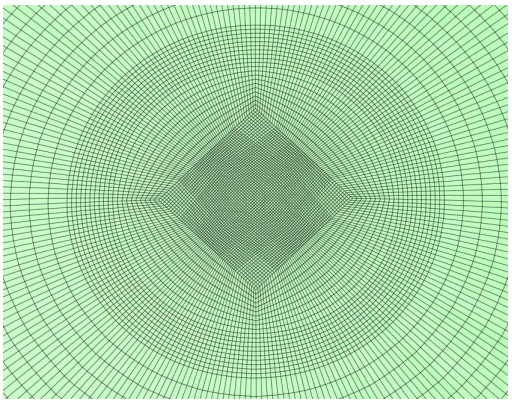

Figure 11-3: Meshing at the top of the dome

11-3 Incorporating nonlinearities in structural model

Nonlinearities can be accounted for in our structural model in several ways. There are different process descriptions and material models, which can be used to incorporate these effects in our model. These choices are offered as various 'settings' in the DIANA, which can be applied prior to analysis. The choice of these options depends on material and structural behaviour. The initial nonlinear settings, that are applied to the shell model, are explained below.

1. **Geometrical Nonlinear settings**

   This is accounted for by using Lagrange's description, which monitors large deformations, with reference to previous configuration. This is done with respect to the time and previous coordinates of that particular point. The Euler description is also available but it applies for flow analysis, hence not applied here.

   The Lagrange description offers two options, which are Total Lagrange and Updated Lagrange formulation. We decide to use the *Total Lagrange* setting which is the default setting. The choice of either is not expected to influence considerable change in results for most structural applications [22]. An important point to be noted for the Updated Lagrange formulation is that the cracking, embedded reinforcements and material anisotropy result in incorrect results [11].

2. **Physical Nonlinear settings**

   Physical nonlinearity is borne out of the non-elastic behaviour of concrete. Ductile properties of UHPC warrant the use of a suitable material model which account for this nonlinear behaviour. Several models are available, the choice of which depends on the type of behaviour under investigation.

- **Material Model**

  To model the UHPC, we choose the 'Modified Maekawa Concrete' model. This model uses a multi-axial damage plasticity model for the compressive action and a total strain based crack model for tensile nature of the concrete [11]. Figure 11-4 shows the tension and compression curves adopted for the nonlinear analysis. UHPC

  This model has two options consisting of a 'fixed' and 'rotating'. it is chosen to use the rotating crack based model for this analysis due to its advantages in numerical calculations and elimination of shear retention factor [22].

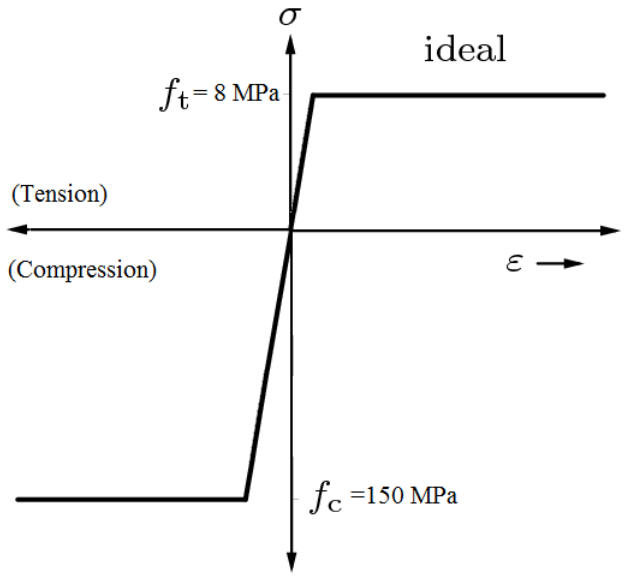

Figure 11-4: Maekawa concrete model used for analysis [11]

- **Cracking**

  UHPC is different from conventional concrete when it comes to tensile behaviour. This because UHPC allows a designer to also design for strength capacity in tension, while controlling the crack widths in the structure. The material model chosen for this analysis contains a curve in tension, thus requiring a certain crack width criteria.

  The calculation of crack widths are done using the concept of 'fracture energy regularisation' [12]. This theory assumes the presence of one crack in each element, the width w of which depends on the equivalent length on the element or crack bandwidth h.

$$\varepsilon = \frac{w}{h} \Rightarrow w = \varepsilon \times h$$

  In the relation above, ε is the strain observed in the element, h is the length of the element and w is the crack width to be calculated. The maximum strains will be extracted from the results and the corresponding crack widths will be calculated in that element, throughout all load steps.

  Now the crack opening criteria has to be established to check the structure for undesirable cracks. This criteria is established based on the recommendation of

AFGC, the widely accepted French guidelines for UHPC [29]. The UHPC sections used in this design confirm to requirements of 'Class IV', without any prestressing reinforcement or passive reinforcing steel bars. The AFGC recommendations provide the following values for crack widths:

- 0.3 mm for normal cracking
- 0.2 mm for detrimental cracking
- 0.1 mm for highly detrimental cracking

3. **Miscellaneous pre-analysis settings**

- Application of external load

  Generally for performing a nonlinear analysis, the external load is applied on the structure in steps. This can be done in two ways: Load control, where the load is directly applied in steps and Displacement Control, where the displacements are allowed to grow at a particular point. Usually displacement control is preferred as it is physically more realistic, except in case of structures which experience snap-back behaviour. Furthermore previous studies have identified, that displacement controls results in the structure behaving stiffer than it actually is [12]. Consequently, it is decided to use 'Load Control' method of external loading.

- Path following techniques

  This technique is extremely important for shell analysis, as it is capable of recording post failure behaviour as well. This is extremely useful for shell structures due to their well recorded snap-back behaviour. 'Arc-length control' is such a technique which is almost always coupled with every nonlinear analysis. Within this technique, there is a choice between 'Update normal plane' or 'spherical path' control. Both options were tested to yield similar results for shell analysis. In absence any further guidelines, the 'spherical path' arc-length control method is chosen.

- Iteration Method

  Diana offers regular and modified Newton-Raphson methods for iterations procedure. The main difference between the two is based on computational times, with the latter being faster. It is judged that either option gives approximately the same results. For this analysis the 'Regular Newton-Raphson' method is chosen.

- Convergence criteria

  The convergence of the iterative procedure mentioned above depends on which criteria the designer specifies in the software. There are options for convergence based on force, displacement or energy. They differ from each other due to the quantity (force, displacement or energy) that is being used to check tolerance. Choice of this criteria depends on the problem at hand. For example force norm is used for pure stress relaxations and displacement norm is used for pure creep deformations [30]. It is decided to adopt 'Force based convergence' criteria using a tolerance of 0.001, which provides a good balance between accuracy of results and computational time [22].

11-4 Details of Analysis

All details prior to analysis have been sorted out, which leads us to the next step of defining the order of analysis. Analysis of the imported structural model can be performed using the command line in DIANA solver. The designer can give commands consisting of different nonlinear options. This is an important step as the designer needs to validate the stability of the roof, and this is fulfilled by studying the roof under various expected load combinations using a suitable material model. Furthermore, the shell has to be checked for settlement of supports, cracking and modelling inadequacies. Overall this results in a complete study of the shell, which enables the designer to make a stronger claim that the shell will not collapse. The sequence in which analysis is carried out is extremely important. This is because DIANA uses the results of a preceding analysis, as initial parameters for any subsequent analysis [11]. As a result, the designer can carry out multiple analysis, using different settings, on the same structure. This property of the finite element program is exploited to study the behaviour of the chosen design, under different loads. These details are mentioned in following subsections.

- **Loads Combinations**

  The behaviour of the shell is checked under the different load combinations, mentioned in pre-modeling details. This includes dead weight of the structure, apex load due to centrehung display along with wind, undistributed and redistributed snow loads. These combinations are summarized in the table below. Is should be noted that load combinations 1,2 and 3 have serviceability safety factors while 4,5 and 6 are using unfavorable ultimate limit state factors.

Load Case	Self Weight	Load due to Centrehung	Wind Load	Undistributed Snow Load	Redistributed Snow Load
	D.L.	L.L.	W.L.	Un.S.L.	Re.S.L.
LC1	1	1	1		
LC2	1	1		1	
LC3	1	1			1
LC4	1.35	1.35	1.5		
LC5	1.35	1.35		1.5	
LC6	1.35	1.35			1.5

Table 11-2: Load Combinations used in nonlinear analysis

- **Imperfections**

  The adverse effects of imperfection are well documented necessitating an investigation under imperfections. This is a precautionary step as small defects can be caused due to improper construction. Incorrect alignment of shell panels or failure of panel to panel connections can also be some causes of imperfections in the shell.

  Diana offers an easy way to examine a shell with imperfections. This can be done by performing a normal *Structural stability* analysis including an imperfection pattern. There are three ways to incorporate an imperfection in *MeshEdit*:

  – Buckling Mode

- Random
- User defined

Random and user defined imperfections simulate real world simulations. The user can define the value of imperfection anywhere in the model, which can be directly incorporated in the structural model and a *stability* analysis can be performed. Meanwhile, buckling mode imperfections need a two step process. Since this option defines an imperfection pattern corresponding to the lowest buckling mode, a normal *stability* analysis has to be initially performed without imperfections. Once this is completed, Diana offers the user a option to re-run the analysis, but this time with the critical buckling mode imperfection.

For this analysis the 'Buckling mode' imperfection pattern corresponding to the first mode is chosen. The thickness t of the shell is 100 mm. Hence, the imperfection, that will be used for the analysis can be calculated as shown below:

$$w_0/t = 0.5 \Rightarrow w_0 = 50mm$$

where w_0 is the amplitude for deflection which defines the imperfection pattern.

- **Comparison with an equivalent simple shell**

  Previously the ribbed version of design 1 was chosen to model the roof. A ribbed shell is preferred over a simple shell due to aforementioned reasons of ease of construction. The roof has quite a large diameter of 110 m, which makes construction of a simple smooth shell difficult and expensive. Also the ribs and stiffeners provide extra strength against buckling. Furthermore, it hypothesized that a simple shell could undergo an undesirable dramatic lose in load carrying capacity.

  Hence, a nonlinear linear analysis is decided to be performed on a simple shell roof having the same panel thickness as that of the ribbed shell, but without ribs and stiffeners. The simple version of design 1 (from the section 'Initial Design Formulation') with a thickness t=100 mm is used here.

11-5 Analysis Results

Several nonlinear analysis are carried out on the shell roof, using the load combination depicted in table 11-2. The first three load cases refer to serviceability while the last three provide ultimate limit state conditions. These cases are applied to all models to obtain a load-deflection curve which will be shown in following paragraphs. The load factor, displayed on the y-axis, represents the weight of the load combination at each step of the analysis, after convergence of the solution.

The first set on calculations are performed on a perfect model of the ribbed shell roof. This is subsequently followed by the analysis for the imperfect shell. The manner of imperfection has already been described in the previous section. Once the aforementioned results are gathered, the prefect and imperfect models are compared to each other to have a better understanding of the effect of imperfection on the shell. This is followed by a nonlinear investigation of a simple dome having similar thickness. This step is undertaken to verify the choice of a ribbed design over a simple shell.

1. **Perfect Shell**

The load displacement (L-D) curves are obtained by performing a nonlinear analysis on the ribbed shell roof. The model is a perfect shell with no imperfections. All load cases from table 11-2 are used to obtain six different curves, which are shown in figure 11-5. The curve stays almost linear upto a load factor of $2 \sim 3$ and only starts showing considerable divergence after that point. Loss of load carrying capacity begins as more load is added, followed by higher deflections. This decrease in load bearing capacity of

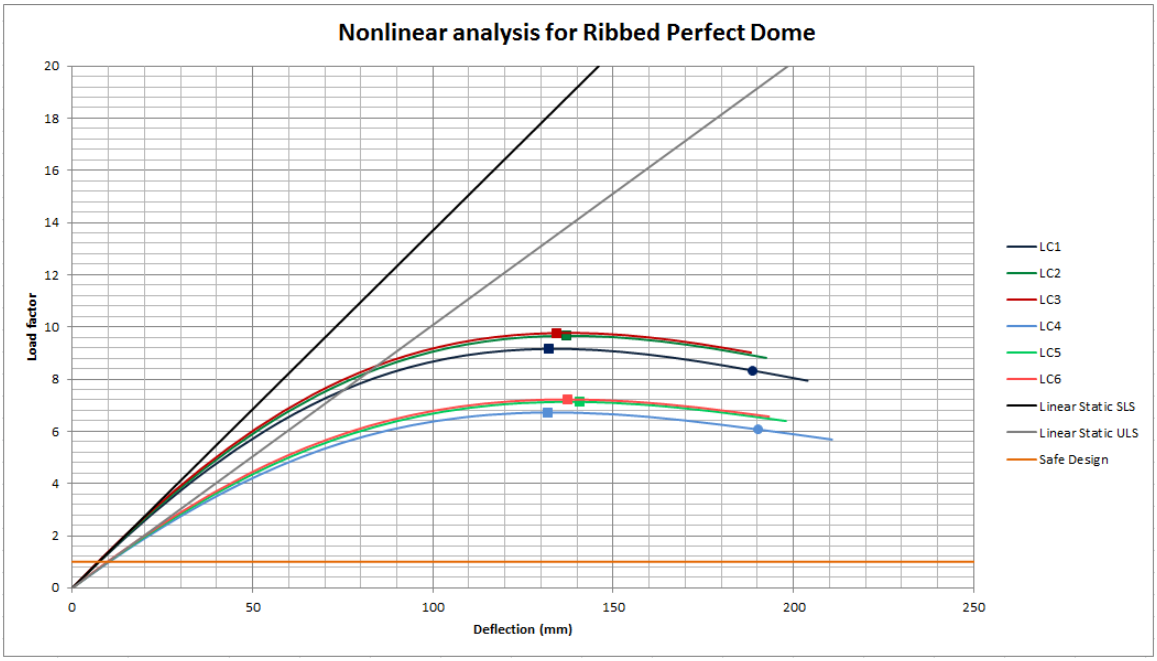

Figure 11-5: Load-Displacement curve for SLS and ULS load combinations

the shell can be attributed to the gradual degradation of UHPC. As the load is increased even further, the concrete starts to crack and the steel fibers start to 'pull out' gradually. In figure 11-5 the square (on the curve) represents the start of appearance of 0.1 mm cracks, while the dot represents a crack with a width of 0.2 mm. It is important to point out that 'highly detrimental' cracks of width 0.1 mm only start appearing after a high load factor of 6 and above.

The orange line in the curve above represents the load factor that the roof will be expected to experience, in reality. The behaviour of the shell until that line is almost linear indicating a safe design. The curves starts to deviate only at higher load factors. One can argue that this is a highly conservative design and the thickness of the shell can be further reduced. But the designer needs to look at the social importance of the structure. This roof is designed to hold above 20,000 people, where structural failure can lead to enormous losses in life. This high risk factor forces the designer to stay away from the edge of safe design, and account for higher load factors, to prevent failure in an event where the structure experiences high accidental forces.

2. **Imperfect Shell**

   The next nonlinear analysis are carried out on an imperfect version of the ribbed shell model. The amount and manner of imperfection have already been defined in the previous section of analysis details. The L-D curves are obtained for all load cases and plotted in figure 11-6. Before comparing an imperfect shell to a perfect shell, it is decided to solely examine the imperfect curves. It is noticed that the curve remains approximately linear until a load factor of 1.5 $\sim$ 2, before it starts diverging from a linear solution.

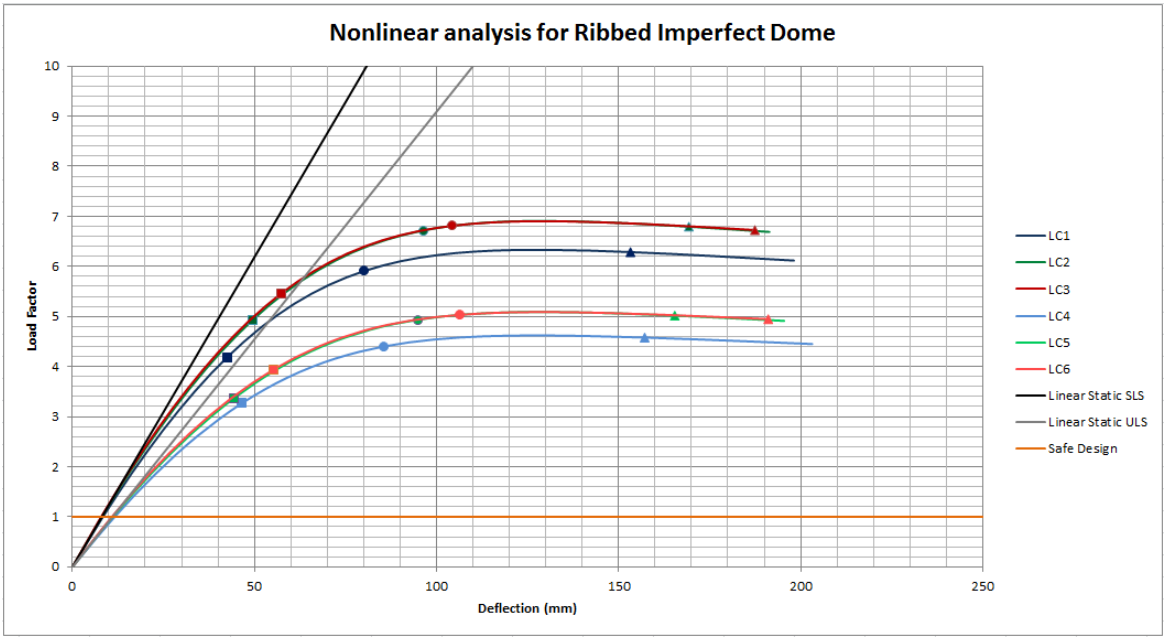

Figure 11-6: Load-Displacement curve for SLS and ULS load combinations

On the curve, the square represents 0.1 mm cracks, the dot shows crack widths of 0.2 mm and the 0.3 mm 'normal' cracks are depicted by the triangles. It can be noticed that even in a imperfect version of the shell, the first micro-cracks only start appearing after a load factor of 3 or more.

3. **Perfect vs Imperfect**

   Once the L-D curves for perfect and imperfect shells are inspected individually, a comparative study is now performed. The L-D curves are plotted for serviceability and ultimate limit states (figure 11-7) separately. Inspection of the L-D curves in both figure show that the perfect and imperfect shell behave linearly up to a load factor of 1.5 $\sim$ 2.5. This means that the designed shell performs well for both design service and ultimate loading conditions.

   Now the formation of cracks are compared for both shell models. The symbols for cracking are the same as used in the previous subsection. It is observed that the severity of cracking is more in the imperfect shell. The perfect shell does not show large micro cracks of 0.3 mm, which can be seen for the imperfect shell towards the latter load steps. For example, in the L-D curve for serviceability load combinations, the imperfect shell

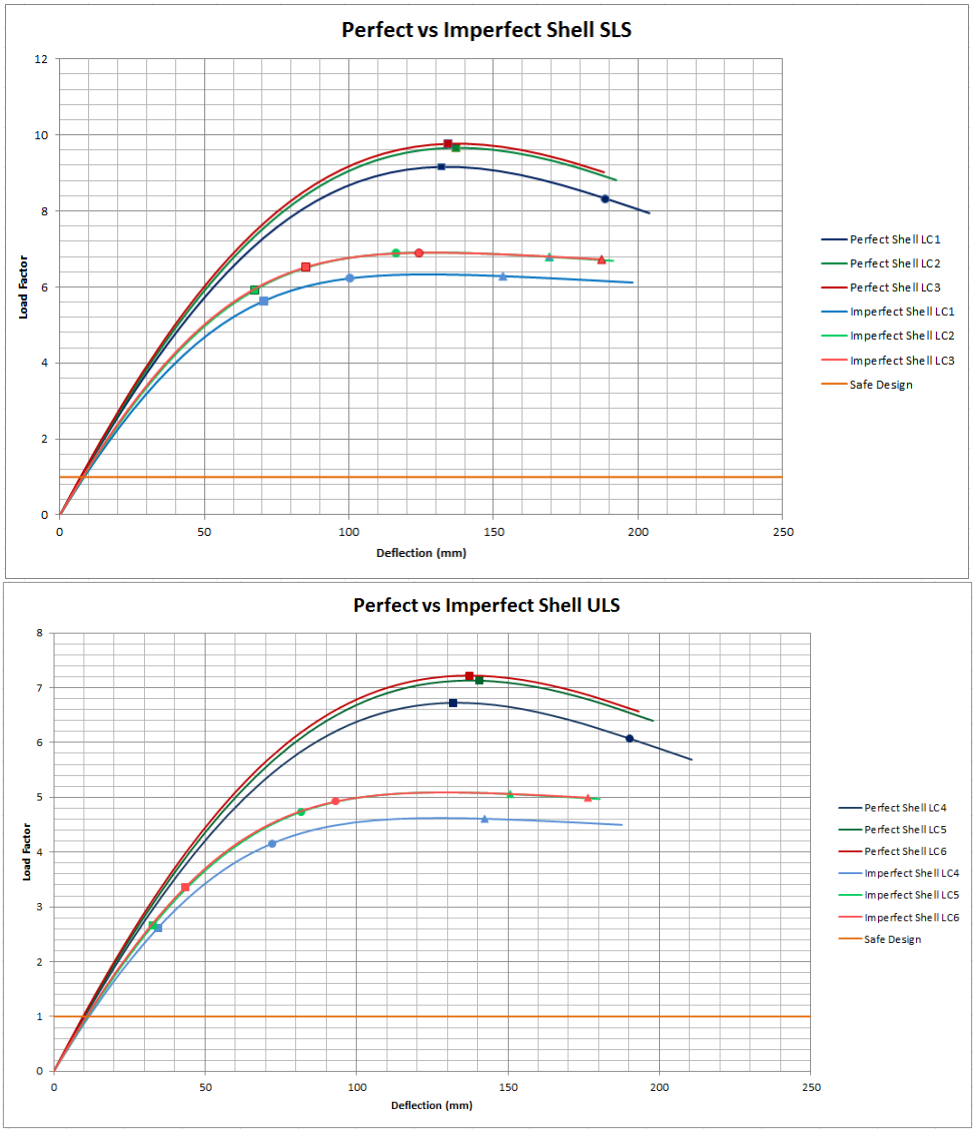

Figure 11-7: Load-Displacement curves for SLS and ULS load combinations

starts to show crack widths of 0.3 mm at the deflection of around 150 mm. But for the same deflection, the perfect shell is able to carry a higher load and shows crack widths of only 0.1 mm, for the corresponding load case. The same pattern can be observed for ultimate load combinations as well.

This confirms the theory of imperfections leading to a considerable decrease in load bearing capacity of the shell. The effect of nonlinearities is compounded with presence imperfections causing the L-D curve to diverge further from a linear solution, than for a perfect shell. Nevertheless these results reiterate the validity of the current shell design for the roof, as the imperfections cause negligible change in the structural response of the shell during initial load steps.

It is also hypothesized that the addition of ribs and stiffeners reduces the sensitivity of the shell roof to imperfections. Usually shells are extremely sensitive to imperfec-

tions causing dramatic lose in load carrying capacity. In this design, the addition of imperfection does cause shell to become weaker but the loss in load bearing capacity is not drastic. The previously shown L-D curves prove this point as the imperfect shell does not experience the 'snap-back' behaviour, mentioned in the literature study. To confirm this theory an equivalent simple (smooth) shell is analyzed, incorporating the same nonlinearities as mentioned before. This is described in the following subsection.

4. **Ribbed vs Simple**

The final verification of the ribbed design is done by comparing to an equivalent simple shell of thickness 100 mm. Only serviceability load combinations are used to conduct the nonlinear analysis. The L-D curves are obtained for the three load cases and plotted below, against the previously calculated ribbed shell values. It should be noted that no imperfections are included in the simple shell, hence they are compared to the L-D curves for the perfect ribbed shell.

Figure 11-8: Load-Displacement curve for SLS and ULS load combinations

This comparison results in display of 'snap back' behaviour in the simple shell. Once the load factor is increased beyond 5, two out of three load cases shown this phenomenon. Furthermore it should be stated absence of imperfections lead one to believe, that including them would further intensify snap back. On the other hand the ribbed shell is protected against this phenomenon, as was justified earlier, due to extra strength provided by ribs and stiffeners.

The nonlinear analysis can lead one to conclude that the designed shell roof performs well up to a load factor of at least 2. From a designer's point of view the shell design is sound for the prescribed loads, in both serviceability and ultimate limit state conditions. The nonlinearities do not seem to effect the shell until extraordinarily large additional loads are applied, which the shell is not expected to carry anyway.

Chapter 12

Validation of Final Design

Once the structural behaviour of the shell has been examined, the final step is to complete the roof design. This includes the design of a structural framework which will efficiently carry the load from the roof to the ground without causing unnecessary stresses in the shell. It is a known fact that a shell, as the one designed in this project, requires additional lateral and rotational stability. This issue is addressed in this section, followed by a check of stresses in the shell. The principal stresses are also calculated to understand how forces flow from the dome to other structural components. Following this the shell panels are arbitrarily designed and shown. The shell pieces need to be connected to each other in such a manner that they behave like one complete isotropic shell. Thus, in the final step an adequate connection strategy is described.

12-1 Structural Framework for the roof

There are some stability problems that can arise due to the inclined geometry of the columns, that will support the dome. These complications arise due to behaviour of the dome as a separate rigid body connected to the supports at the edges. Unusual forces, like in an earthquake or just abnormally high wind speeds, can cause the dome to lose lateral and/or rotational stability. The manner of failure is shown in the following figure.

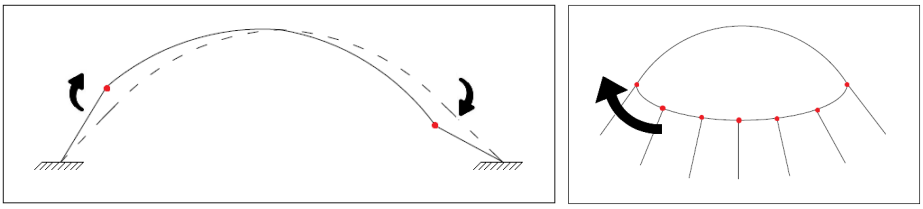

Figure 12-1: Lateral and rotational deformation of a dome on inclined supports

This issue needs to be addressed while designing the support framework for the dome. Figure 12-1 shows the main areas of the structure which will require a strategic design. These areas

are mainly the points (red dots) where the structural fans connect to the edge of the dome, and also where the fans continue on to the outer columns. Previously conducted hanging model analysis showed weaknesses in the same areas as well. Thus, a structural framework is now designed, which is based on intuition and experience from structures in the past.

The most elegant and efficient way to deal with the problem of rotational stability is to use 'forked' outer columns, shown in figure 12-2. This enables a single column to be connected to the dome at two points instead of one, and consequently provides extra strength to the shell against rotation. The validity of this solution is proven by structures in existence today, like the Norfolk Scope and the Sports Palace in Rome, just to name a few.

Lateral support is provided by designing a second set of structural fans which are more vertical, and play the role of inner columns supporting the shell. Figure 12-2 shows a small segment of the entire structure, with the red dots depicting the new orientation of structural elements at the shell edge. The bottom of two fans are connected to each other to provide extra stability against buckling.

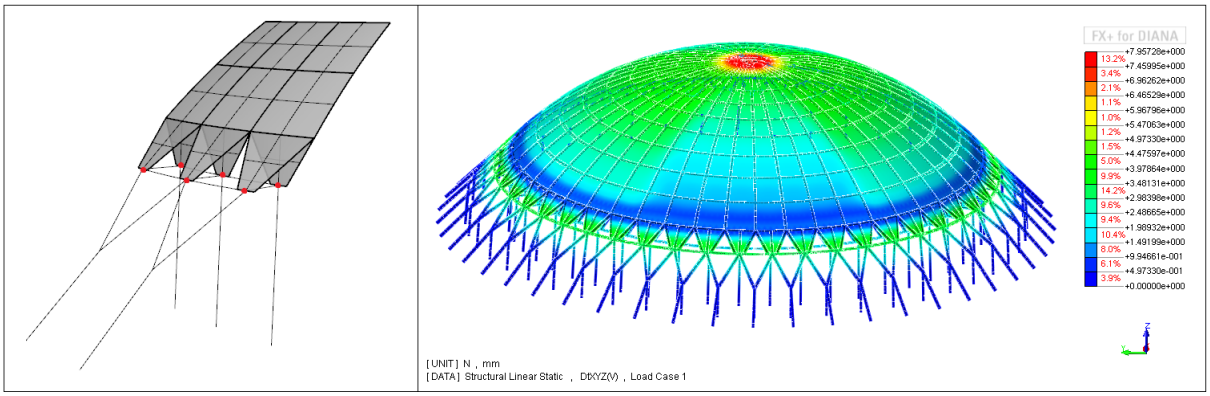

Figure 12-2: Solution adopted for lateral and rotational stability

These structural modifications are modeled in *Rhinoceros* and transferred to *FX+*, where a linear static analysis is performed to check deflections and the critical points of the structure. Load combination 1 is used for this analysis, as the wind load is unsymmetrical and is judged to be the most severe load case. The resulting deflections are below a centimeter, while the edge of the dome appears to not be the critical area any more.

12-2 Stresses in the Shell

Now that the an arbitrary structural framework has been designed, the stresses have to be verified in the shell. This is done so by performing a linear static analysis on the entire structure, under all serviceability load combinations. The curved shell elements (CQ40S), used to design the roof, are characterized by three layers corresponding to the top, middle and bottom surface of the shell panel. Naturally the stress has to be checked at all surfaces to verify the presence of compressive forces, on major parts of the shell. Representation of stresses in the shell is done using *iDiana* instead of *FX+*, which has been used until now. This is because *iDiana* enables the user to show results in a local spherical co-ordinate system of the elements. This provides the user with the ring and hoop stresses directly, which are

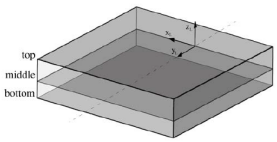

Figure 12-3: CQ40S Element surfaces

a more appropriate form of presenting stresses in the shell. This also facilitates the stress diagrams to be symmetrical simplifying the interpretation of results. In this section the stress diagrams pertaining to load case 1 (with wind loads) are shown. Please refer to Appendix D for load cases 2 and 3.

12-2-1 Results for Load Combination 1

Now that the Ring and Hoop stresses for all surfaces have been calculated, it is time to interpret the results. The Hoop stresses are looked at first, and a graph is plotted for its variation along a line across the shell. This is shown in figure 12-7 superimposed for all surfaces. It can be inferred that majority of the shell surfaces are in compression, with the exception of a small part near the edges. This stress state is favorable for shells, and validates the efficiency of the design.

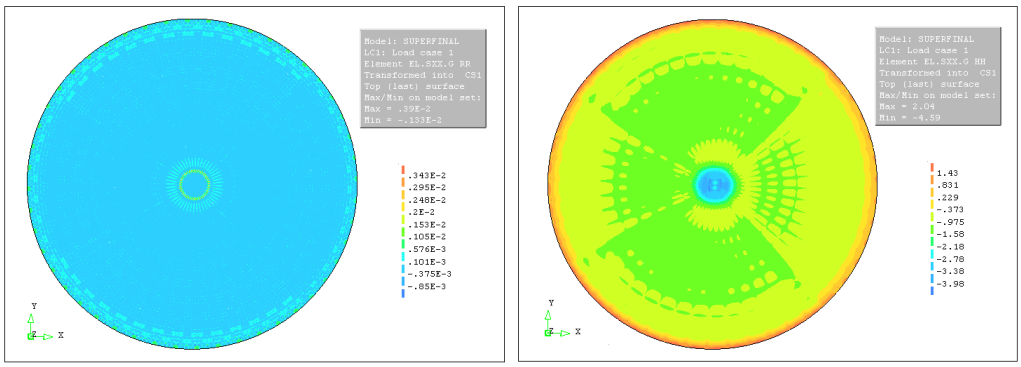

Figure 12-4: Ring and Hoop stresses on the top surface of the shell for LC1

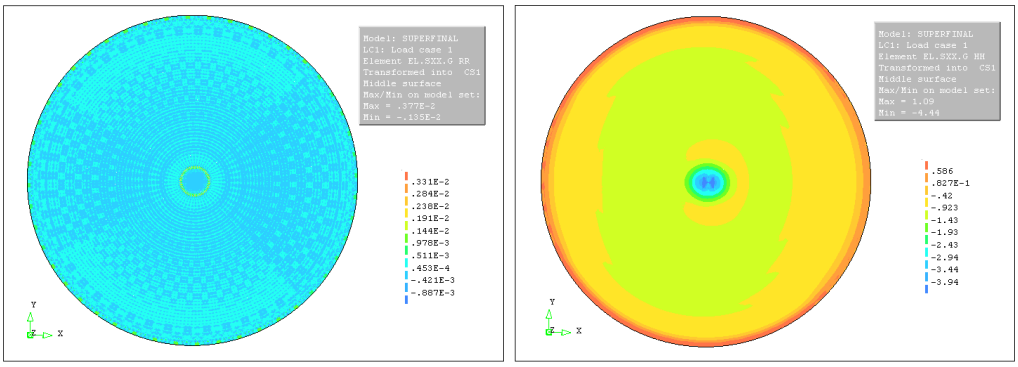

Figure 12-5: Ring and Hoop stresses on the middle surface of the shell for LC1

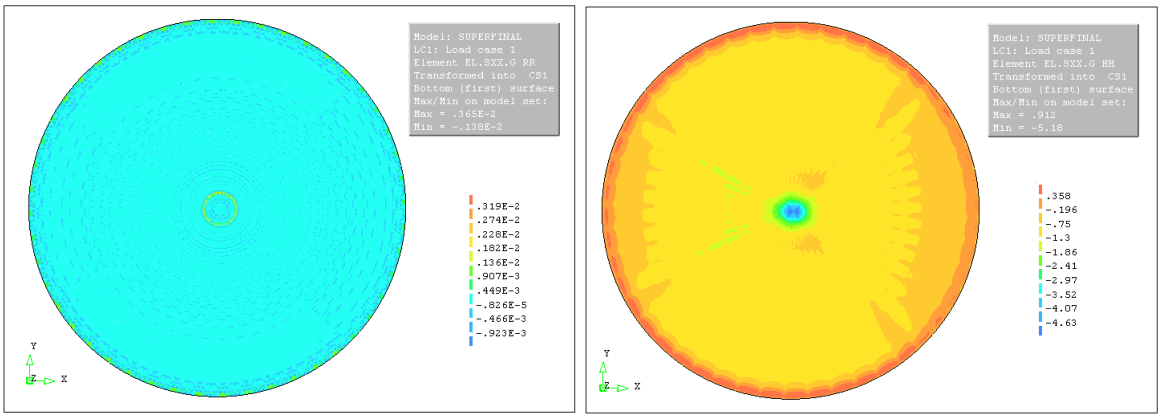

Figure 12-6: Ring and Hoop stresses on the bottom surface of the shell for LC1

Hereafter, the ring stresses are checked. Only the top surface has been shown to make the graph more readable. From the figure plotted below, it is easily observed that majority of the shell experiences a low value of tensile stresses. This is not ideal but is expected, due to the presence of a concentrated load at the shell apex. The structural geometry is such that it causes the shell to 'expand' in radial directions. it should be pointed out that the tensile ring stresses have an order of 10^{-3}, the values being much lower when compared to that of the hoop stresses. It is decided that the panel connections have to be designed accordingly, to account for these radial forces.

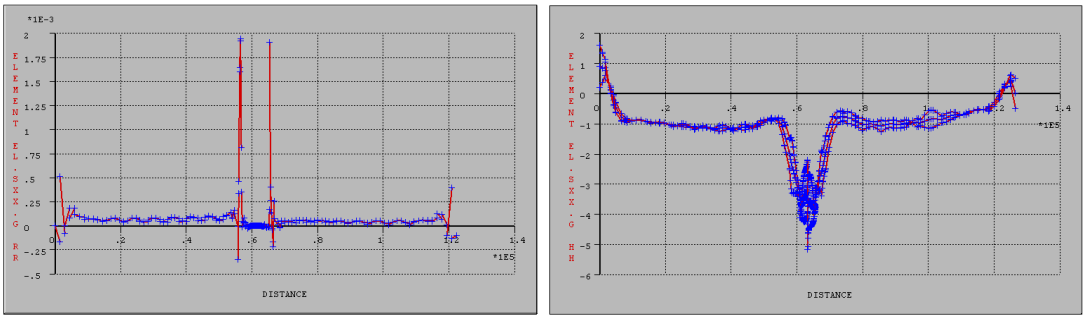

Figure 12-7: Variation of Ring and Hoop stress across a cross section of shell

12-2-2 Principal Stresses

The next step is to determine the flow of forces in the dome, which is done using principal stresses in the shell. *iDiana* used for this purpose where all the principal stresses are calculated and plotted. This is performed for the wind load combination, and can be seen in the following figure. Only the top surface is shown to declutter the figure for better visual representation. Figures for the other load combination can be found in Appendix E. It can be seen in the

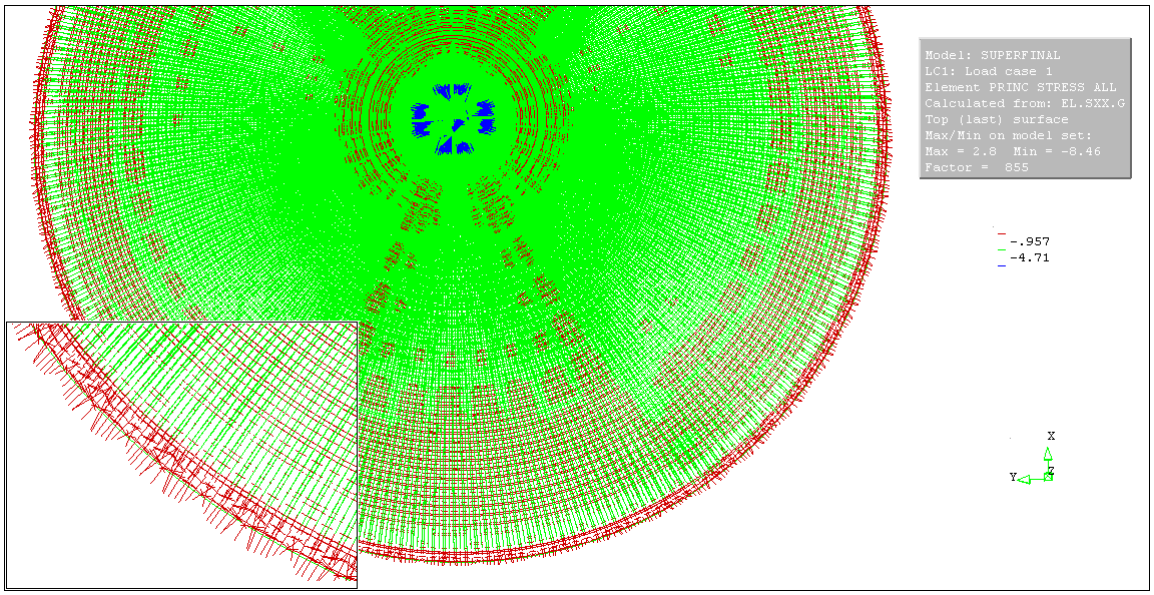

figure above, how the stresses flow and change direction at the edges of the shell. The zoomed part of the figure represents the flow of forces into the structural fans from the shell. The directions of the red lines roughly confirms to the shape of the fans just outside the edge. It illustrates how these forces change from a radial direction due to the geometry of the structure.

12-3 Paneling and Connections

The merits of breaking up a shell structure into panels have been discussed in previous sections. These prefabricated slabs need to mimic the behaviour of a shell with ribs and stiffeners. The shell surface has to be divided in such a way that one can obtain a set of equally shaped panels. This makes the process of prefabrication quicker and more efficient. Ideally, the best outcome is that all panels have the same dimensions but this makes the division of the surface a lot more complex. For the sake of simplicity the shell is radially divided into 10 concentric rings where the panels in each ring are of the same dimensions. This division is figuratively depicted in Appendix C.

The shell thickness is 100mm while the dimensions of the ribs are 250 $\times$ 200 mm. As a result, 'open-box' panels are drafted having a uniform thickness of 100 mm. This is done using *Rhinoceros*. These UHPC curved panels are used to build up the surface of the shell as shown in figure 12-8. These panels are specially suited to create a ribbed shell surface when they are

connected together. The edges of the panels have a greater depth to account for space that needs to be provided for connections.

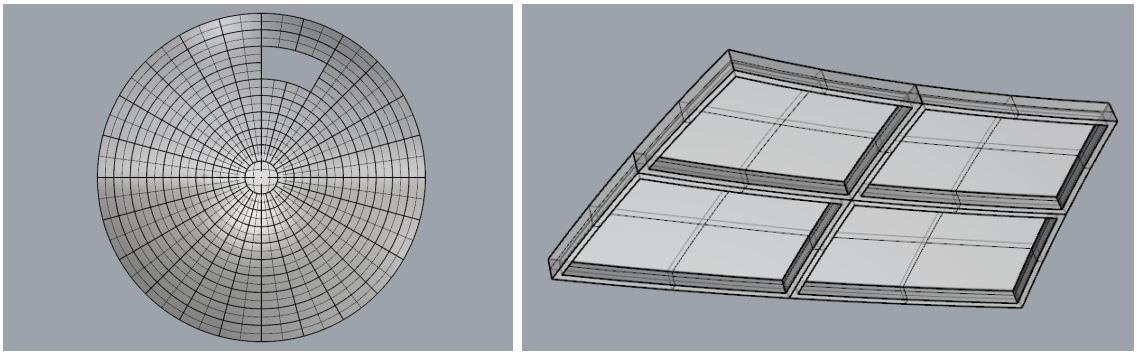

Figure 12-8: Shell panels used for construction of the ribbed shell

The edge faces of the individual panels, need make perfect contact with their neighbours, in order to behave like a smooth shell surface. To ensure this proper connections need to be defined, which is the last step of this design formulation. The structural behaviour of the shell will exert tensile forces over the connections. There are several ways in which shell panels can be connected to each other. A designer has choice of wet, bolted, welded, glued and fiber jointed connections [31]. For UHPC panels bolted and welded joints are suitable but the most favorable ones are the fiber jointed connections as they can carry all kinds of forces through the connection.

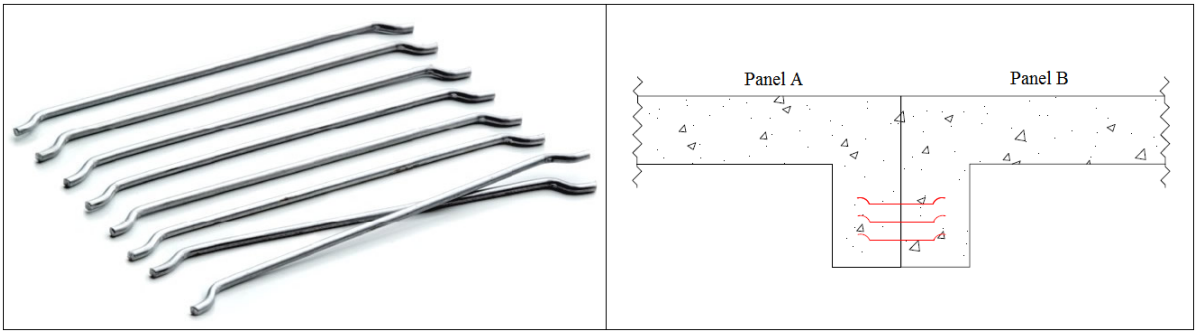

Figure 12-9: Connecting steel fibers and their orientation in panel-to-panel connections

As a result, it is decided to adopt fiber connections for the shell panels. The connection fibers are different from those present in the UHPC, the latter being of insufficient length to form satisfactory connections. An example of connection fibers is shown in the figure above. They have hooks at the end to ensure that the fibers do not slip out of position. During calculation of ring stresses it was discovered that the panels will experience low tensile forces in radial directions. To counteract this the fibers are oriented as shown in the figure above. The exact value of fiber content in the connections, overlapping length and diameter needs to be calculated based on the ring forces. This calculation is not part of this project and only the concept used for the connection has been shown.

Fiber joints can be constructed using supporting ribbons, which can also function as formwork for panel edges. During assembly these ribbons can be used to insert the connecting fibers

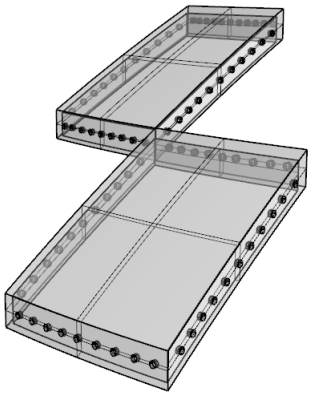

Figure 12-10: Orientation of connections in the panels

between to adjacent panels. Special holes need to be provided at panel edges to facilitate this process. Example of such panels can be seen in the figure 12-10. Once this is done the seam between the panel edges can be injected with shotcrete or plain mortar. This is a relatively laborious process as the filler material needs to be allowed to harden sufficiently. This would increase assembly time but is necessary for the joint to gain full strength. Care should also be taken so as to not bend the connecting fibers during installation.

Chapter 13

Conclusions

A thin concrete shell structure has been designed, for a basketball arena of 20,000 spectator capacity. This is the overlying conclusion of this thesis. The roof is required to cover an arena, which can house 20,000 spectators at one time. To ensure that the designed roof is able to do that, its dimensions were calculated in accordance to the capacity. This required a sightline analysis, to help with the formulation of seating levels, to be used in the capacity analysis. Subsequently in was concluded that the final capacity requirements are met.

The main objective was to create a functioning concrete roof structure, which was expected to maintain a fine balance between aesthetical, structural and constructional efficiency. Attempts have been made throughout the thesis, to create such a shell structure by taking these factors into account.

- The spherical dome has captured the imagination of generations of builders proving the timeless beauty of the simplest of shapes. The dome is elegantly combined with rest of the arena to provide a better visual representation of the roof. This is an attempt to enhance the aesthetical efficiency of the roof system, although it should be pointed out that the fulfillment of this objective is subjective to the reader.
- Structural efficiency of the final design can be verified using the results of the nonlinear analysis and the stresses calculated thereafter. The realistic behaviour of the shell, based on the nonlinearity settings, remains close to the linear analysis results, within the design values. This implies that the nonlinear effects are almost negligible under expected serviceability and ultimate limit state conditions, indicating a well designed shell structure.
- During the design process, it is decided to construct the shell using prefabricated curved shell panels. To incorporate this into the design process, the shell is provided with ribs and stiffeners. Panels which can be easily connected to each other, are chosen for making up the roof. These panels, which can be easily hauled into place, eliminating the requirement of complex curved form-work, for in-situ shell surface creation. This efficient form of construction enables us to achieve the third and final objective of this thesis.

Based on arguments discussed above, it can be concluded that the designed roof is aesthetically pleasing, structurally efficient and easy to construct. This is the underlying conclusion of this thesis.

Chapter 14

Recommendations

- Additional research is needed to incorporate realistic creep effects in the structure. Also the visco-elastic and visco-plasticity settings needs further studies, to provide the designer with more knowledge on how and when to incorporate this effects in nonlinear analysis.
- An attempt could be made to provide a hole or opening at the apex of the shell, and then proceed with the design process. The shell can then be analyzed and studied to see any changes in structural responses.
- This shell roof is proposed to be built up using individual panels. A study should be performed to analyze the shell with one panel missing. This is to recreate a situation if one or more panels need to be repaired or replaced.
- Although the designed shell roof has been proven to be satisfactory, the imperfections included were based on buckling patterns. Additional analysis should be performed by incorporating more realistic imperfections, based on practical experiences of working with domes.
- The connections between panels need to be accurately calculated based on parameters like bond strength and tensile ring stresses developing in the shell. These calculation may also slightly modify the shape and/or orientation on panels.
- A dynamic analysis needs to be preformed on the shell, to assess its behaviour against abnormal loading conditions like wind storms and earthquakes. This will make the design more comprehensive.

Appendix A

Sightline Calculations

The seating arrangement is divided into three tiers. An average C-value is calculated for each of the tiers. Values for minimum seat width and seat depth(T) are chosen in accordance with recommended values stipulated in the Netherlands [24].

$$N = \frac{(R + C) \times (C + T)}{R} - R$$

$$\Rightarrow C = \frac{D(N + R)}{D + T} - R$$

R = Vertical height between the eye and the point of focus

D = Horizontal distance between the eye and the point of focus

N = Seating step height

T = Seating step width

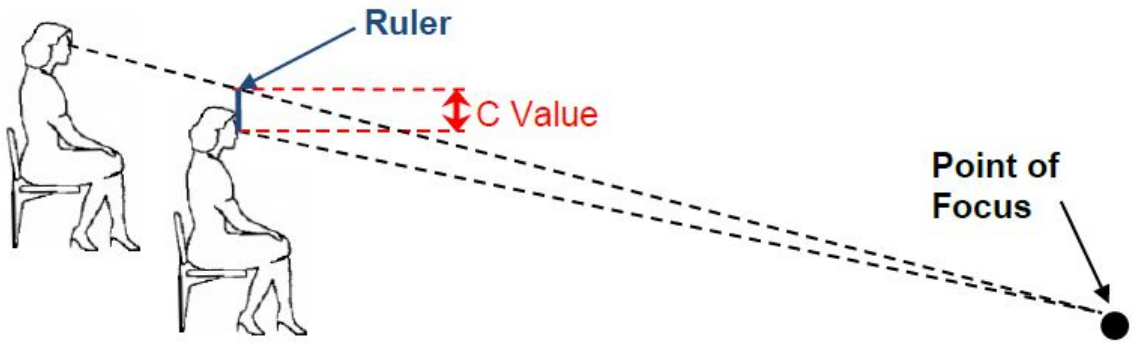

Figure A-1: Concept of C-value

C Value (mm)	Description
60	Need to look between heads in front
90	Can see well with head tilted backwards
120	Optimal viewing standard
150	Can see well even if over spectators with hats

Figure A-2: C-values with description

The C-value calculations for all the zones is done using the formula shown above. This is shown in the following figures. Zones are divided into three parts namely 1,2 and 3. Zone 1 and 3 are designed normally while Zone 2 is designed for VIPs where the seats are provided with extra space for more comfort. This calculation is incorporated in Appendix 4.

Zone 1	(Lower Tier)							
Level	Row	Seating step width = T (m)	Step height = N (m)	Distance from field = D (m)	Height above field = R (m)	Eye Height = h (m)	C-Value	
1	1	0.800	0.240	4.00	0.240	1.44	0.160	
1	2	0.800	0.240	4.80	0.480	1.68	0.137	
1	3	0.800	0.240	5.60	0.720	1.92	0.120	
1	4	0.800	0.255	6.40	0.975	2.18	0.118	
1	5	0.800	0.255	7.20	1.230	2.43	0.107	
1	6	0.800	0.255	8.00	1.485	2.69	0.097	
1	7	0.800	0.270	8.80	1.755	2.96	0.101	
1	8	0.800	0.270	9.60	2.025	3.23	0.093	
1	9	0.800	0.270	10.40	2.295	3.50	0.087	
1	10	0.800	0.285	11.20	2.580	3.78	0.094	
1	11	0.800	0.285	12.00	2.865	4.07	0.088	
1	12	0.800	0.285	12.80	3.150	4.35	0.083	
1	13	0.800	0.300	13.60	3.450	4.65	0.092	
1	14	0.800	0.300	14.40	3.750	4.95	0.087	
1	15	0.800	0.300	15.20	4.050	5.25	0.083	
1	16	0.800	0.315	16.00	4.365	5.57	0.092	
1	17	0.800	0.315	16.80	4.680	5.88	0.088	
1	18	0.800	0.315	17.60	4.995	6.20	0.084	
1	19	0.800	0.330	18.40	5.325	6.53	0.094	
1	20	0.800	0.330	19.20	5.655	6.86	0.091	
1	21	0.800	0.330	20.00	5.985	7.19	0.087	
1	22	0.800	0.345	20.80	6.330	7.53	0.098	
1	23	0.800	0.345	21.60	6.675	7.88	0.094	
1	24	0.800	0.345	22.40	7.020	8.22	0.091	Avg.
1	25	0.800	0.360	23.20	7.380	8.58	0.102	0.099

Zone 2	(Middle Tier)				(1 m gap)			
Level	Row	Seating step width = T (m)	Step height = N (m)	Distance from field = D (m)	Height above field = R (m)	Eye Height = h (m)	C-Value	
2	1	0.800		22.40	8.380	12.500	0.146	
2	2	0.800	0.475	23.20	8.855	12.975	0.164	
2	3	0.800	0.475	24.00	9.330	13.450	0.159	
2	4	0.800	0.475	24.80	9.805	13.925	0.154	
2	5	0.800	0.475	25.60	10.280	14.400	0.149	
2	6	0.800	0.475	26.40	10.755	14.875	0.120	
2	7	0.800	0.475	27.20	11.230	15.350	0.141	
2	8	0.800	0.475	28.00	11.705	15.825	0.137	
2	9	0.800	0.475	28.80	12.180	16.300	0.133	Avg.
2	10	0.800	0.475	29.60	12.655	16.775	0.129	0.143

					(1 m gap)			
Zone 3	(Upper Tier)							
Level	**Row**	**Seating step width = T (m)**	**Step height = N (m)**	**Distance from field = D (m)**	**Height above field = R (m)**	**Eye Height = h (m)**	C-Value	
3	1	0.800		28.80	13.655	16.300	0.096	
3	2	0.800	0.540	29.60	14.195	16.840	0.094	
3	3	0.800	0.540	30.40	14.735	17.380	0.091	
3	4	0.800	0.540	31.20	15.275	17.920	0.089	
3	5	0.800	0.540	32.00	15.815	18.460	0.086	
3	6	0.800	0.540	32.80	16.355	19.000	0.084	
3	7	0.800	0.540	33.60	16.895	19.540	0.082	
3	8	0.800	0.540	34.40	17.435	20.080	0.080	
3	9	0.800	0.540	35.20	17.975	20.620	0.078	**Avg.**
3	10	0.800	0.540	36.00	18.515	21.160	0.077	**0.086**

Appendix B

Arena capacity calculations

The design requirement requires the arena to hold 20,000 spectators. An approximate calculation is done where the entire seating plan is divided into 8 equal segments. The plan is shown in figure 6-3. The number of spectators in each zone are calculated separately and then combined to get the total capacity. These calculations along with notations are shown in the following page.

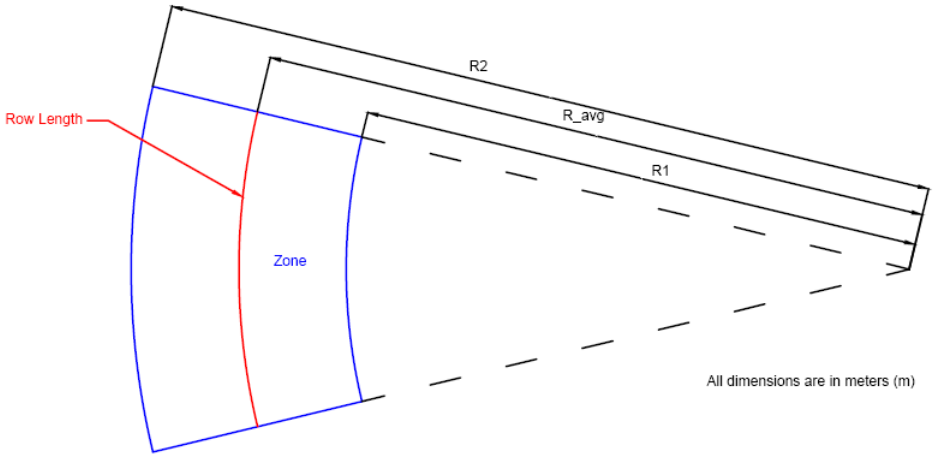

Figure B-1: Notations for capacity calculations

R_1 = Radius of inner edge of zone

R_2 = Radius of outer edge of zone

R_{avg} = Average radius for design row

w_{seat} = Width of one seat in the zone

n_{avg} = Number of spectators in design row

n_{row} = number of rows in the zone

N = Number of spectators in one zone

N_{total} = Number of spectators in one tier (combining all 8 zones in that tier)

	R_1(m)	R_2(m)	R_{avg}(m)	Row length(m)	w_{seat}(m)	n_{avg}	n_{row}	N	N_{total}	
Zone 1	19	38.2	28.6	22.47	0.450	50	25	1248	9987	
Zone 2	37.4	44.6	41	32.21	0.500	64	10	644	5154	
										Total capacity
Zone 3	43.8	51	47.4	37.24	0.450	83	10	828	6621	21763

Appendix C

Division of shell surface

The main arc of the shell is divided in 10 equal segments facilitating the creation of 10 rings of varying dimensions. This means that the shell is made up of 10 different types of panels, which are highlighted in the figure below. Each of these panels follows the same characteristics as described in the final design. Division of the shell is purely based on symmetry, and makes computational modelling easier.

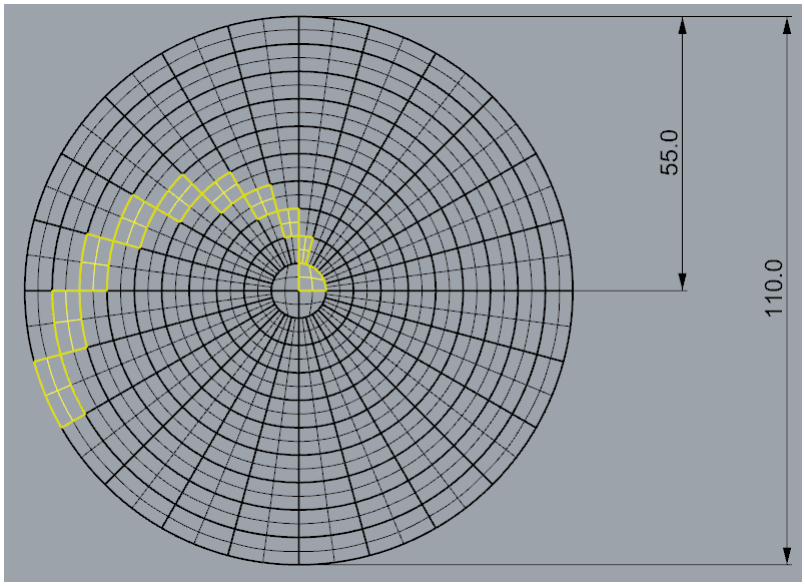

Figure C-1: Division of shell surface

Dimensions shown are in meters.

Appendix D

Stress diagrams

The ring and hoop's stress diagrams for Load combination 2 and 3 are shown here.

- **Load Combination 2**

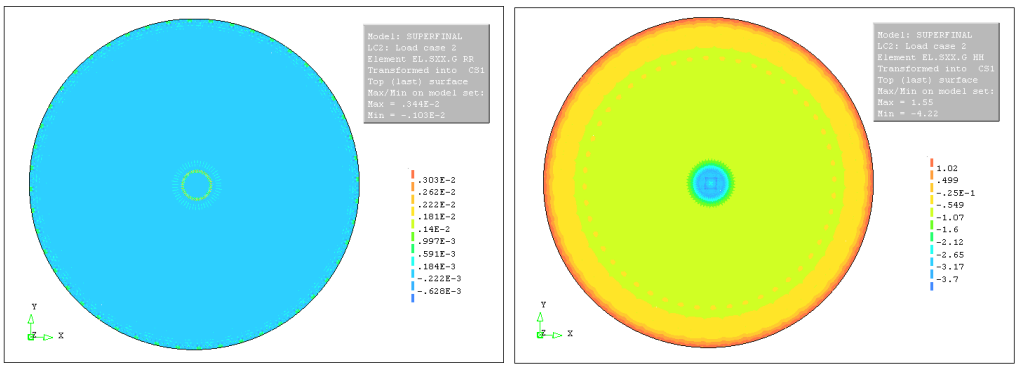

Figure D-1: Ring and Hoop stresses on the top surface of the shell for LC2

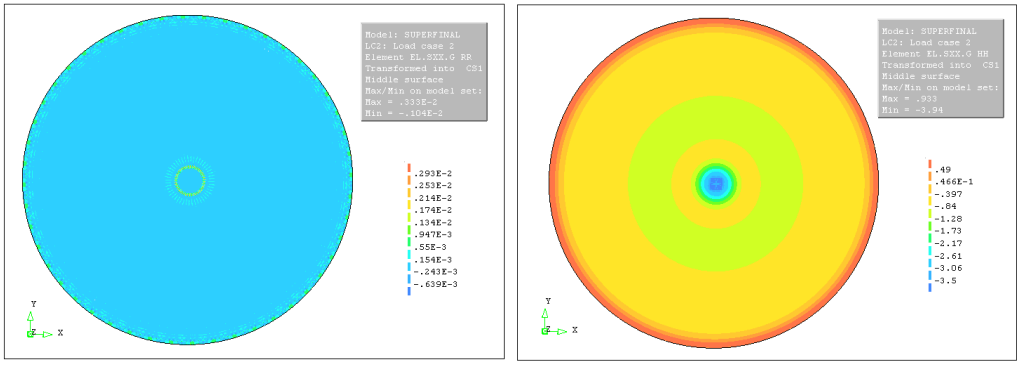

Figure D-2: Ring and Hoop stresses on the middle surface of the shell for LC2

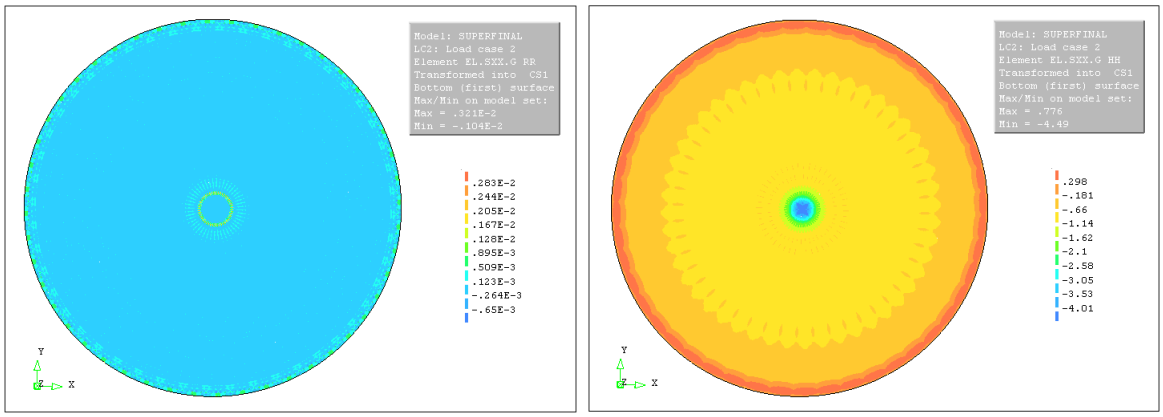

Figure D-3: Ring and Hoop stresses on the bottom surface of the shell for LC2

- **Load Combination 3**

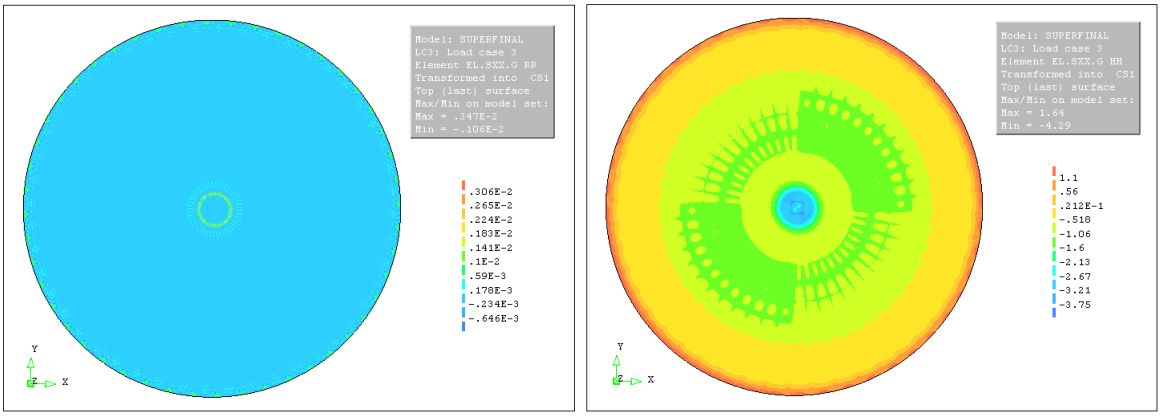

Figure D-4: Ring and Hoop stresses on the top surface of the shell for LC3

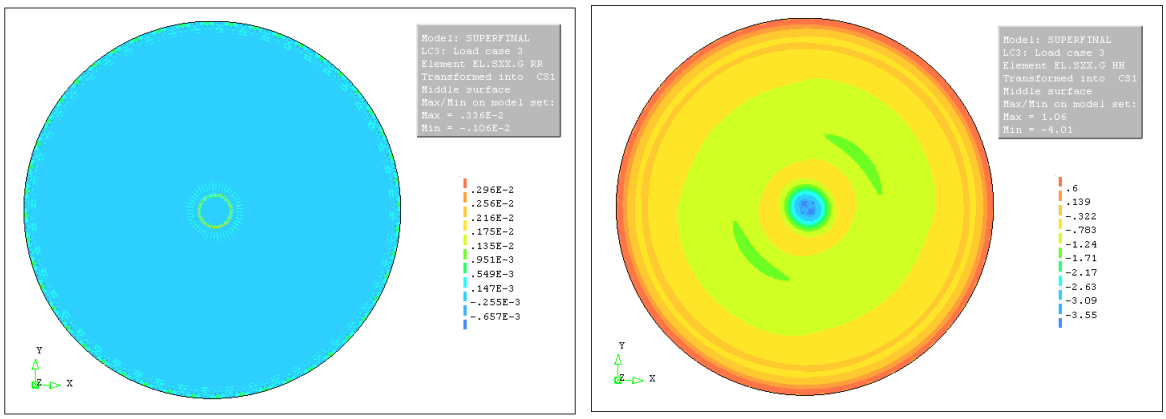

Figure D-5: Ring and Hoop stresses on the middle surface of the shell for LC3

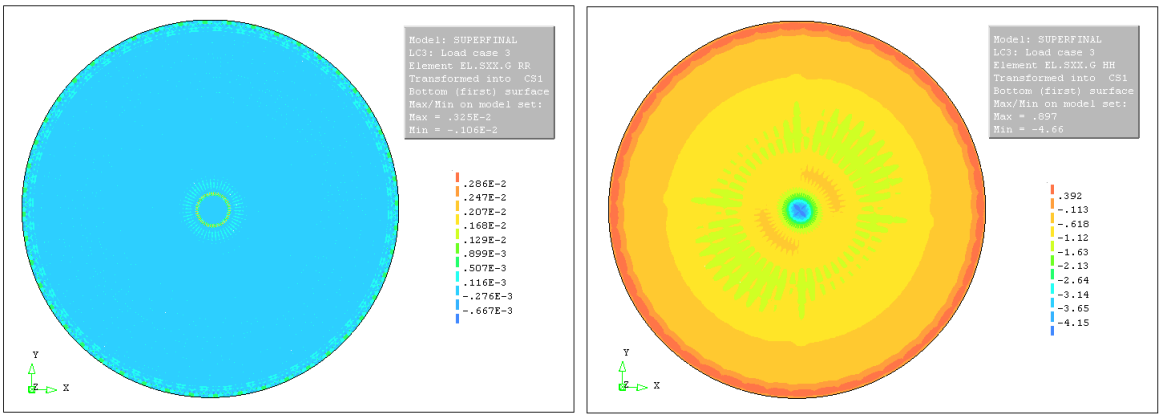

Figure D-6: Ring and Hoop stresses on the bottom surface of the shell for LC3

Appendix E

Principal Stress diagrams

The principal stress directions for load combinations 2 and 3 are shown here.

- Load Combination 2

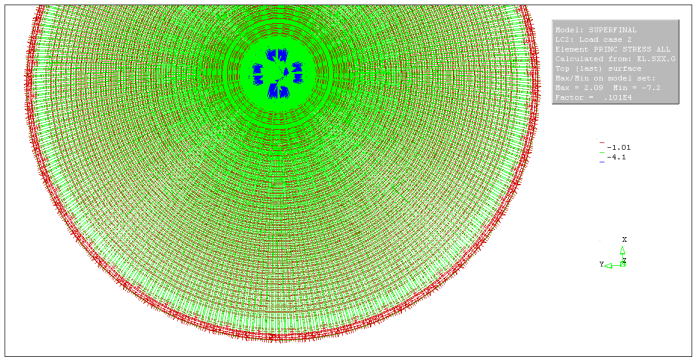

- Load Combination 3

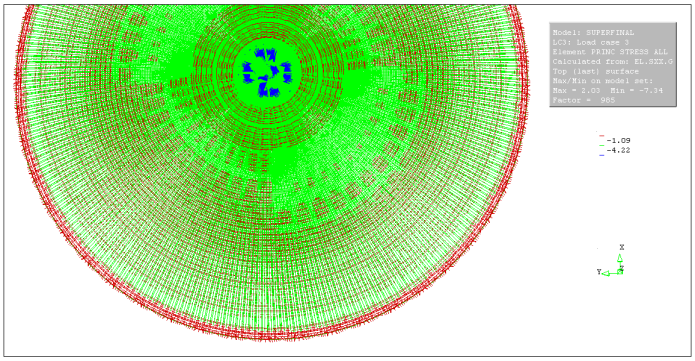

Bibliography

[1] P. Hoogenboom, "Lectures on CIE4143 Shell Analysis, Theory and Application."

[2] J. Blaauwendraad and J. H. Hoefakker, *Structural Shell Analysis*, vol. 200 of *Solid Mechanics and Its Applications*. Dordrecht: Springer Netherlands, 2014.

[3] E. Ramm and G. Mehlhorn, "On shape finding methods and ultimate load analyses of reinforced concrete shells," *Engineering Structures*, vol. 13, no. 2, pp. 178–198, 1991.

[4] E. Ramm, *Ultimate Load and Stability Analy sis of Reinforced Concrete Shells*.

[5] V. Weingarten, E. Morgan, and P. Seide, "Elastic stability of thin-walled cylindrical and conical shells under combined internal pressure and axial compression," 1965.

[6] L. Samuelson and S. Eggwertz, *Shell Stability Handbook*. 1992.

[7] R. Motro and B. Maurin, "Bernard Laffaille, Nicolas Esquillan, Two French Pioneers," 1968.

[8] A. L. Huxtable, *Pier Luigi Nervi*. G. Braziller, 1960.

[9] N. Walliman and B. Baiche, *Ernst and Peter Neufert Architects' Data*. Blackwell Science.

[10] R. N. Maten, "Ultra High Performance Concrete in Large Span Shell Structures," tech. rep., 2011.

[11] T. Diana, *Diana 9.5 User's Manual*, 2014.

[12] B. Peerdeman, "Analysis of thin concrete shells revisited," tech. rep., TU Delft, 2008.

[13] E. Chao, "Pier Luigi Nervi 1891-1979," pp. 32–38, 2005.

[14] J. F. Abel and J. C. Chilton, "Heinz Isler - 50 years of "new shapes for shells"," *Journal of the International Association for Shell and Spatial Structures*, vol. 52, no. 169, pp. 131–134, 2011.

[15] M. Millais, *Building Structures: From Concepts to Design*. Taylor and Francis, 2005.

[16] T. Iori and S. Poretti, "Pier Luigi NerviâĂŹs Works for the 1960 Rome Olympics," *Small*, pp. 27–29, 2005.

[17] Amway Center, "Production Guide Version 2,"

[18] L. T. Ltd., "LED Display Solutions at Bradley Center," 2011.

[19] H. Cowan, *A history of masonry and concrete domes in building construction*, vol. 12 of *Building and Environment*. Jan. 1977.

[20] F. v. H. F. Huijben and R. Nijsse, "Concrete Shell Structures Revisited: Introducing a new 'Low-Tech' construction method using Vacuumatics Formwork," 2011.

[21] D. Roylance, "Finite Element Analysis," tech. rep., Department of Materials Science and Engineering, Massachusetts Institue of Technology, 2001.

[22] L. Sluys and R. de Borst, "Lecture Notes for CIE5142 Computational Methods in Non-Linear Solid Mechanics," May 2013.

[23] M. Schmidt and E. Fehling, "Ultra-high-performance concrete: Research, development and application in Europe," *Concrete, ACI Special Publication*, vol. 228, pp. 51–78, 2005.

[24] P. Shepherd, "Notes on Sightlines," 2012.

[25] E. C. of Standardization, "Eurocode 1: Actions on structures part 1-1: General actions-densities, self-weight, imposed loads for buildings," 2002.

[26] E. C. of Standardization, "Eurocode 1: Actions on structures part 1-3: General actions-snow loads," 2002.

[27] E. C. of Standardization, "Eurocode 1: Actions on structures part 1-4: General actions-wind actions," 2002.

[28] E. C. of Standardization, "Eurocode-basis of structural design," April 2002.

[29] Association Française de Génie Civil, "Ultra High Performance Fibre-Reinforced Concretes - Interim Recommendations," 2002.

[30] J. Rots and M. Hendricks, "Lecture Notes for CIE5142 Computational Modelling of Structures." September 2012.

[31] E. D. Hartog, "Prefabrication of concrete shells," 2009.